COPY 1 3

RD 75/153

Report No. FAA-RD-75-153

FAA WJH Technical Center
00090604

INSTRUMENT LANDING SYSTEM MEASUREMENT PROGRAM

NAFEC
LIBRARY
OCT 28 1975
RECEIVED

APRIL 1975

FINAL REPORT

Document is available to the public through the
National Technical Information Service,
Springfield, Virginia 22161.

Prepared for

U.S. DEPARTMENT OF TRANSPORTATION
FEDERAL AVIATION ADMINISTRATION
Systems Research & Development Service
Washington, D.C. 20590

NOTICE

This document is disseminated under the sponsorship of the Department of Transportation in the interest of information exchange. The United States Government assumes no liability for its contents or use thereof.

Technical Report Documentation Page

1. Report No.	2. Government Accession No.	3. Recipient's Catalog No.
FAA-RD-75-153		

4. Title and Subtitle	5. Report Date
INSTRUMENT LANDING SYSTEM MEASUREMENT PROGRAM	April 1975
	6. Performing Organization Code
	8. Performing Organization Report No.
7. Author(s) AVIONICS STAFF	EER 22-1
9. Performing Organization Name and Address Avionics Engineering Center Department of Electrical Engineering Ohio University Athens, Ohio 45701	10. Work Unit No. (TRAIS) 11. Contract or Grant No. FA74WA-3371
12. Sponsoring Agency Name and Address U. S. Department of Transportation Federal Aviation Administration Systems Research and Development Service Washington, D. C. 20590	13. Type of Report and Period Covered Final Report October, 1973 to April, 1975 14. Sponsoring Agency Code

15. Supplementary Notes

16. Abstract

Results of an extensive series of experiments to determine the characteristics and performance of the Watts slotted-cable, end-fire, glide-slope array are presented. Measurements made at the Tamiami ILS test site, specially prepared under this work program, show that the Watts array will produce a flyable path for Category I operations, but improvements are needed to give greater azimuth coverage of path information. Also, increased RF gain is needed to meet usable distance requirements when operating with solid state transmitting equipment.

Image glide-slope systems and a slotted-cable localizer course array were also measured for performance characteristics and these items are discussed.

For improved accuracy when tracking flight-check aircraft, two automatic tracking theodolites were designed, fabricated, and tested. The video-type tracker, suitable for night-time tracking, gave the greatest range of operation. A modification of the commonly used Warren Knight Model 83 theodolite was made to include drive motors operating on error signals derived from a photocell. This system was found earlier to operate in daytime conditions with ranges up to 3 miles but suffered reliability problems because of confusion created in the processing due to background lighting. This confusion was overcome by replacing incandescent lights on the aircraft with pulsed light emitting diodes to give a signature. With the diodes available for this project, only 1.5 miles maximum range was obtained under laboratory conditions.

17. Key Words	18. Distribution Statement
slotted-cable end-fire glide slope, slotted-cable localizer, video automatic theodolite, light-emitting diode source automatic theodolite	Document is available to the public through the National Technical Information Service, Springfield, Virginia 22161.

19. Security Classif. (of this report)	20. Security Classif. (of this page)	21. No. of Pages	22. Price
Unclassified	Unclassified	127	

Form DOT F 1700.7 (8-72) Reproduction of completed page authorized

METRIC CONVERSION FACTORS

Approximate Conversions to Metric Measures

Symbol	When You Know	Multiply by	To Find	Symbol
		LENGTH		
in	inches	*2.5	centimeters	cm
ft	feet	30	centimeters	cm
yd	yards	0.9	meters	m
mi	miles	1.6	kilometers	km
		AREA		
in^2	square inches	6.5	square centimeters	cm^2
ft^2	square feet	0.09	square meters	m^2
yd^2	square yards	0.8	square meters	m^2
mi^2	square miles	2.6	square kilometers	km^2
	acres	0.4	hectares	ha
		MASS (weight)		
oz	ounces	28	grams	g
lb	pounds	0.45	kilograms	kg
	short tons (2000 lb)	0.9	tonnes	t
		VOLUME		
tsp	teaspoons	5	milliliters	ml
Tbsp	tablespoons	15	milliliters	ml
fl oz	fluid ounces	30	milliliters	ml
c	cups	0.24	liters	l
pt	pints	0.47	liters	l
qt	quarts	0.95	liters	l
gal	gallons	3.8	liters	l
ft^3	cubic feet	0.03	cubic meters	m^3
yd^3	cubic yards	0.76	cubic meters	m^3
		TEMPERATURE (exact)		
°F	Fahrenheit temperature	5/9 (after subtracting 32)	Celsius temperature	°C

*1 in = 2.54 (exactly). For other exact conversions and more detailed tables, see NBS Misc. Publ. 286, Units of Weights and Measures, Price $2.25, SD Catalog No. C13.10:286.

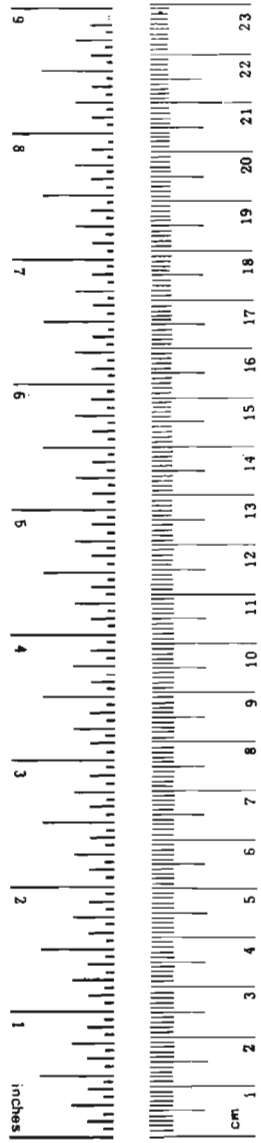

Approximate Conversions from Metric Measures

Symbol	When You Know	Multiply by	To Find	Symbol
		LENGTH		
mm	millimeters	0.04	inches	in
cm	centimeters	0.4	inches	in
m	meters	3.3	feet	ft
m	meters	1.1	yards	yd
km	kilometers	0.6	miles	mi
		AREA		
cm^2	square centimeters	0.16	square inches	in^2
m^2	square meters	1.2	square yards	yd^2
km^2	square kilometers	0.4	square miles	mi^2
ha	hectares (10,000 m^2)	2.5	acres	
		MASS (weight)		
g	grams	0.035	ounces	oz
kg	kilograms	2.2	pounds	lb
t	tonnes (1000 kg)	1.1	short tons	
		VOLUME		
ml	milliliters	0.03	fluid ounces	fl oz
l	liters	2.1	pints	pt
l	liters	1.06	quarts	qt
l	liters	0.26	gallons	gal
m^3	cubic meters	35	cubic feet	ft^3
m^3	cubic meters	1.3	cubic yards	yd^3
		TEMPERATURE (exact)		
°C	Celsius temperature	9/5 (then add 32)	Fahrenheit temperature	°F

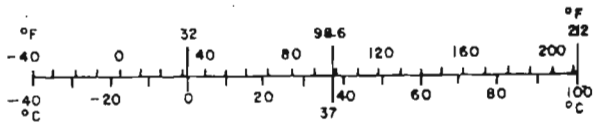

TABLE OF CONTENTS

		PAGE
	List of Figures	iii
	List of Tables	ix
I	INTRODUCTION AND SUMMARY	1
II	INSTALLATION OF FACILITIES	2
	A. Installation of Semi-Permanent Localizer and Glide Slope.	2
	B. Installation and Flight Check of the V-Ring Localizer Array.	3
	C. Installation and Flight Check of an Image Glide-Slope Array and Monitor.	3
III	WATTS LOCALIZER	8
IV	WATTS GLIDE-SLOPE EVALUATION	11
	A. Tamiami Tests.	11
	B. Staunton Tests.	38
	C. Signal Strength Calibration and Rationalization.	61
	D. Conclusions Concerning Performance of the Watts End-Fire Glide-Slope Array.	64
V	FABRICATION OF AN AUTOMATIC TRACKING RADIO THEODOLITE SYSTEM	67
	A. Video System.	68
	B. ARTT with Modulated Light Source.	73
	1. LED Range Calculations and Experiments.	76
	2. LED Control Design.	82
	3. LED ARTT Receiver.	84
	C. Telemetry Interface.	94
	1. Operating Considerations and Functional Design.	94
	2. Detailed Circuit Description.	97
	a. Signal Conditioning Section.	97
	b. Servo-Loop.	97
	c. Receiver.	101
	d. Tone Decoder.	101
	e. Power Supply.	101
	D. Conclusions Concerning the Recently Fabricated ARTT Devices.	109

TABLE OF CONTENTS (Continued)

		PAGE
VI	INVESTIGATORS	111
VII	REFERENCES	112
VIII	APPENDICES	113
	A. Field Strength Considerations	114
	B. Circuit Diagrams for Video ARTT Processor	121
	C. Position Sensor	127

LIST OF FIGURES

		PAGE
Figure 1.	Aerial Photograph of Tamiami Site Prior to Installation of Facilities. (Courtesy of Coast Geodetic Survey)	4
Figure 2.	The 12-Element V-Ring Test Localizer on Runway 9L at the Ohio Site at Tamiami.	6
Figure 3.	Image Glide-Slope Facility at Tamiami with Tracking and Flight-Check Equipment.	7
Figure 4.	End View of the Watts Slotted-Cable Localizer Course Array in Place for the Stability Tests Run During February, 1974 at the Ohio University ILS Test Site, Albany, Ohio.	9
Figure 5.	Watts Slotted-Cable Glide-Slope Array Shown at the Ohio University Tamiami Test Site Looking East Toward the Rear Antenna from the Front Antenna Element.	12
Figure 6.	Watts Slotted-Cable Glide-Slope Layout at Tamiami.	13
Figure 7.	Use of Clark Tower for Elevating Probe Antenna.	15
Figure 8.	Watts Slotted-Cable Glide Slope, Tamiami Airport, November 13, 1973. Ground-Derived Data Using Clark Tower.	16
Figure 9.	Mini-lab Package Which is Installed in the Beechcraft Model 35 Aircraft.	17
Figure 10.	Level Pass Made on Centerline Inbound at 1500 Feet.	19
Figure 11.	Level Pass Made on Centerline Inbound at 1000 Feet.	20
Figure 12.	Low Approaches on Centerline Beginning Near Point A and Extending to the Threshold, Runs 14-13, 14-16, 16-16.	21
Figure 13.	Low Approaches on Centerline Beginning Near Point A and Extending to the Threshold, Runs 15-9, 14-12, 14-14.	22
Figure 14.	Recordings of CDI Made on Opposite Direction Flights Perpendicular to Localizer at 2000 Foot Range, Altitude 130 Feet. Runs 16-9, 16-10, November 16, 1973.	23

LIST OF FIGURES (Continued)

		PAGE
Figure 15.	Recordings of CDI Made on Opposite Direction Flights Perpendicular to Localizer at 13,000 Foot Range, Elevation 650 Feet. Runs 16-7, 16-8, November 13, 1973.	24
Figure 16.	Recordings of CDI Made on Opposite Direction Flights Perpendicular to Localizer at 30,000 Foot Range, Elevation 1000 Feet. Runs 16-11, 16-12, November 16, 1973.	25
Figure 17.	Recordings of CDI Made on Opposite Direction Flights Perpendicular to Localizer at 30,000 Foot Range, Elevation 1300 Feet. Runs 16-13, 16-14, November 16, 1973.	26
Figure 18.	Recordings of CDI Made on Opposite Direction Flights Perpendicular to Localizer at 30,000 Foot Range, Elevation 1600 Feet. Runs 16-15, 16-16, November 16, 1973.	27
Figure 19.	Recordings of CDI Made on Opposite Direction Flights Perpendicular to Localizer at 30,000 Foot Range, Elevation 1900 Feet. Runs 16-17, 16-18, November 16, 1973.	28
Figure 20.	Diagram to Show the Conical Structure of the Watts Array.	29
Figure 21.	Position 5, Perpendicular Cut North to South, Range 1 Mile, Altitude 300 Feet, December 20, 1973, Run No. 30.	32
Figure 22.	Position 5, Perpendicular Cut North to South, Range 2.1 Miles, Altitude 700 Feet, December 20, 1973, Run No. 28.	33
Figure 23.	Position 5, Perpendicular Cut North to South, Range 5.4 Miles, Altitude 1600 Feet, December 20, 1973, Run No. 21.	34
Figure 24.	Plot of CDI Current Made with Ground-Based Vehicle Moving Perpendicular to Runway Centerline, 2000 Feet in Front of Antenna Reference. Probe Height = 7 Feet.	35
Figure 25.	On-Path Approach, Tamiami Airport, December 20, 1973.	36
Figure 26.	Typical Recording of Differential Amplifier and Course Deviation Indicator Values During Low Approach, Tamiami Airport, February 18, 1974, Antenna 5.	37
Figure 27.	Aerial View of Glide-Slope Site at Shenandoah Valley Airport, Staunton, Virginia, March, 1974.	39

LIST OF FIGURES (Continued)

		PAGE
Figure 28.	Extended Centerline Profile Runway 4 - Shenandoah Valley Airport.	40
Figure 29.	View of the Upslope Area Looking Out Into the Approach Region for Runway 6 at the Shenandoah Valley Airport, Staunton, Virginia.	41
Figure 30.	Mr. Ban Tran and Mr. Chester Watts in the Process of Collection Data on the Forward Slotted-Cable Antenna Installed at the Shenandoah Valley Airport, Staunton, Virginia.	42
Figure 31.	Watts Array - Position 5 - Effect of Lateral Offset of Rear Antenna, Perpendicular Cuts, March 25, 1974.	43
Figure 32.	Watts Array - Position 5 - Approach on Path 48", Lateral Movement of Rear Antenna, March 25, 1974.	44
Figure 33.	Watts Array Layout - Position 6 - Shenandoah Valley Airport, March 28, 1974.	45
Figure 34.	Watts Array - Position 6 - Effect of Lateral Offset of Rear Antenna, Perpendicular Cuts March 1, 1974.	47
Figure 35.	Perpendicular Cuts, Position 5 - Tamiami, Position 6 - Staunton.	48
Figure 36.	Approach on Path - Comparison Positions 5 and 6.	49
Figure 37.	Comparison Watts Array versus Sideband Reference - Position 6 with Optimized Offset - April 11, 1974.	50
Figure 38.	Slotted Cable at Reduced Height for Purposes of Evaluating Performance in This Configuration.	51
Figure 39.	Width Measurements by Level Runs.	52
Figure 40.	Differential Amplifier Recordings - Position 6 - Staunton, Virginia, April 23, 1974, Runs 23-12, 23-13, 23-14.	54
Figure 41.	Width Envelope, Staunton, Virginia, Runs 23-12, 23-13, 23-14.	55
Figure 42.	Differential Amplifier Recordings - Position 6 - Staunton, Virginia.	56

LIST OF FIGURES (Continued)

		PAGE
Figure 43.	Width Envelope - Position 6 - Broad, Staunton, Virginia.	57
Figure 44.	Perpendicular Cut, Watts Array - Position 7 - Staunton, Virginia, Run 25-15.	58
Figure 45.	Approach on Path, Watts Array - Position 7 - Staunton, Virginia, Run 25-20.	59
Figure 46.	Approach Distance versus Horizontal Angle of Watts Array. Phase Center 169' from Centerline.	60
Figure 47.	Directional Glide-Slope Antenna.	65
Figure 48.	Block Diagram of Video ARTT System.	70
Figure 49.	Display on Operator's Monitor After Cursors Are Generated.	70
Figure 50.	Functional Diagram of Cursor Generator, Video Brightening, and Rating Circuits.	71
Figure 51.	Block Diagram of Sync. Extraction Circuit.	71
Figure 52.	Block Diagram of Target Threshold and Target Location Circuitry.	74
Figure 53.	Video ARTT - Two Consecutive Runs Overlaid, April 2, 1975.	75
Figure 54.	Preamplifier Circuit for SC-10.	76
Figure 55.	Equivalent Circuit for SC-10 Photocell.	77
Figure 56.	SC-10 and Preamplifier Circuit Shown in Transfer Function Form.	77
Figure 57.	Circuit Response for Varying Pulse Widths.	79
Figure 58.	Output Voltage Amplitude of Preamp for Varying Range in Pulse Width.	81
Figure 59.	LED Control Bolck Diagram.	82
Figure 60.	Light Emitting Diode Wing Unit and Control Box.	83
Figure 61.	1 KHz Trigger Circuit.	85

LIST OF FIGURES (Continued)

		PAGE
Figure 62.	High Voltage Power Supply.	86
Figure 63.	LED Firing Circuit.	87
Figure 64.	LED Monitor Circuit.	87
Figure 65.	Low-Voltage Power Supply.	88
Figure 66.	LED Receiver Block Diagram.	90
Figure 67.	SC-10 Photodetector Equivalent Circuit.	91
Figure 68.	SC-10 Photodetector Utilization.	91
Figure 69.	ARTT Preamp.	92
Figure 70.	ARTT Amplifier and Bandpass Filter (One Channel).	93
Figure 71.	DC Processor Circuit.	95
Figure 72.	Receiver Power Supplies.	96
Figure 73.	Block Diagram of the Converter/Receiver.	98
Figure 74.	Signal Conditioning Section Circuit Diagram.	99
Figure 75.	Servo-Loop Circuit Diagram.	100
Figure 76.	Receiver Circuit Diagram.	102
Figure 77.	Tone Decoder Circuit Diagram.	103
Figure 78.	Complete Circuit Diagram of Converter/Display.	104
Figure 79.	Test Setup for Converter/Display.	105
Figure 80.	Calibration of Converter/Receiver Using DC Feedback.	107
Figure 81.	Calibration of Converter/Receiver Using RF Feedback.	107
Figure 82.	Stepped Response of Converter/Display Unit.	108
Figure 83.	Dynamic Response of Converter/Display Unit.	110

LIST OF FIGURES (Continued)

		PAGE
Figure A-1.	Equivalent Circuit.	116
Figure B-1.	Board 1 - Video Amp, Sync. Separators/Amplifiers, Target Separator/Limiter.	122
Figure B-2.	Board 2 - Vertical Ramp Generator and Gate Generator.	123
Figure B-3.	Board 3 - Horizontal and Vertical Sample/Holds, Ramp Generators, Location Detectors, Gate Generators, and and Bright-Line Generators.	124
Figure B-4.	Board 4 - Video Booster/Isolator, Video Gating, Cursor Adder.	125
Figure B-5.	Cabinet-Mounted Functions - Mode Switch and Power Supply and Tracking Regulator.	126

LIST OF TABLES

		PAGE
Table 1.	Maximum Far-Field Changes Noted During Icing, Heavy Frost, and 3" Snowfall.	10
Table 2.	Listing of Gap Locations for Positions 1 and 5 for Watts Array.	30
Table 3.	Comparison of Ground Measurement and Calculated Field Strength of Watts Array.	62
Table 4.	Laboratory Test Data on Converter/Display Unit.	106
Table 5.	Laboratory Test Data on Converter/Display Unit (RF Feedback).	106

I INTRODUCTION AND SUMMARY

This report documents the results of work performed under Contract FA74WA-3371, entitled Establishment of ILS Test Facilities. The main purpose of this effort was to establish a semi-permanent ILS test facility at a site featuring the ideal electromagnetic environmental conditions required for the precise evaluation of overall system standards and components as related to newly-developed antenna arrays, monitor systems, and flight inspection techniques. In addition, the work performed under this contract included the evaluation of a new end-fire antenna array, the environmental study of a new localizer array, and the design of an automatic radio telemetering theodolite.

A basic antenna test facility had previously been established by Ohio University at the New Tamiami Airport, Miami, Florida, and utilized under Contract FA69WA-2066. Because of the extremely fine electromagnetic environmental characteristics of the site, it was decided that it would be suitable for the ILS work required under this contract. Consistent with the requirements of this contract, a V-ring localizer array and an image glide-slope array along with its associated monitors were established at the site. The image glide slope installed has such flexibility that it can be operated in the null-reference, sideband reference, or capture-effect modes.

Also at the Ohio University test site at Tamiami, a new end-fire glide slope was installed and tested. This new glide slope was designed and built by the Watts Prototype Company, Annandale, Virginia. The purpose of the test on this glide slope was to evaluate the flyability and overall performance of the system.

A new localizer array also designed and built by the Watts Prototype Company was installed at the Ohio University localizer test site at Albany, Ohio. The purpose of the study of this array was to determine environmental effects on path stability.

Finally, in an area related to flight checking of ILS facilities, an automatic radio telemetering theodolite (ARTT) conceived by Forrest Yetter of the FAA was designed and fabricated by Ohio University personnel. In the ARTT portion of the program, several different approaches to the problem were evaluated to determine the optimum in performance versus cost of the tracking systems for use in testing prototype arrays.

II INSTALLATION OF FACILITIES

A. Installation of Semi-Permanent Localizer and Glide Slope. Typically, experimentation with localizer and glide-slope antenna arrays involves aircraft flight measurements and requires for best results large open areas unobstructed with no buildings, wires, hills and other reflecting objects. In the ideal case this suggests a large flat area, say an uncluttered airport, located where climatic conditions insure high probabilities of good weather especially the kind that will permit visual tracking of flight-check aircraft to distances of 6 miles or better. Another highly desirable factor is that the weather be reasonably warm so that personnel may work out-of-doors at any time without great discomfort and attendant inefficiencies of cold weather operation.

Experience at Ohio University compelled the management to search for a site to supplement the test facilities at the Ohio University Airport in Albany, Ohio. Contacts with the Dade County Aviation Department, Miami, Florida, revealed that space at their New Tamiami Airport could be made available on a cooperative basis to enable Ohio University to obtain data on instrument landing system components. Investigation of the site revealed that it was indeed flat, almost totally unobstructed, and possessed almost continual weather conditions that would permit flight checking and visual tracking. The glide-slope antenna and monitor at the Tamiami site under Contract FA69WA-2066[1] permitted some rudimentary facilities to predate this contract work thus saving effort in moving to the goals of this work program.

An instrument landing system located at Dobbins Air Force Base, Georgia, was made available to this project by the FAA. Ohio University personnel removed it from Dobbins and had it shipped to Tamiami. The V-ring localizer was reconfigured to 12 elements and set up on a specially poured concrete pad 1700 feet from the stop end of runway 9 left. This array was energized by an Airborne Instruments Laboratories Model LE-1 transmitter from Dobbins to give a high quality course structure. One-half inch foam-filled coaxial cables were buried in a run of 300 feet between the transmitter hut and the array. A new Alford 12-element distribution unit was used in the feed system.

Provisions were made for maximum flexibility in setting up this localizer array. The anticipation was that other arrays, distribution units, and transmitters may eventually be used with this facility and the least possible complication in changeover is desired. This was accomplished to a large extent by mounting the V-ring antenna elements on unistrut steel channels which permit easy relocation and allow ready access to the cabling.

The glide-slope facility was located to conform to a standard installation plan if the 9L runway is assumed to extend 1435 feet to the west beyond the present threshold. This simulated runway extension was desirable for several reasons. First, the glide-slope location appropriate for the existing hard surface would be very close to the grove of scrub trees and would have a drainage depression of approximately 3 feet parallel to the runway between the transmitting antennas and the runway. Experience has shown that when investigating Category II performance, such a depression can have significant effects.

Second, by moving into the approach region beyond the operational threshold, it was possible to gain access to the effective centerline of the runway for tracking and other purposes without disturbing aircraft operations. This proved to be an important convenience when working with the Watts end-fire array because the center of the coordinate system and reference for tracking were on centerline. Personnel and equipment could be located there without closing a runway or causing other operational problems. Approximately 2600 feet of flat ground exists to the west of the threshold of runway 9L and the airport boundary so no access problems or other difficulties were encountered. Flags were located on the grass area to give the flight-check pilot the visual cues as to where the simulated runway threshold and boundaries were located. Figure 1 shows the location of the localizer and glide-slope sites on the airdrome.

B. Installation and Flight Check of the V-Ring Localizer Array. In the Fall of 1973 installation work was completed on the 12-element V-ring array at Tamiami. The initial purpose of this array was to provide lateral guidance to the flight-check aircraft operating on the glide-slope systems. Flight measurements on this localizer operating at 111.9 MHz showed the facility to have less than three microamperes of roughness and adequate clearance to beyond 35 degrees either side of the runway. All indications are that the array performs very well as might be expected when considering the excellent site conditions.

Figure 2 shows the localizer array in place at Tamiami. After the photograph was taken, another set of localizer transmitting equipment was made available by the FAA. This was a TUR transmitter capable of generating over 100 watts of RF power in contrast to the 10 watts available from the LE-1.

C. Installation and Flight Check of an Image Glide-Slope Array and Monitor. As mentioned in a previous section, the image glide-slope site was located 385 feet to the west of the threshold of runway 9L and 450 feet north of the centerline. This particular location permitted an area greater than 50 acres of smooth terrain to exist to the front and sides of the transmitting array. The term "smooth" means that variations in elevation are on the order of ± 6 inches or less. It should be noted that the land looking out into the approach region for the first 1500 feet has a uniform uptilt of 0.1 degree. Drainage depressions and scrub tree growth are behind the array site. See Figure 3.

The simulated runway threshold was located so as to give a threshold crossing height as defined by TERPS (FAA Handbook 8260.3A)[2] of 55 feet with a 3 degree angle.*

---

*It should be noted that later in the contract work period the simulated threshold was moved to 1595 feet from the threshold of 9L to permit the center of the Watts system to be exactly 1000 feet from the simulated threshold.

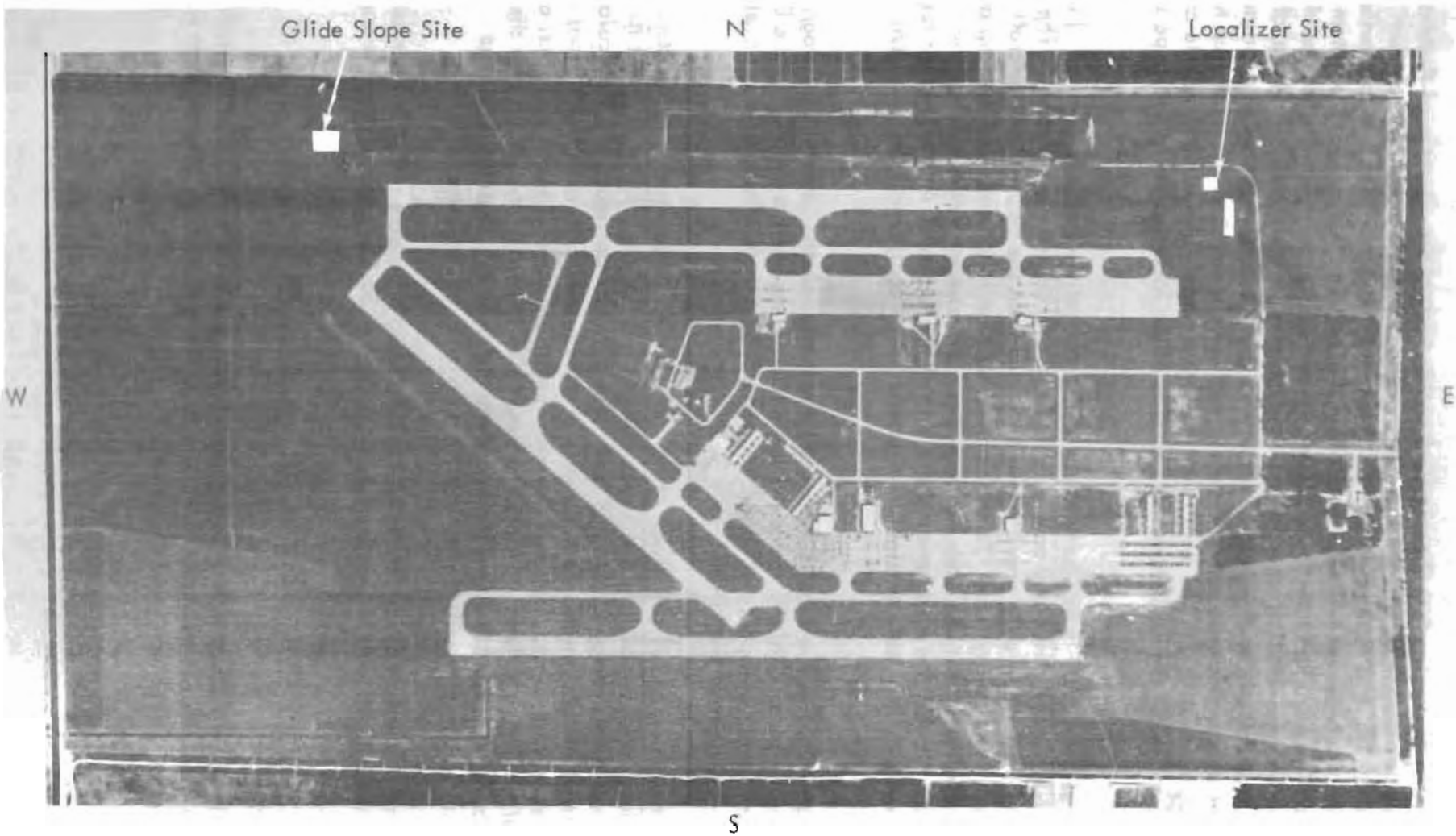

Figure 1. Aerial Photograph of Tamiami Site Prior to Installation of Facilities. (Courtesy of Coast Geodetic Survey)

The image systems played very well at the Tamiami site. A capture-effect and a null-reference type system were set up and test flown. Path roughness of ±8 microamperes was recorded with the theodolite located as specified in the U. S. Flight Inspection Manual[3]. This is on the surface of the reference cone whose vertex is at the antenna mast at the elevation of the runway opposite the mast. A standard 62-inch theodolite height was used.

A check of integral monitors was made for the image system, but with the emphasis on the Watts end-fire system these tests were abbreviated in scope. Sufficient signal level and quality were found for adequate monitoring.

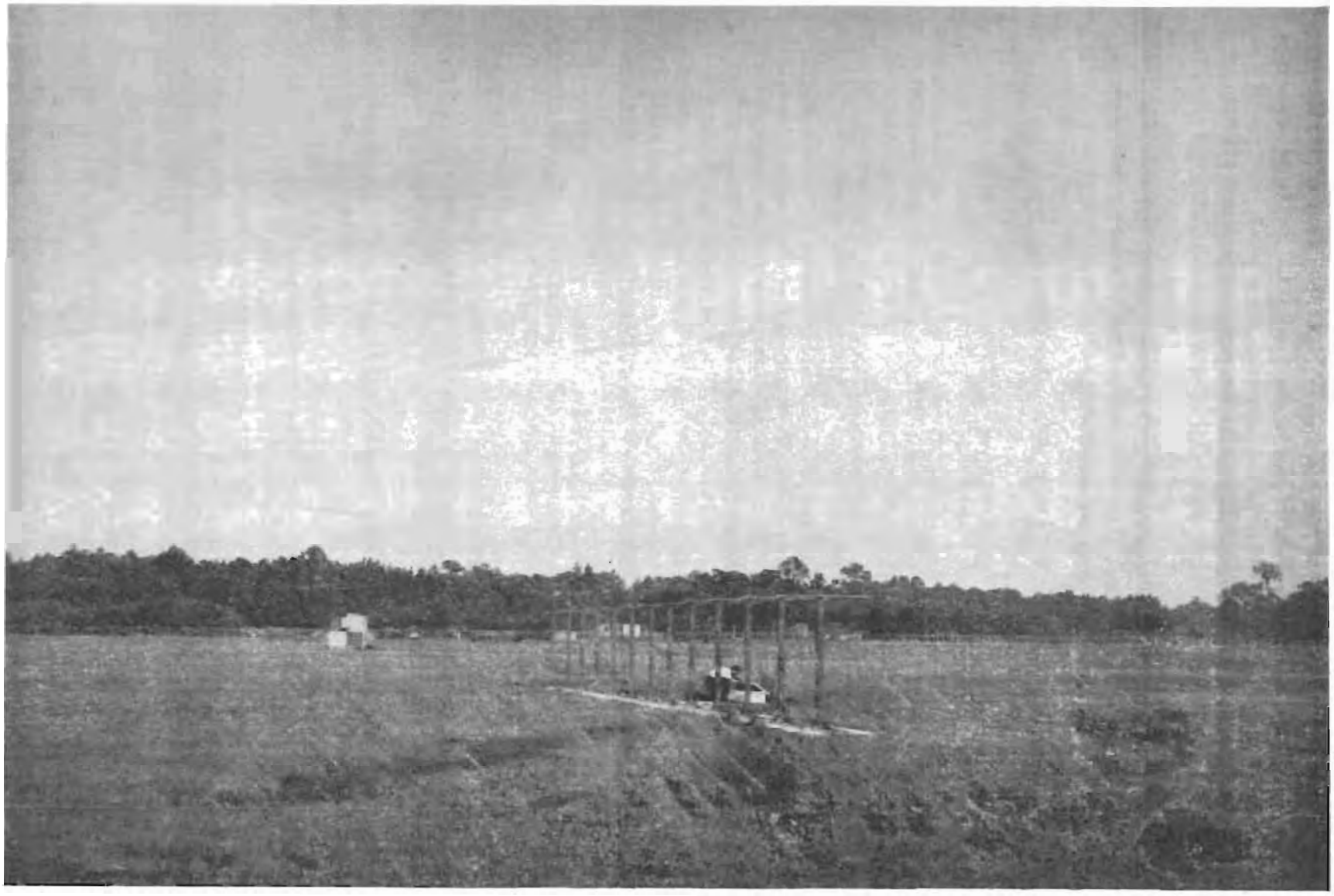

Figure 2. The 12-Element V-Ring Test Localizer on Runway 9L at the Ohio Site at Tamiami. This is presently operating from the special Alford distribution unit for this array.

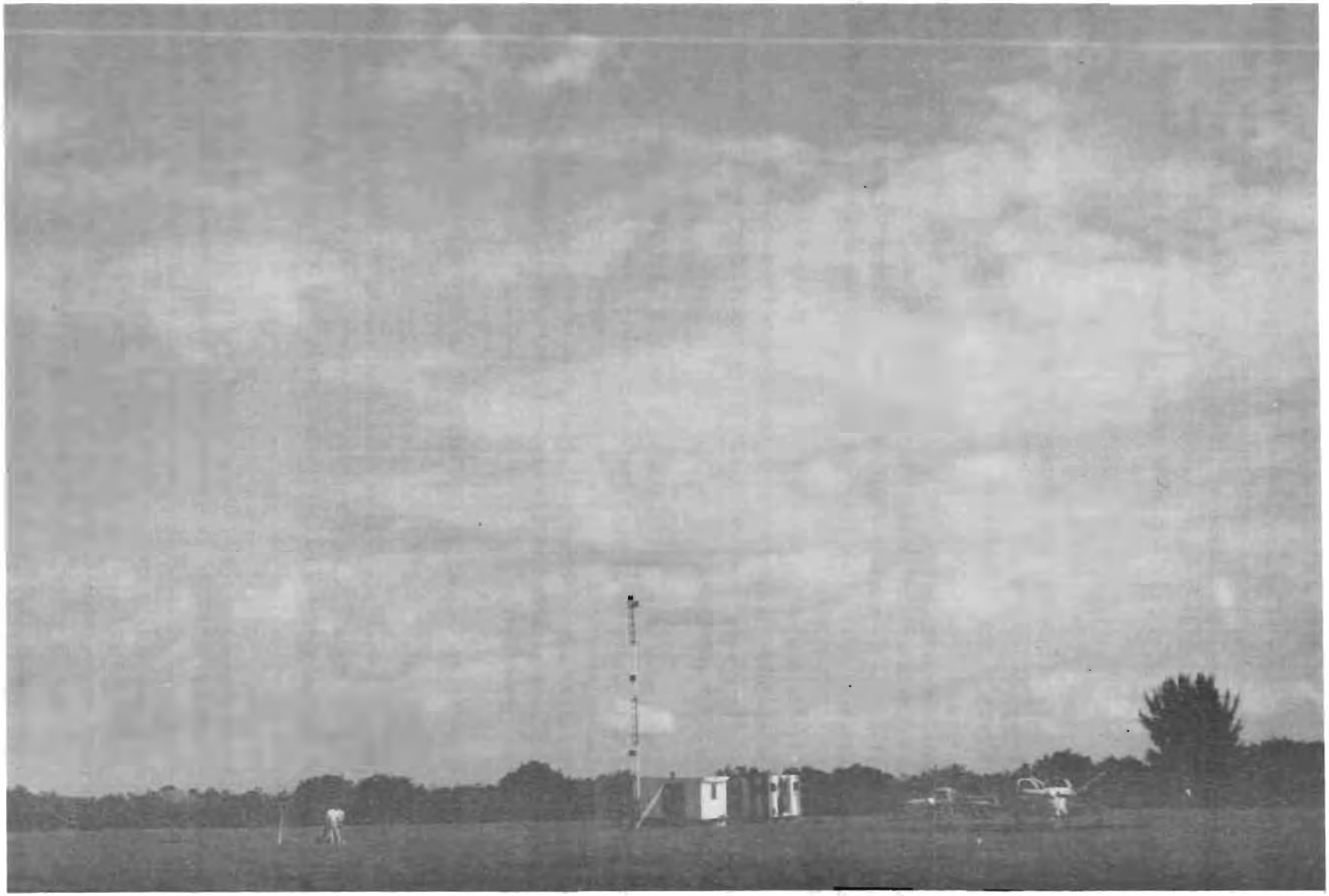

Figure 3. Image Glide-Slope Facility at Tamiami with Tracking and Flight-Check Equipment.

III WATTS LOCALIZER

The Watts Prototype Company, Annandale, Virginia, (under an FAA contract) developed a 200-foot aperture, slotted-cable antenna array and integral monitor system for use as the course array in a two-frequency capture-effect localizer system. An investigation of this system was undertaken to determine the effects of environmental factors on the transmitting array and the monitor system. Specific objectives were to assess:

1. Overall system stability,
2. Effects of humidity and temperature changes,
3. Effects of ice and snow,
4. Effects of electrical storms.

This work was done at the Ohio University localizer test site at Albany, Ohio. The site, which has been used for other localizer experiments, was specially prepared for these tests by installation of a 4-foot by 200-foot concrete pad and the installation of far-field course and width monitors at 7500 feet from the transmitting antennas. See Figure 4 for installation.

The slotted-cable integral monitor was connected to two ARN-14C receivers and records were obtained using Honeywell Model 17 recorders which were calibrated with a Collins 479S-3 test generator.

Far-field records were obtained using a standard far-field monitor type FA-5699 connected to a 10-element Yagi antenna that was located 7500 feet from the transmitting array and on runway centerline. A similar antenna was positioned 7500 feet from the transmitting array with an offset of 2.34 degrees on the 90 Hz side. Course and width monitor outputs were recorded on a Honeywell Electronik 17 recorder calibrated with a Collins 479S-3 generator.

Course and width values, ±11 μa and ±30 μa, respectively, were used as alarm limits.

Integral versus far-field monitor correlation was established using fault insertion at the transmitter by the use of tone balance and sideband attenuation adjustments. The course monitor tracked within 2 μa (worst case) while the far-field tracked within 5 μa (worst case).

The testing period on the Watts localizer ran through the month of February and parts of March and April, 1974. During this time, no adjustments were required on the transmitting array or the monitor once the initial setup was completed. The maximum far-field course deviations during the tests were 3 μa in the 150 Hz side and 5 μa in the 90 Hz side, while the far-field width readings varied from 155 to 166 μa in the 90 Hz. The Watts integral monitor response was generally within 2 μa of the far field except for one case of a 6 μa difference during inclement weather. During the tests, the site

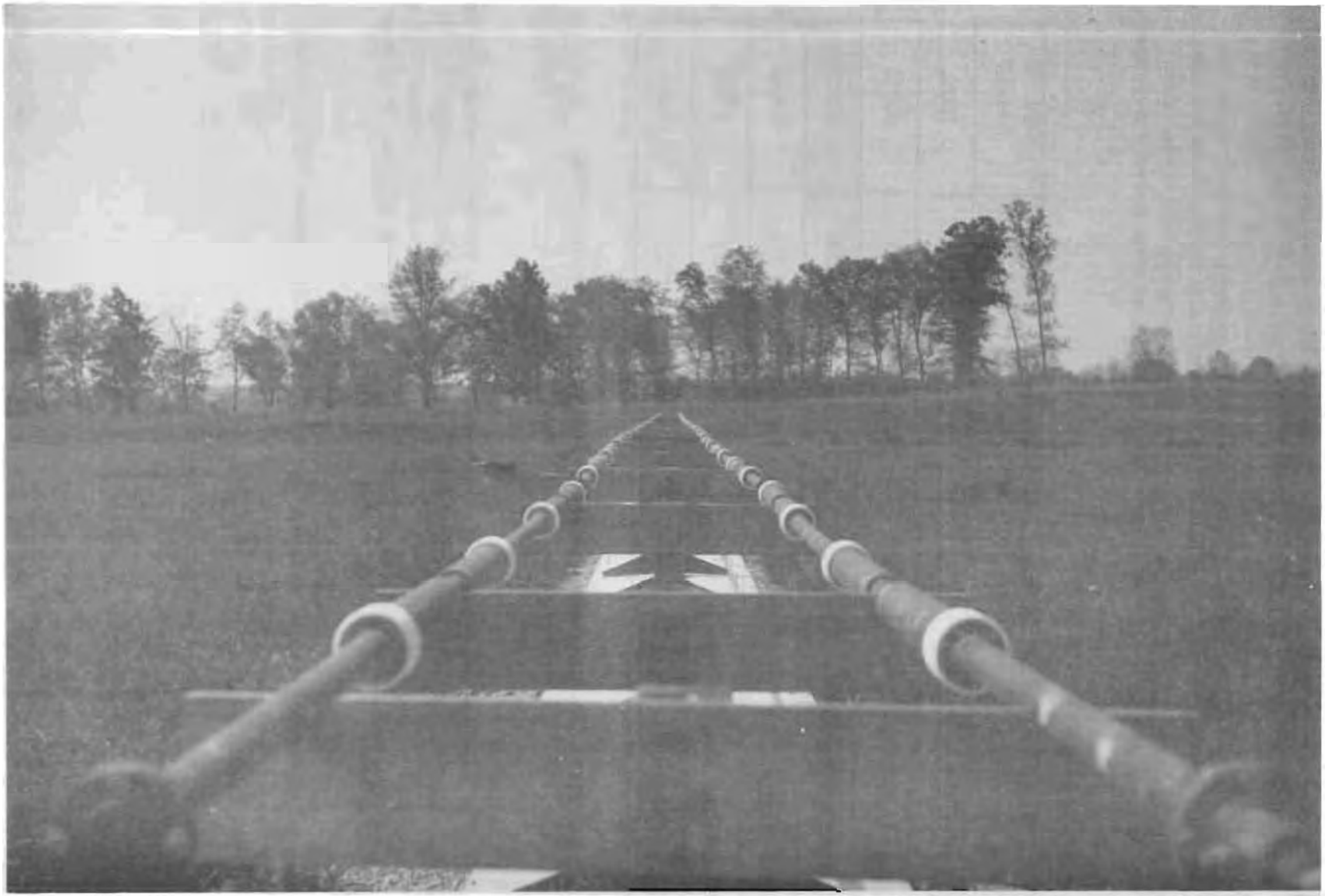

Figure 4. End View of the Watts Slotted-Cable Localizer Course Array in Place for the Stability Tests Run During February, 1974 at the Ohio University ILS Test Site, Albany, Ohio.

FAA WJH Technical Center
00090604

temperature varied from 13 degrees to 78 degrees Fahrenheit and the humidity from 45 percent to 100 percent with no temperature or humidity effects noted on either the Watts integral monitor or the far-field monitor. Neither ice nor snow showed any unacceptable effects on the array. All data for these tests are summarized in Table 1. During the testing period a major thunderstorm with severe electrical activity occurred at the test site. The storm produced no deviations on either the integral or the far-field monitors. During this storm commercial power was interrupted for 10 minutes, and it should be noted that the monitors were back to normal within two minutes after power was restored.

Ice or Frost Accumulation	Course Error	Width Error	RF % Normal	Mod. % Normal
Ice 3/8" Slots 1-4	0 μa	0 μa	100%	100%
Ice 3/8" Slots 1-8	0 μa	1 μa	100%	100%
Ice 3/8" Right Half Array	1 μa	3 μa	100%	100%
Ice 3/8" Entire Array	2 μa	4 μa	98%	100%
Heavy Frost on all Antennas	0 μa	6 μa	100%	100%
3" Snowfall Melting	0 μa	4 μa	100%	100%

Table 1. Maximum Far-Field Changes Noted During Icing, Heavy Frost, and 3" Snowfall.

In summary, the course and width values as seen by the far-field monitors are stable to within 10 percent of the established Category II limits during a variety of mid-west winter conditions. The installation of the array was very straightforward and it did not require any further adjustment following initial setup. The integral monitor, in contrast to the far-field monitor, shows no effects of overflights.

The in-depth results of this program may be found in Report Number FAA-RD-74-94[4].

IV WATTS GLIDE-SLOPE EVALUATION

The Watts Prototype Company has also developed a slotted-cable glide-slope antenna array which has several important properties to give it a potential for installation at sites where limited or irregular ground planes exist. The Watts system is a compatible, end-fire, non-image type which can operate at heights 18 inches or greater above ground. As is typical with end-fire systems, the inherent path is a cone whose axis is nearly parallel to the runway but with a very small (6 degrees) vertex angle. To make an end-fire system practical as an operational glide path, the cone must be flattened or broadened in azimuth. The Watts Prototype Company has employed the slotted cables to obtain aperture and to control the azimuth energy distribution. This control permits the cone to be essentially flattened on top to provide the glide-slope surface within the localizer limits. Ohio University flight checks have been designed to permit careful examination of the effective broadening of the basic cone, and to determine how well the end result serves as an operational glide slope.

A. Tamiami Tests. In November, 1973 an experimental investigation of the Watts Prototype Company's end-fire glide slope was begun at the Ohio University Tamiami Airport test site, Miami, Florida. Tests were run at 331.1 MHz with the antennas to the north side of the runway. The Watts end-fire glide slope utilizes slotted-cable antennas for the two array elements. Two of the principal advantages claimed for the Watts glide slope are its broadened azimuth coverage compared to previous end-fire systems and its high directivity.

One of the more satisfying aspects of the end-fire evaluation program was the ease of the temporary installation of the glide-slope array. The installation took less than two days with two people involved in the establishment of antenna location, running the transmission lines, and pressurizing the system. Electrical adjustments were made on the ground in one day's time, and ground-based data collection was accomplished in one additional day after flight checking began. The only system adjustment made was an increase in power level at the TU4 transmitter. After initial data was obtained, numerous changes were made to check for optimization.

The physical layout of the antenna array is shown in Figure 5. The array center was located 1000 feet back from the simulated threshold and set to radiate a 3-degree glide slope. The slotted-cable antennas were mounted on 42-inch high supporting wood stands. A photograph of the Watts glide-slope installation at Tamiami is given in Figure 6.

The experiments performed during this program were designed and executed not only for the purpose of identifying the usual glide-slope characteristics, but also with the purpose of examining the characteristics peculiar to end-fire arrays, determining the requirement for azimuthal path broadening, and checking for optimum performance given these prototype slot antennas. To this end a number of special measurements were made with flights perpendicular to the runway centerline at various altitudes and distances from the transmitting array. These were in addition to those made in compliance with the U. S. Flight Inspection Manual.

Figure 5. Watts Slotted-Cable Glide-Slope Array shown at the Ohio University Tamiami Test Site looking east toward the rear antenna from the front antenna element. The plastic radome covering the slotted cable is evident with tape bands marking the individual slot positions. The portable wooden stands support the slotted cables, the front 130.2 feet long, the rear 132.8 feet. The white loop on the right of the front antenna is the plastic pressure line which couples the transmission line to the antenna so that all are pressurized from the same source. The air-filled coaxial transmission line carries the pressure to the antenna.

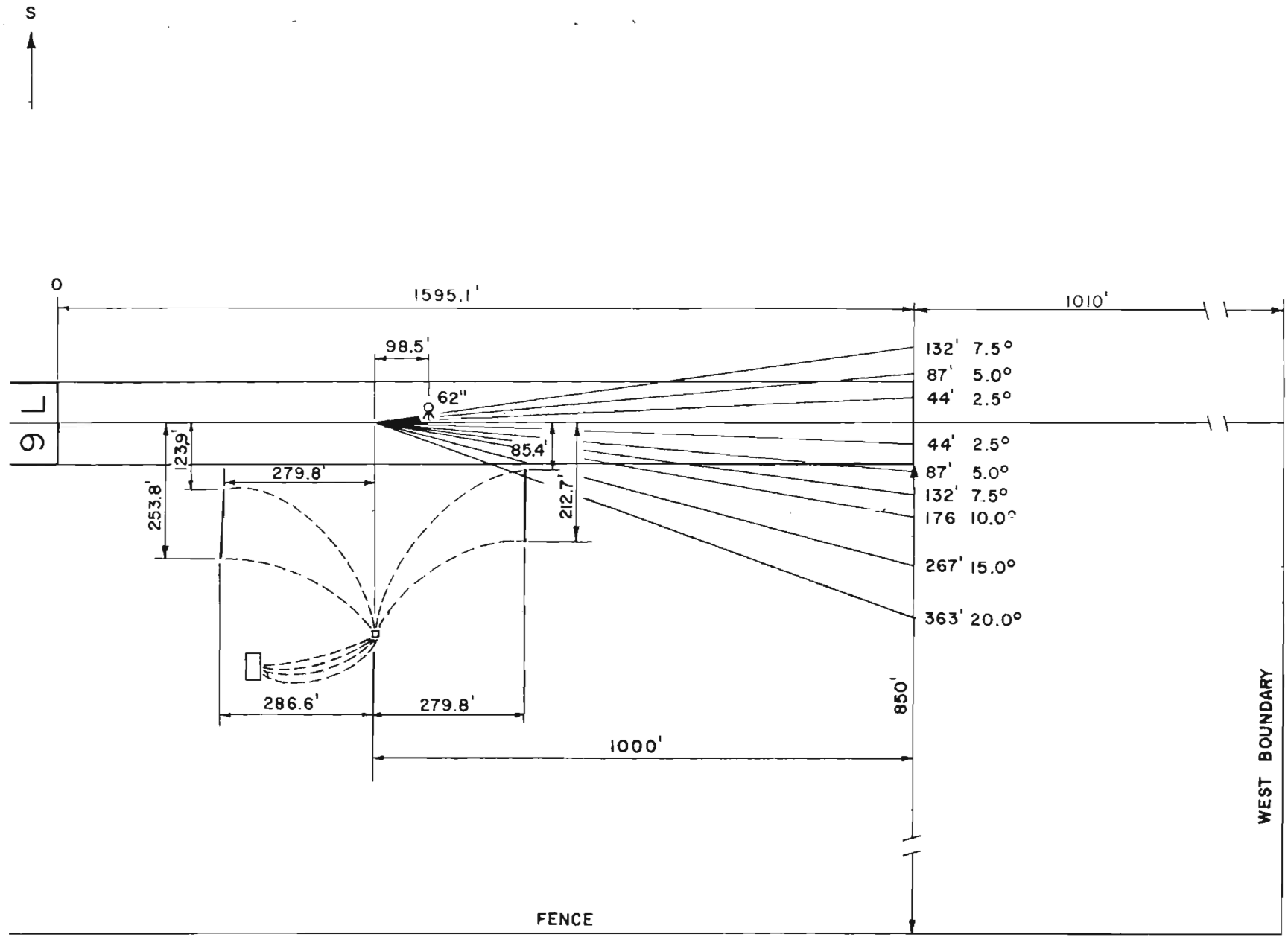

Figure 6. Watts Slotted-Cable Glide-Slope Layout at Tamiami.

Ground-based measurements were also made with a telescoping tower to give an indication of the path structure at a distance of 1000 feet from the array center. The ground-based measurements consisted of inserting a vertical probe in the path at a distance of 1000 feet from the phase center of the array. The specific points were at azimuth angles of 7.5°, 5°, 2.5° left and 0°, 2.5°, 5.0°, 7.5°, 10°, 15° and 20° right, as measured from a point on the runway centerline that was opposite the phase center of the array. Probe heights up to 60 feet were achieved with the Clark Tower shown in Figure 7. Figure 8 provides a summary of the ground-based data measurements.

A Beechcraft Model 35 aircraft was used for the flight checks. Recordings were made of the course deviation indicator of the glide slope using a NARCO UGR-2 receiver and a Honeywell Electronik 19 dual-channel recorder. Figure 9 shows the flight-check package. Telemetry from the theodolite was received on another NARCO UGR-2 receiver. A differential amplifier was used to subtract the theodolite signal from the glide-slope signal and this difference was usually recorded on the other recorder channel. Optionally, flag current level or theodolite position could be recorded instead of the differential amplifier output. Specially built UHF preamplifiers giving 20 dB gain were planned ahead of the NARCO receivers to bring their sensitivities to an equivalent of 2 microvolts. An Aircraft Radio Corporation A13B antenna was used for normal path measurements and a NARCO UGA-1 antenna which has side-looking characteristics was used for perpendicular cut measurements. Calibration reference was a Boonton 232A signal generator.

The following types of airborne measurements were made on the Watts glide slope. From these a reasonable inference can be made concerning the three-dimensional path in space.

ON PATH APPROACHES	On runway centerline -	Above nominal angle At nominal angle Below nominal angle Below path clearance
	Off runway centerline -	At nominal angle
LEVEL PASSES	On runway centerline -	1000 feet 1500 feet
	Off runway centerline -	1500 feet
CUTS PERPENDICULAR TO RUNWAY CENTER-LINE	Range 1000 feet -	130 feet elevation
	Range 13,000 feet -	650 feet elevation
	Range 20,000 feet -	1000 feet elevation
	Range 30,000 feet -	1000 feet elevation 1300 feet elevation 1600 feet elevation 1900 feet elevation

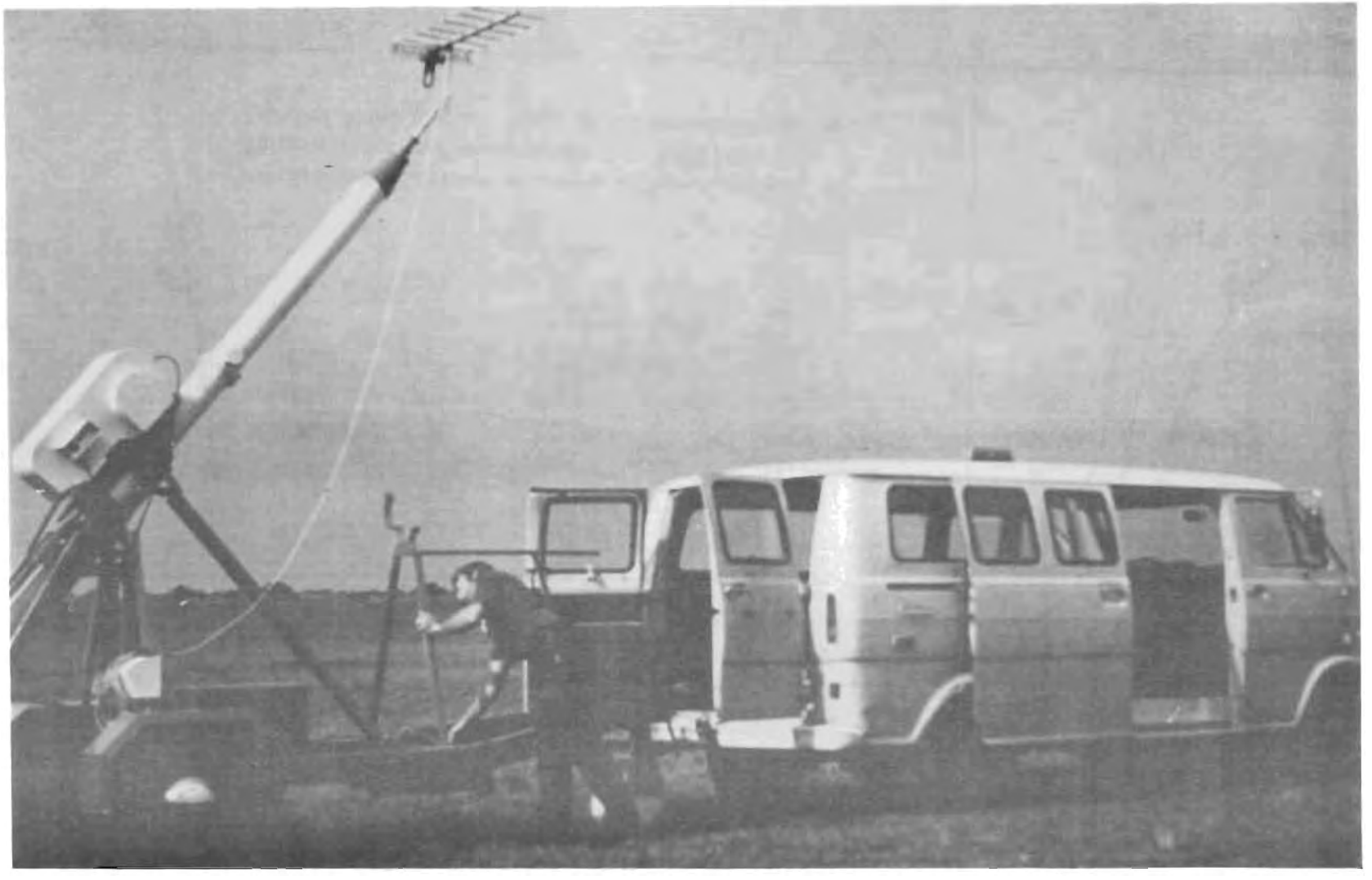

Figure 7. Use of Clark Tower for Elevating Probe Antenna.

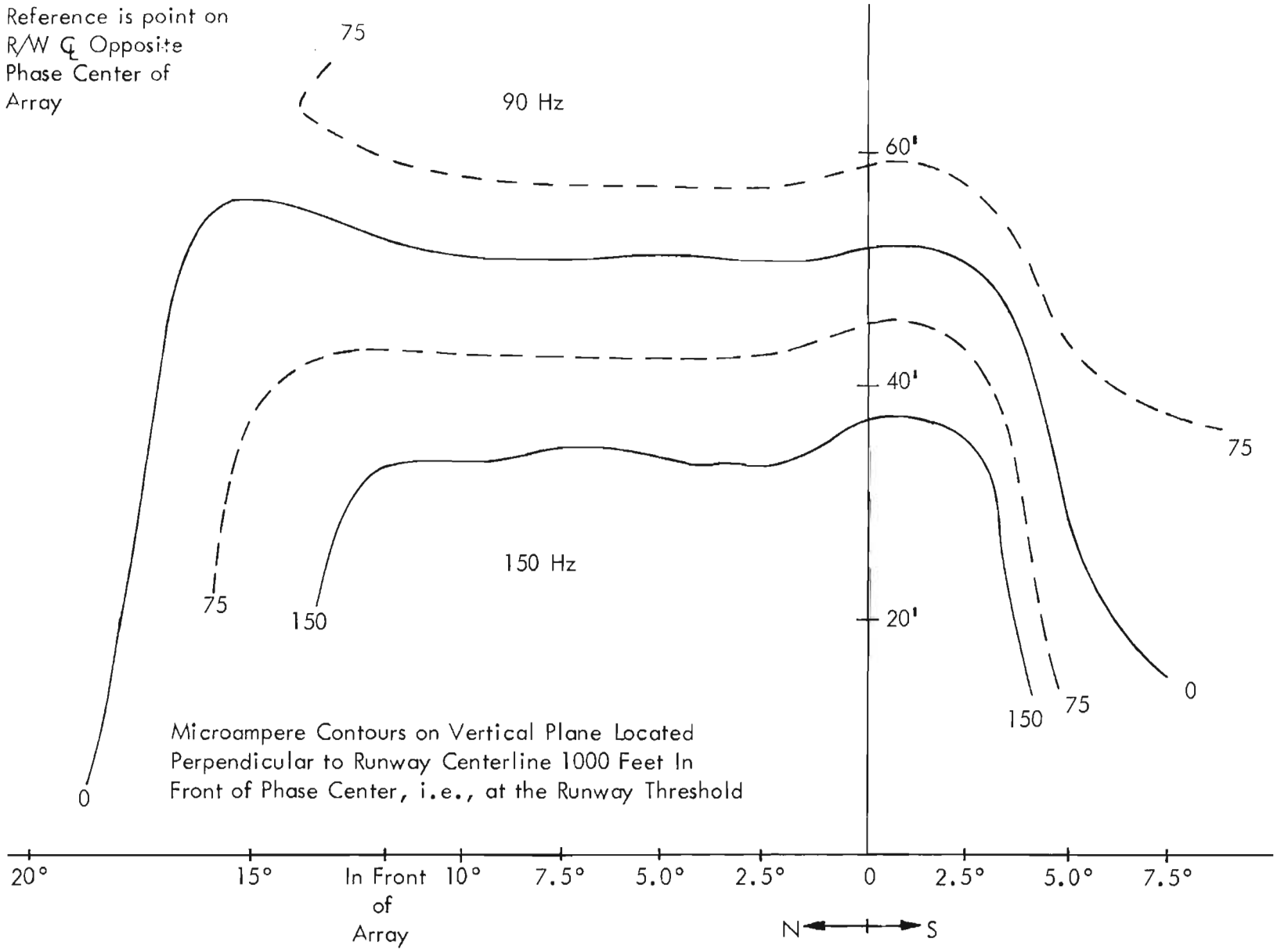

Figure 8 . Watts Slotted-Cable Glide Slope, Tamiami Airport, November 13, 1973. Ground-Derived Data Using Clark Tower.

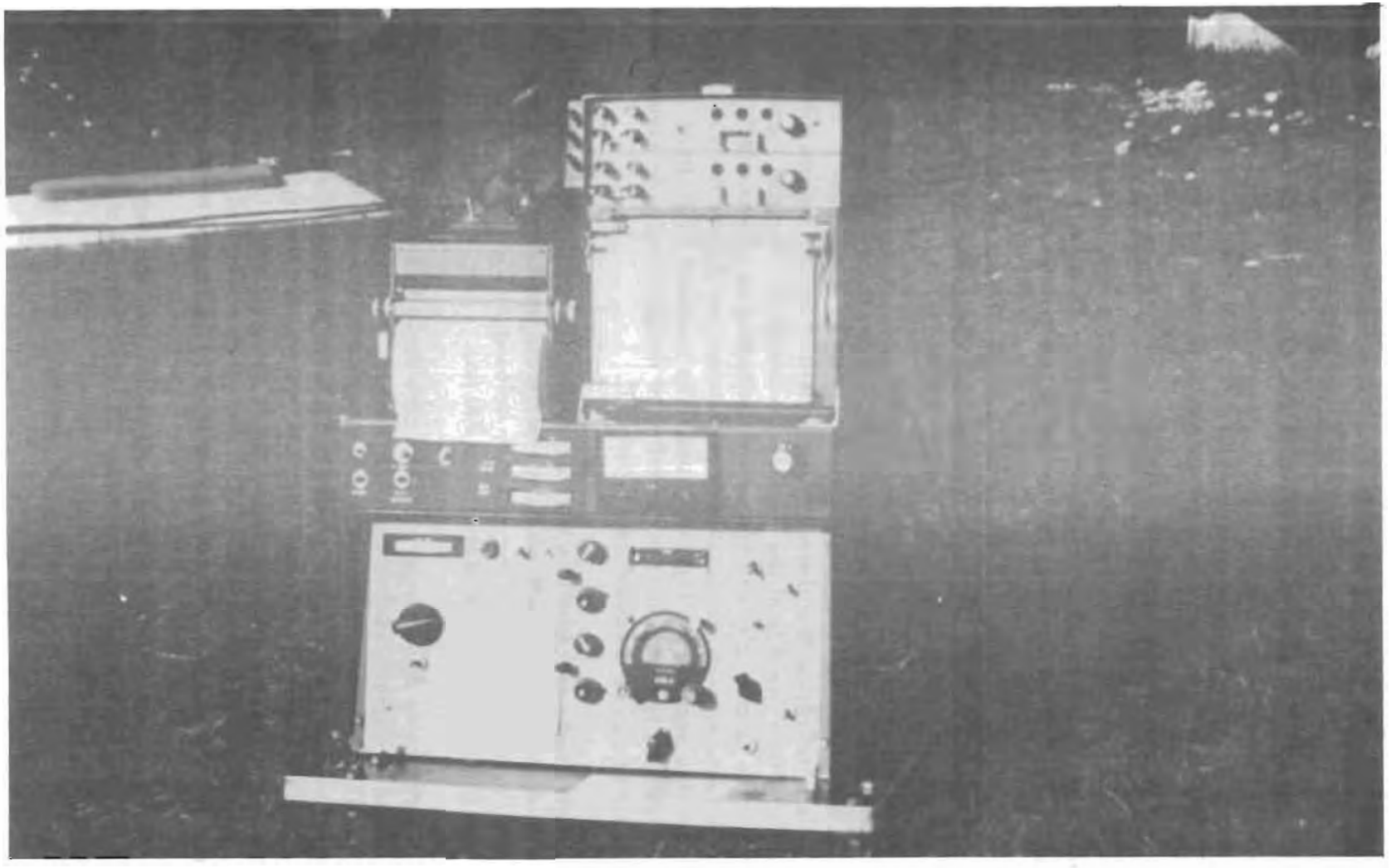

Figure 9. Mini-lab Package Which is Installed in the Beechcraft Model 35 Aircraft. It provided for three channels of analog recording with selection of localizer, marker beacon, and glide slope plus theodolite, and differential amplifier outputs.

Several examples of these types of flight measurements are included in Figures 10 through 19. From Figures 10 and 11, the width value of the path was found to be 0.69 degree between the 75 μa points and was essentially constant from run to run. The symmetry was typically 1.16:1 with the larger segment below. The low approaches were in general quite repeatable. As shown in Figures 12 and 13, the path begins 0.1 degree below the nominal value and then between points A and B makes a smooth transition to 0.08 degree above the nominal value. From point B to the threshold, one and one-half periods of CDI oscillation occur with a peak-to-peak amplitude of 40 μa.

At the threshold, the CDI indication is a fly-up signal. Past the threshold the signal oscillation continues; however, due to the rapidly increasing spatial frequency the pilot does not receive a fly-up or fly-down command, rather he receives a near zero indication due to the CDI's inability to follow the rapid oscillations.

Flights made on the centerline above and below the nominal path angle gave much the same command information indicating that the vertical path structure is reasonably constant.

Perpendicular path structures measured between the ± 2.4 degree localizer course limits as set for an 8300 foot runway are shown in Figures 14 through 19. From these there is clear indication that there are undulations in the glide-slope surfaces longitudinally extending from one side of the localizer to the other. Because the path structure was established to be at an angle with the runway centerline of approximately 5 degrees so as to give the best coverage, these undulations become manifest as the 40 μa peak-to-peak oscillations that occur in the flyability runs. The approach flight track is drawn across the undulations when tracking the centerline of the localizer. An idea of the three-dimensional structure can be obtained from Figure 20.

Width checks on centerline were exceptionally good. However, at 15 degrees to the south the maximum below-path clearance available was 120 μa. To the north side, at 5 degrees off localizer centerline the maximum below-path clearance was 92 μa, at 4 degrees it was 150 μa, and at 3 degrees it was 200 μa.

A satisfactory course sector could be considered to exist only between 4 degrees North and 13 degrees South at the outer marker, whereas the coverage is adequate only to the localizer limits at ILS point C (approximately 1000 feet out from the threshold). Greater azimuth coverage was clearly needed and the Watts Company responded by furnishing another orientation of the antennas. The plan was to place the antennas closer to the runway thus requiring less effective transverse cut of the glide-slope azimuth structure with the runway centerline. Initial measurements of the system performance over a period of time indicated that the system was stable, for at least 25 degrees of temperature change.

On December 3, 1973, a second data collection was begun at the Tamiami test site with the Watts array in a new position. The main purpose of this task was to determine the performance with a new position, denoted Position 5, by the Watts Company. Table 2 lists explicitly the location of two antenna positions. As with the initial

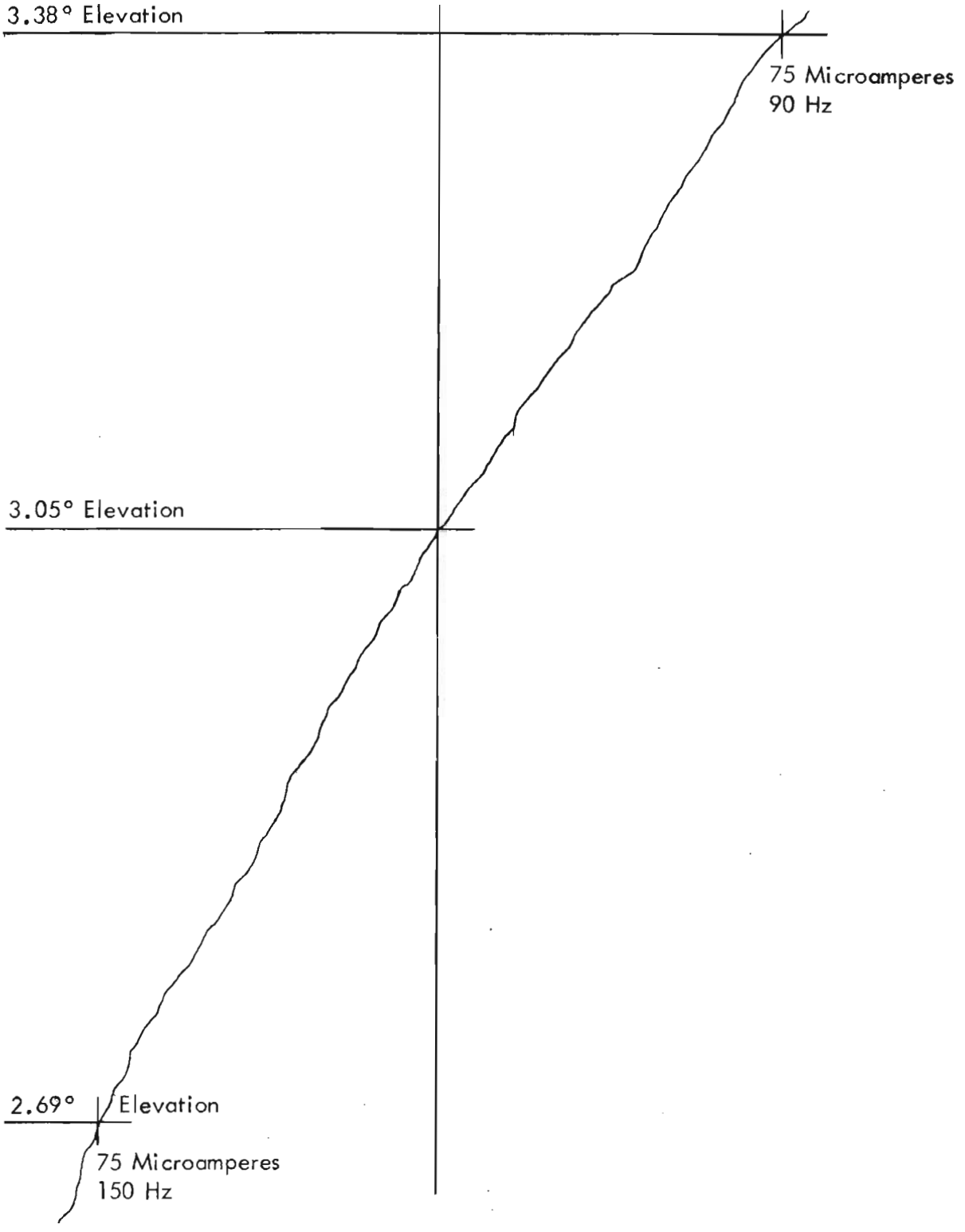

Figure 10. Level Pass Made on Centerline Inbound at 1500 Feet. Width between 75 microampere points is 0.69 degree and the path angle is 3.05 degrees. For this flight and all others in this series, H. F. Hooghkirk was the theodolite tracker, A. S. Swearingen was the airborne panel operator, and R. H. McFarland was the pilot. Run 13-7, November 13, 1973.

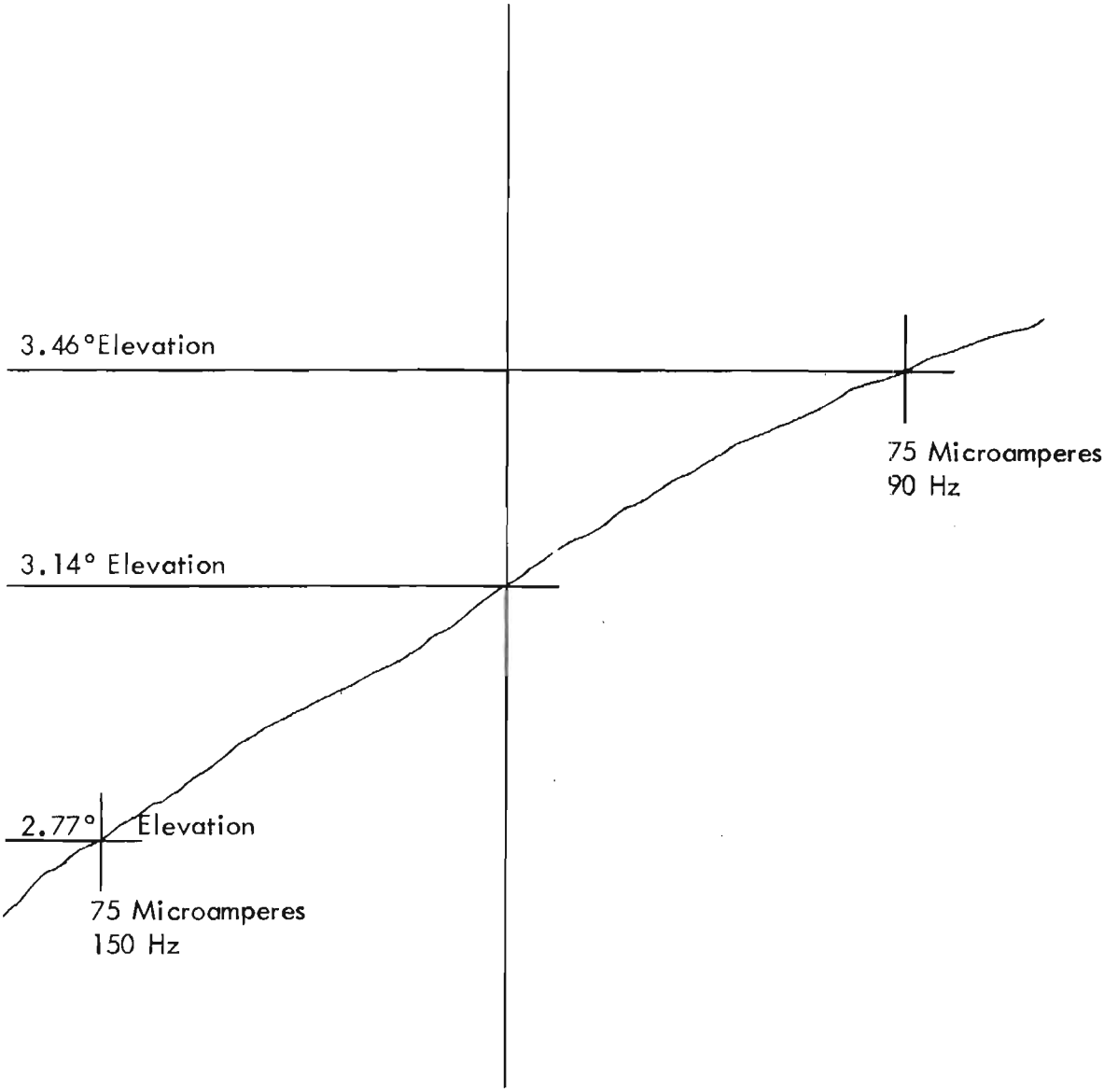

Figure 11. Level Pass Made on Centerline Inbound at 1000 Feet. Width between 75 microampere points is 0.69 degree and the path angle is 3.14 degrees. Run 13-4, November 13, 1973.

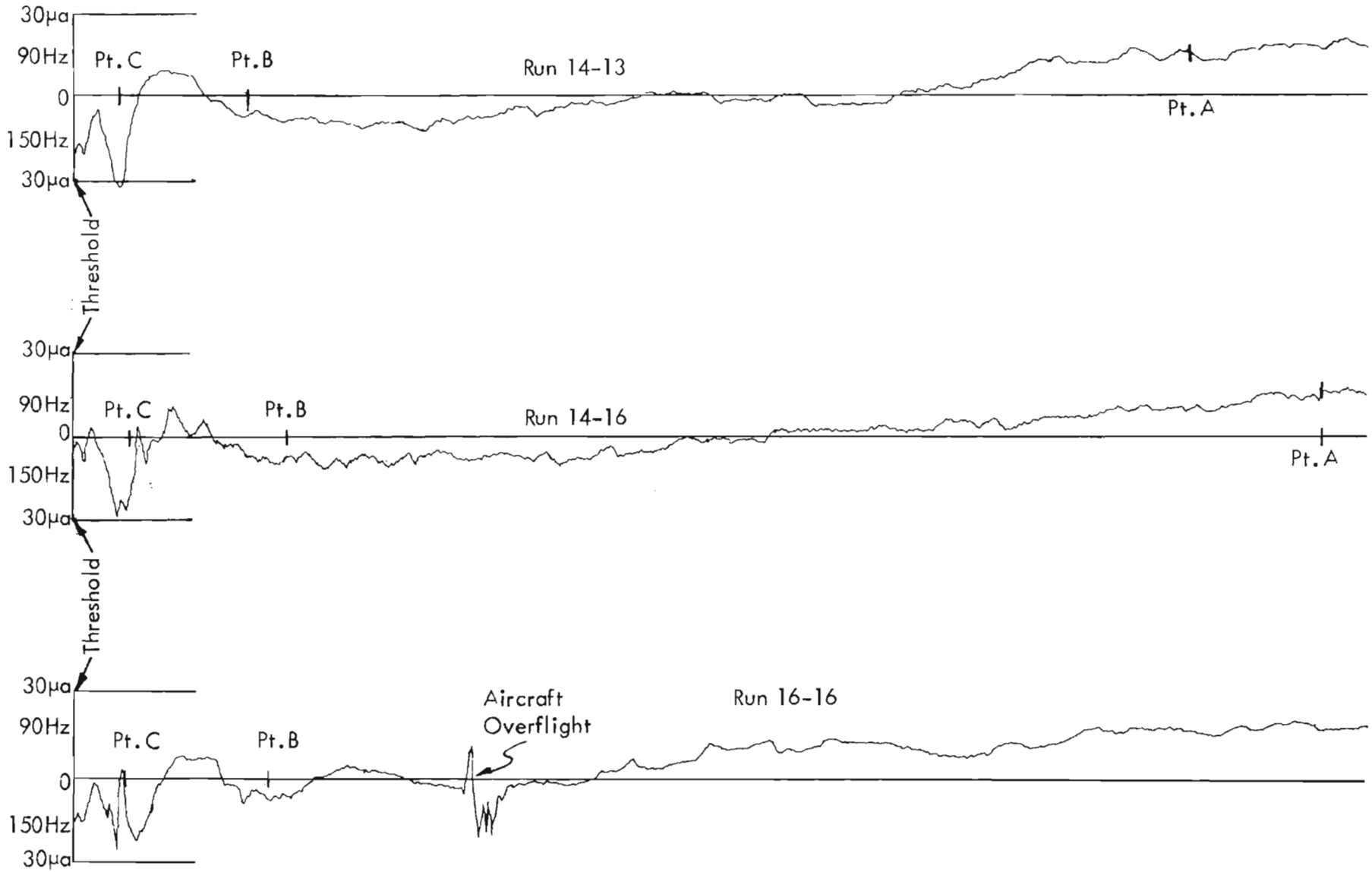

Figure 12. Low Approaches on Centerline Beginning Near Point A and Extending to the Threshold. Runs 14-13, 14-14, 16-16.

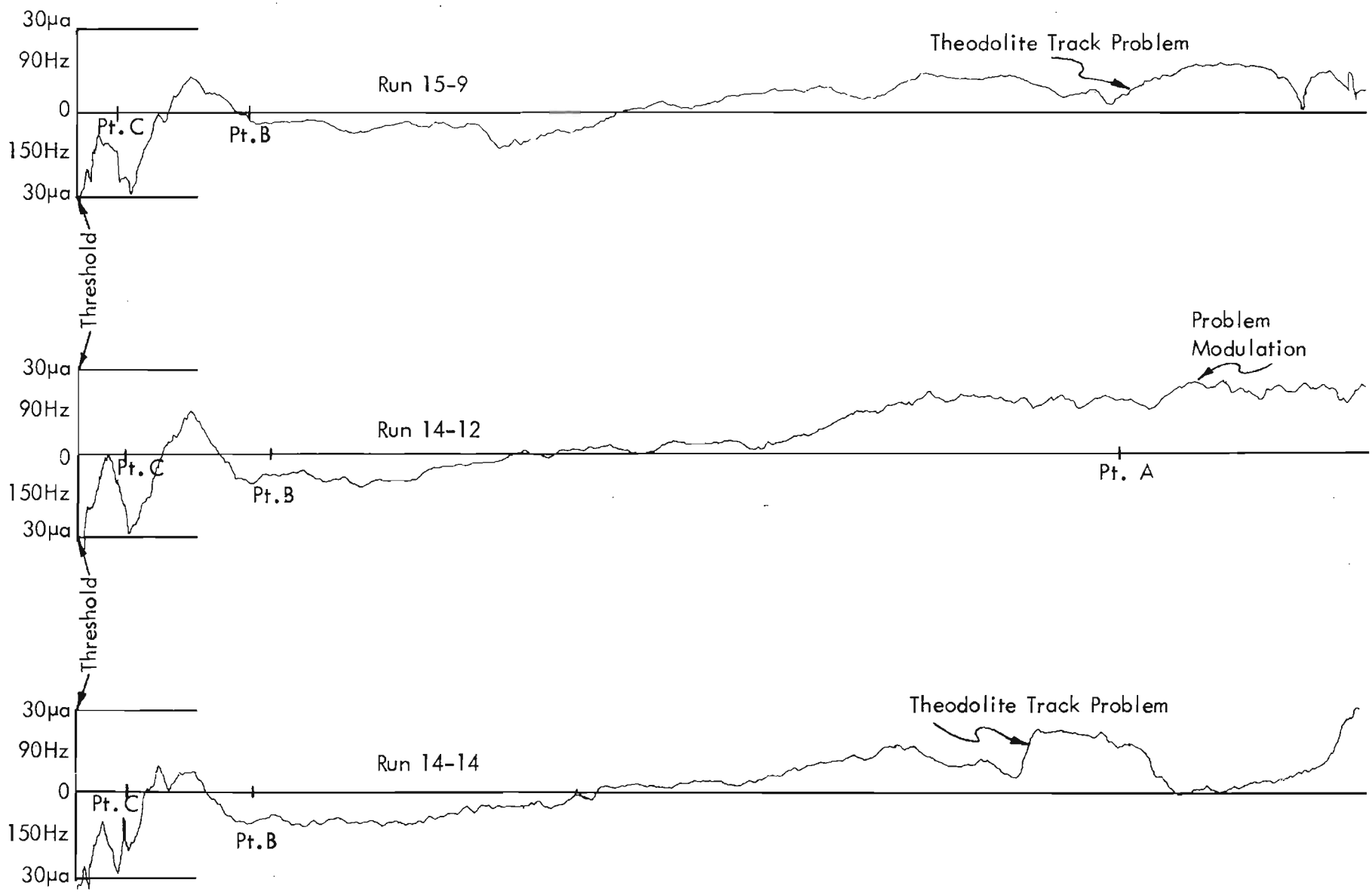

Figure 13. Low Approaches on Centerline Beginning Near Point A and Extending to the Threshold, Runs 15-9, 14-12, 14-14.

For Figures 14 through 19 recordings are of microamperes of CDI current for a fixed angle in space; hence, with 90 Hz plotted to the top of the graph, a rise in the curve indicates a depression of the path or zero DDM line. Although contradictory to intuitive reference, these curves are consistent with sensing used in FAA recordings. In other words, a rise in the curves will indicate a depression in the path in space.

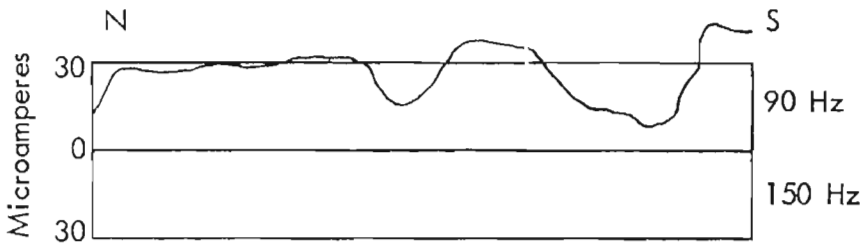

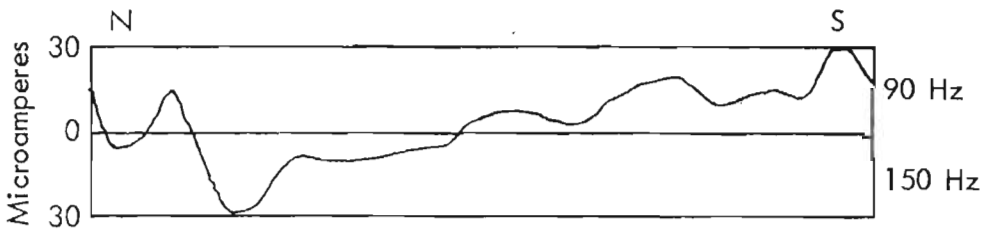

Figure 14. Recordings of CDI Made on Opposite Direction Flights Perpendicular to Localizer at 2000 Foot Range, Altitude 130 Feet. Runs 16-9, 16-10, November 16, 1973.

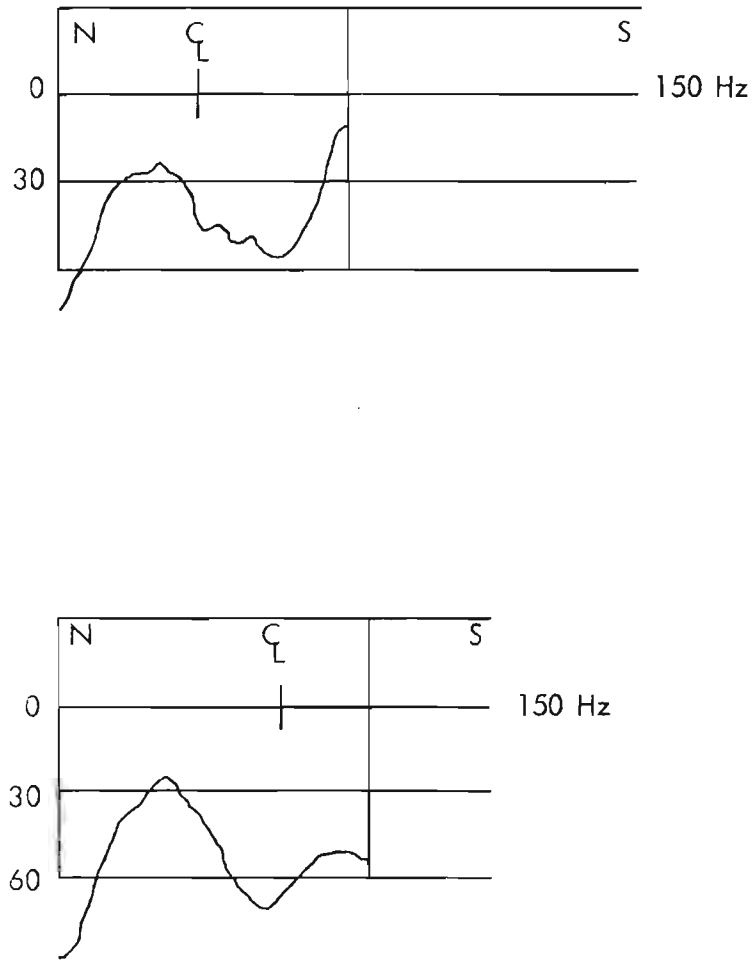

Figure 15. Recordings of CDI Made on Opposite Direction Flights Perpendicular to Localizer at 13,000 Foot Range, Elevation 650 Feet. Runs 16-7, 16-8, November 13, 1973.

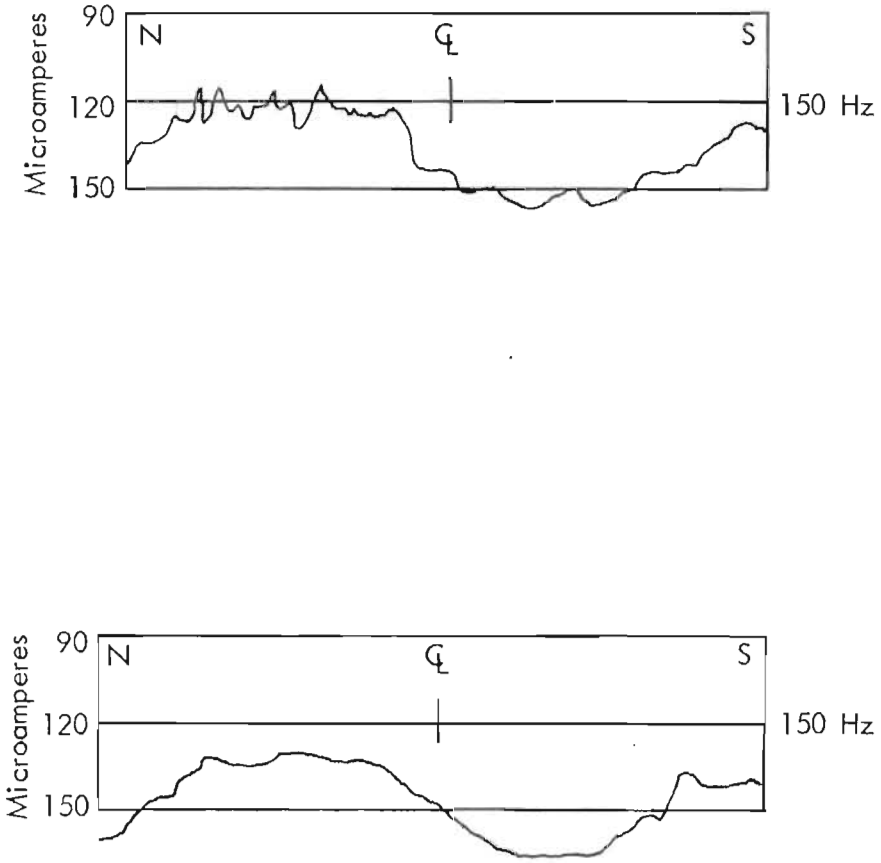

Figure 16. Recordings of CDI Made on Opposite Direction Flights Perpendicular to Localizer at 30,000 Foot Range, Elevation 1000 Feet. Runs 16-11, 16-12, November 16, 1973.

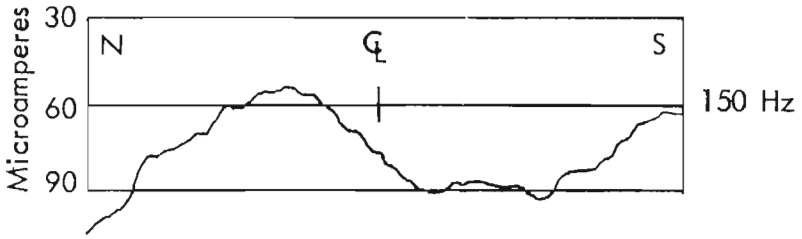

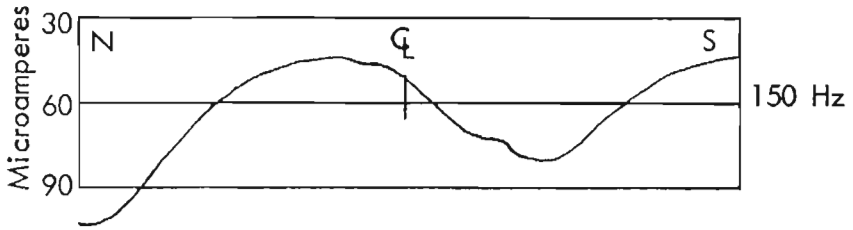

Figure 17. Recordings of CDI Made on Opposite Direction Flights Perpendicular to Localizer at 30,000 Foot Range, Elevation 1300 Feet. Runs 16-13, 16-14, November 16, 1973.

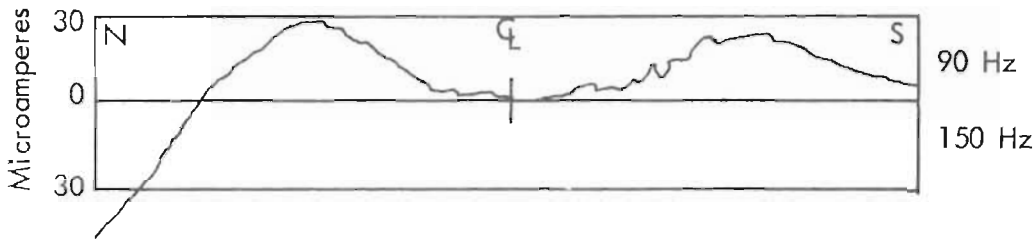

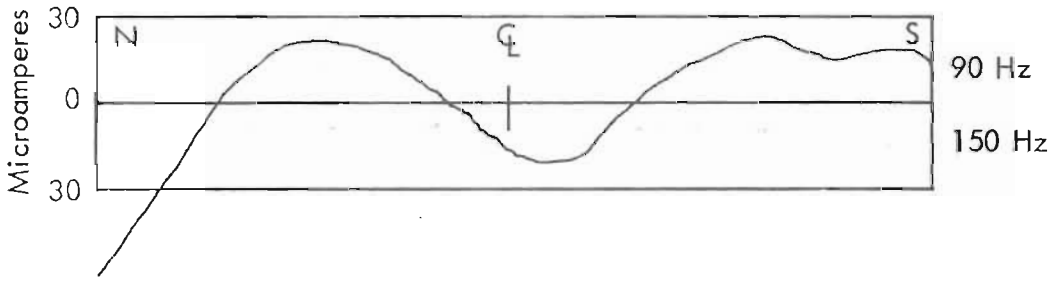

Figure 18. Recordings of CDI Made on Opposite Direction Flights Perpendicular to Localizer at 30,000 Foot Range, Elevation 1600 Feet. Runs 16-15, 16-16, November 16, 1973.

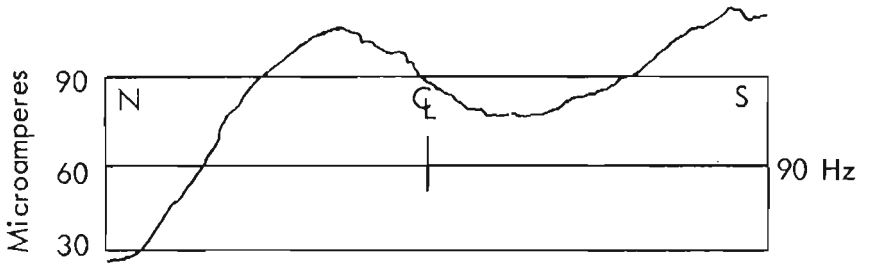

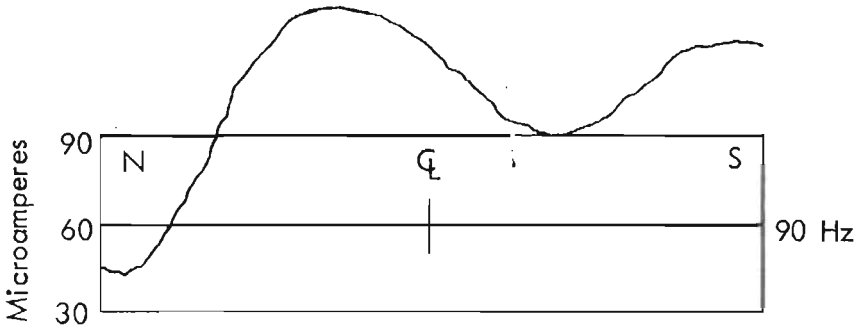

Figure 19. Recordings of CDI Made on Opposite Direction Flights Perpendicular to Localizer at 30,000 Foot Range, Elevation 1900 Feet. Runs 16-17, 16-18, November 16, 1973.

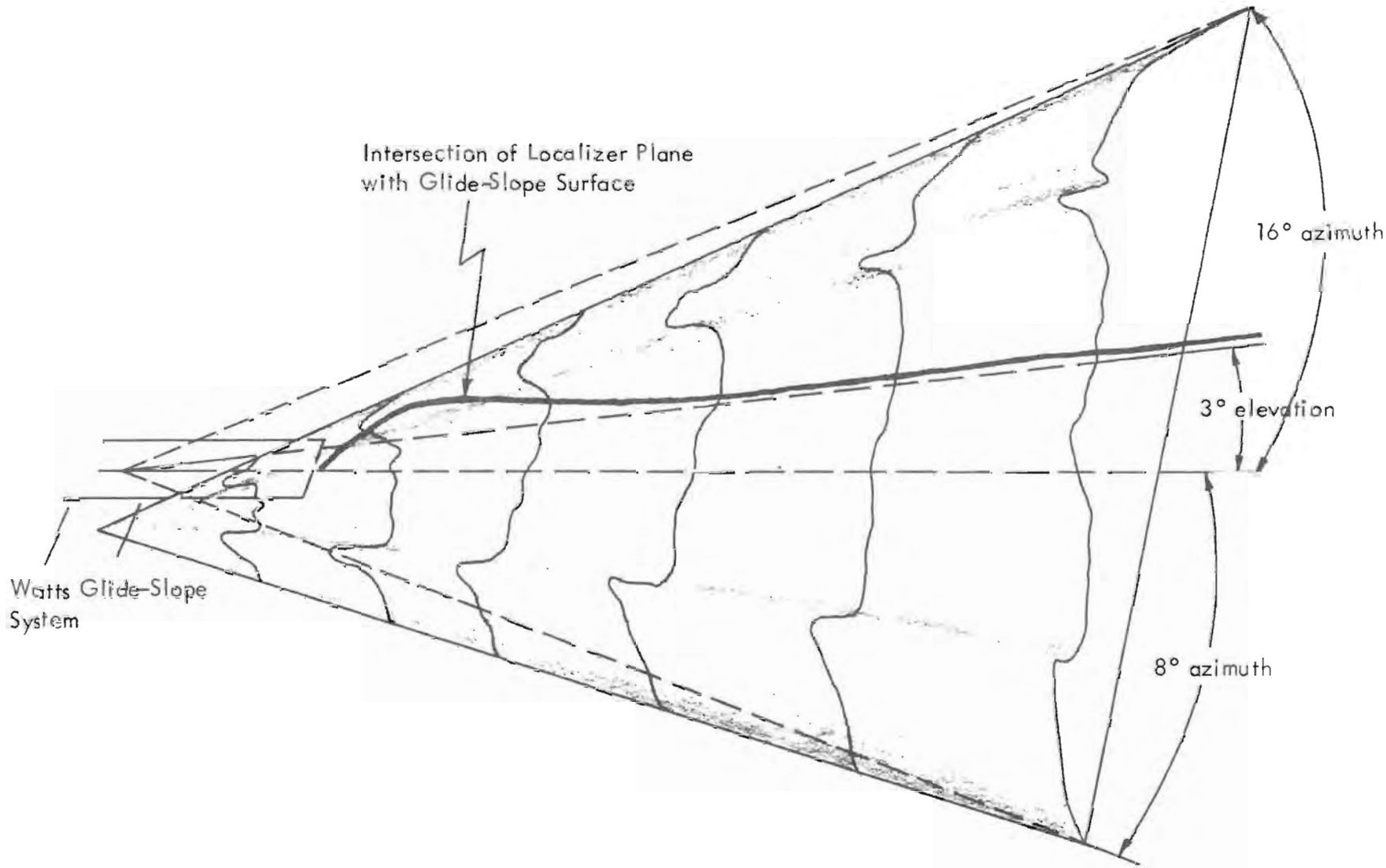

Figure 20. Diagram to Show the Conical Structure of the Watts Array.

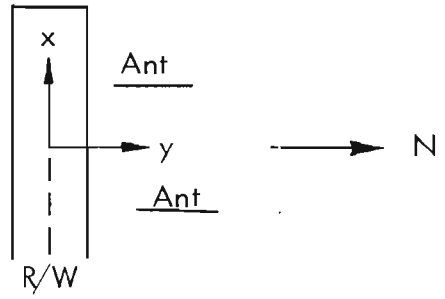

Position 1 Path Characteristics Measured in November, 1973 and During First Part of Period in December, 1973.

Rear Antenna	Gap 1	x = 297.8;	y = 162.9
	Gap 99	x = 297.8;	y = 293.0
Front Antenna	Gap 81	x = 300.0;	y = 106.7
	1	x = 300.0;	y = 234.0

Position 5 Path Characteristics Measured in December, 1973.

Rear Antenna	Gap 1	x = 279.8;	y = 123.9
	Slot 99	x = 286.6;	y = 253.8
Front Antenna	Slot 81	x = 279.8;	y = 85.4
	Slot 1	x = 279.8;	y = 212.7

Table 2. Listing of Gap Locations for Positions 1 and 5 for Watts Array. All dimensions are given in feet.

positioning, both ground-based and flight data were obtained for Position 5. Figures 21 through 23 show perpendicular cuts to the runway centerline taken for Position 5 at distances of 1.0, 2.1, and 5.4 miles, respectively, from the antenna array. Figure 24 shows the results of ground-based measurements of azimuth glide-slope coverage. Clearly evident from these figures is the increased coverage as compared to data from Position 1, but at the same time there occurs a steep upward slope of the zero DDM line in space as one proceeds from the antenna side of the runway to the opposite side.

Figure 25 shows the results of an on-path approach with the steeply-sloped azimuth coverage. All data presented is representative of the repeatable results obtained. It is noted that this glide-path condition did not meet Category II tolerances and further work (explained below) was undertaken to correct this.

An experiment was also performed in which the rear antenna was lowered to approximately 24 inches above the ground. Sideband power was increased to compensate for the reduced clearance that resulted beyond the outer marker. Improvement was noted with 160 μa being obtained; however, limited time prevented a complete adjustment to obtain the desired 180 μa. Another significant result of lowering the antennas was to reduce the available signal strength in the far field by more than 6 dB. Other than path softening and reduced signal strength, lowering the height of the antennas had no effect on the system performance.

Further work was undertaken in January and February, 1974, to help correct the objectionably steep transverse slope to the zero DDM surface as occurred at Position 5. In order to cure the problem, the Watts Prototype Company suggested that the rear antenna of the array should be moved laterally with respect to the runway. Accordingly, measurements were made for a number of antenna lateral positions. Results of this revealed that the transverse slope of the zero DDM line could be reduced, but only at the expense of path roughness. Reduction of the transverse slope caused a depression in the path just inside point B. This gives the pilot a fly-down signal just prior to point C with a reversal occurring approximately 1000 feet later, thus giving the path a strong fly-up or flare condition.

By careful adjustment, it was possible to produce a path which would stay within Category II limits and give a flare in the path approaching the runway. Depressions of 20 μa were considered acceptable with a flare of 50-70 μa at the threshold. This yields a path that can be flown within ± 10 μa on the CDI. Based on all considerations involving azimuth coverage, path structure in azimuth, path straightness, flyability, and Category II limits, an antenna position was determined that was considered to be optimum. Figure 26 shows a typical path shape for this position.

Special experiments were also performed on the advice of the Watts Prototype Company that involved lowering a section of the antennas. Displacement of a 10-foot section of the front antenna by only 3 inches produced very noticeable changes in path shape. Because of these observations, it is clear that a tolerance of better than one inch must be held in the horizontal on antenna positioning in the horizontal plane.

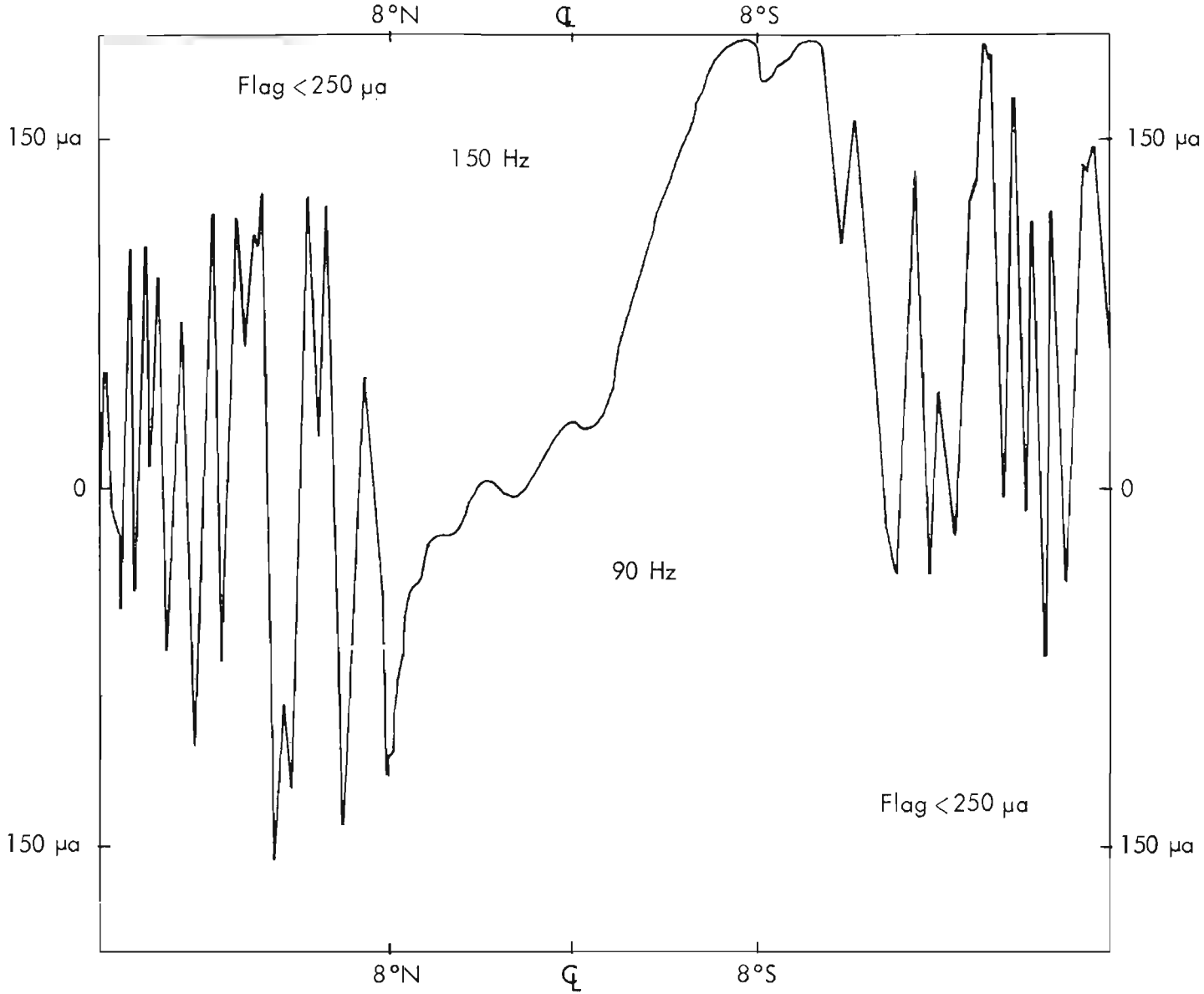

Figure 21. Position 5, Perpendicular Cut North to South, Range 1 Mile, Altitude 300 Feet, December 20, 1973, Run No. 30. (Note that for Figures 21, 22, and 23 the 90 and 150 Hz sides of the charts have been exchanged to give an intuitive feel for a rise in the glide-slope surface; in other words, up in space is represented by up on the chart.)

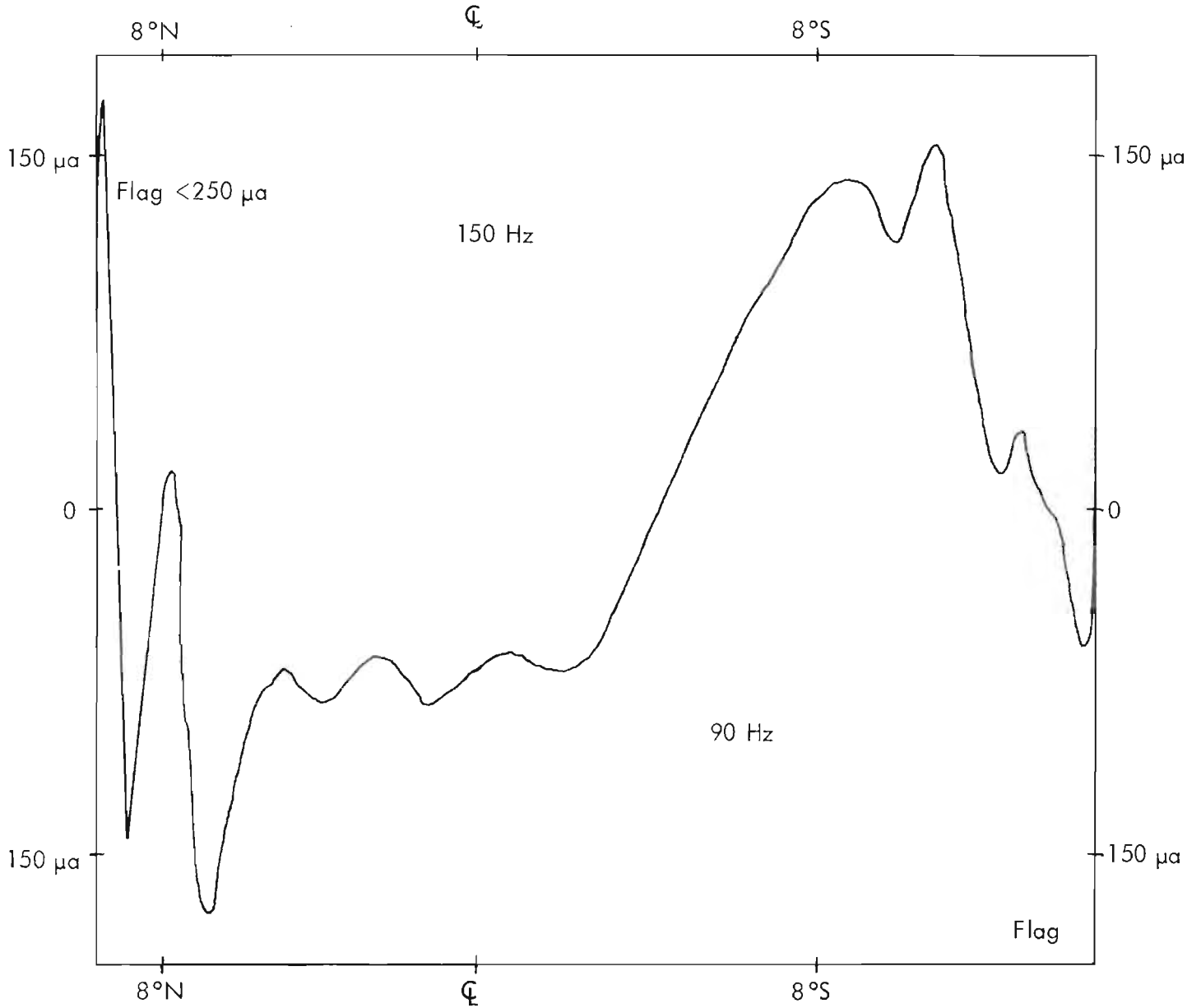

Figure 22. Position 5, Perpendicular Cut North to South, Range 2.1 Miles, Altitude 700 Feet, December 20, 1973, Run No. 28.

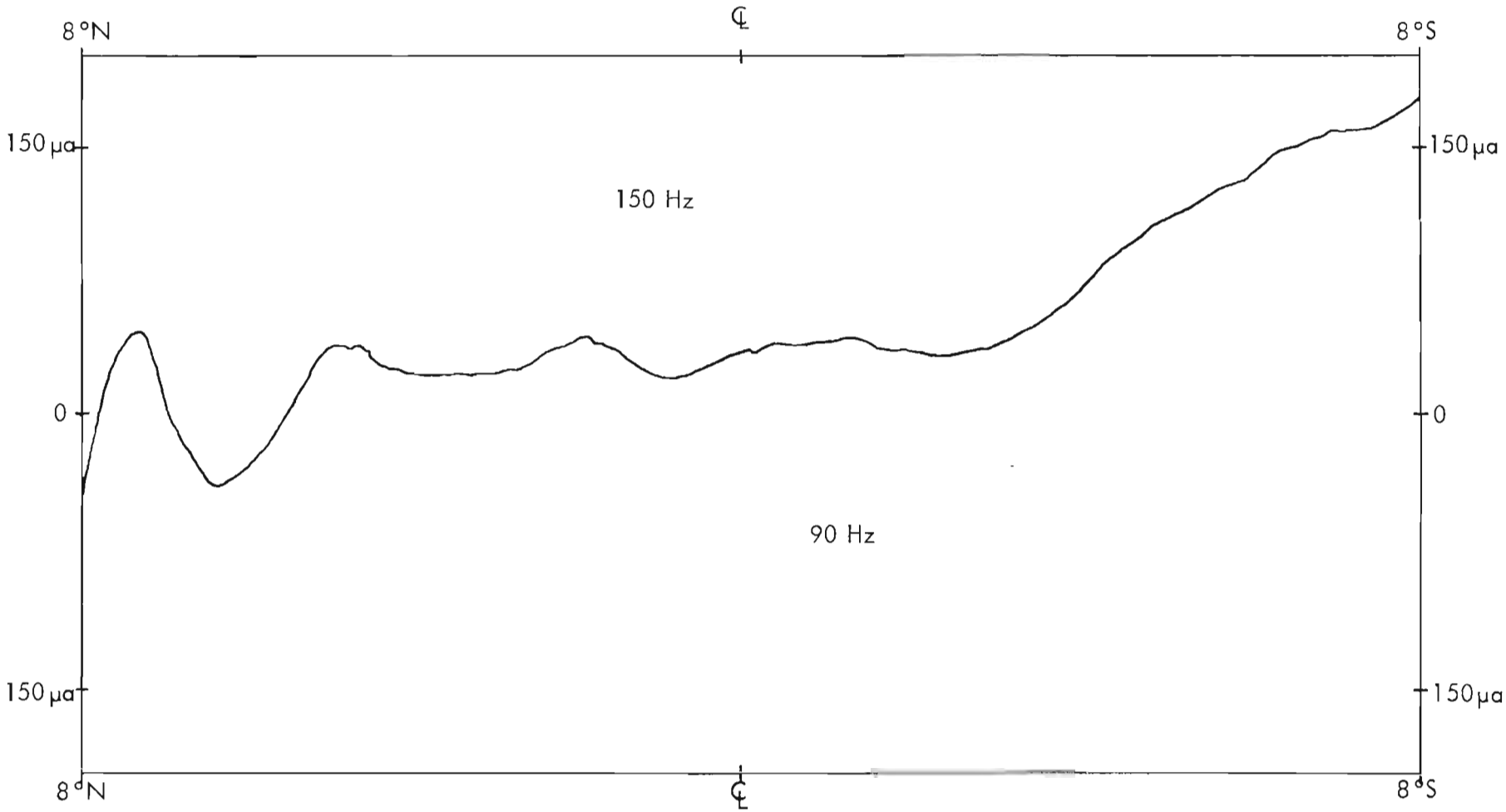

Figure 23. Position 5, Perpendicular Cut North to South, Range 5.4 Miles, Altitude 1600 Feet, December 20, 1973, Run No. 21.

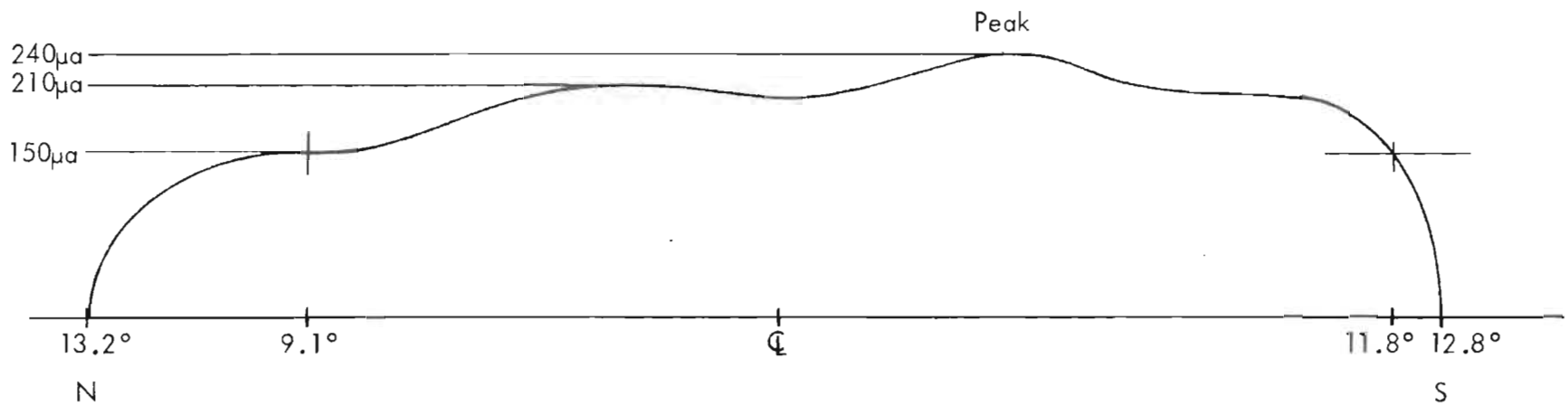

Figure 24. Plot of CDI Current Made with Ground-Based Vehicle Moving Perpendicular to Runway Centerline, 2000 Feet in Front of Antenna Reference. Probe Height = 7 Feet.

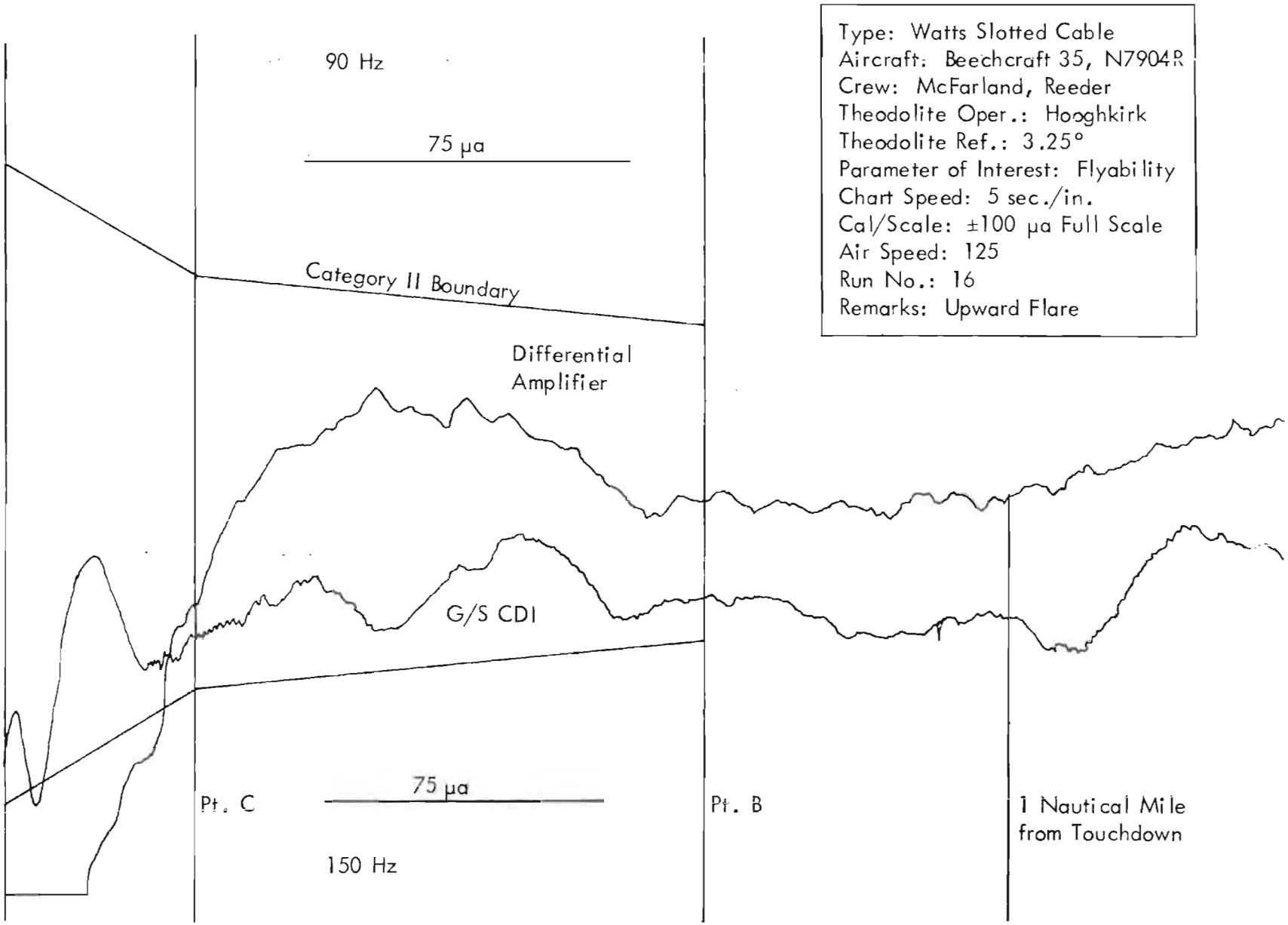

Figure 25. On-Path Approach, Tamiami Airport, December 20, 1973.

Type: Watts Glide Slope Aircraft: Beechcraft 35, N7904R Crew: McFarland, Swearingen Theodolite Oper.: Hooghkirk Theodolite Ref.: 3.0°	Parameter of Interest: Flyability Chart Speed: 5 sec./In. Cal/Scale: ± 100 μa Full Scale Air Speed: 130 Run No.: 24

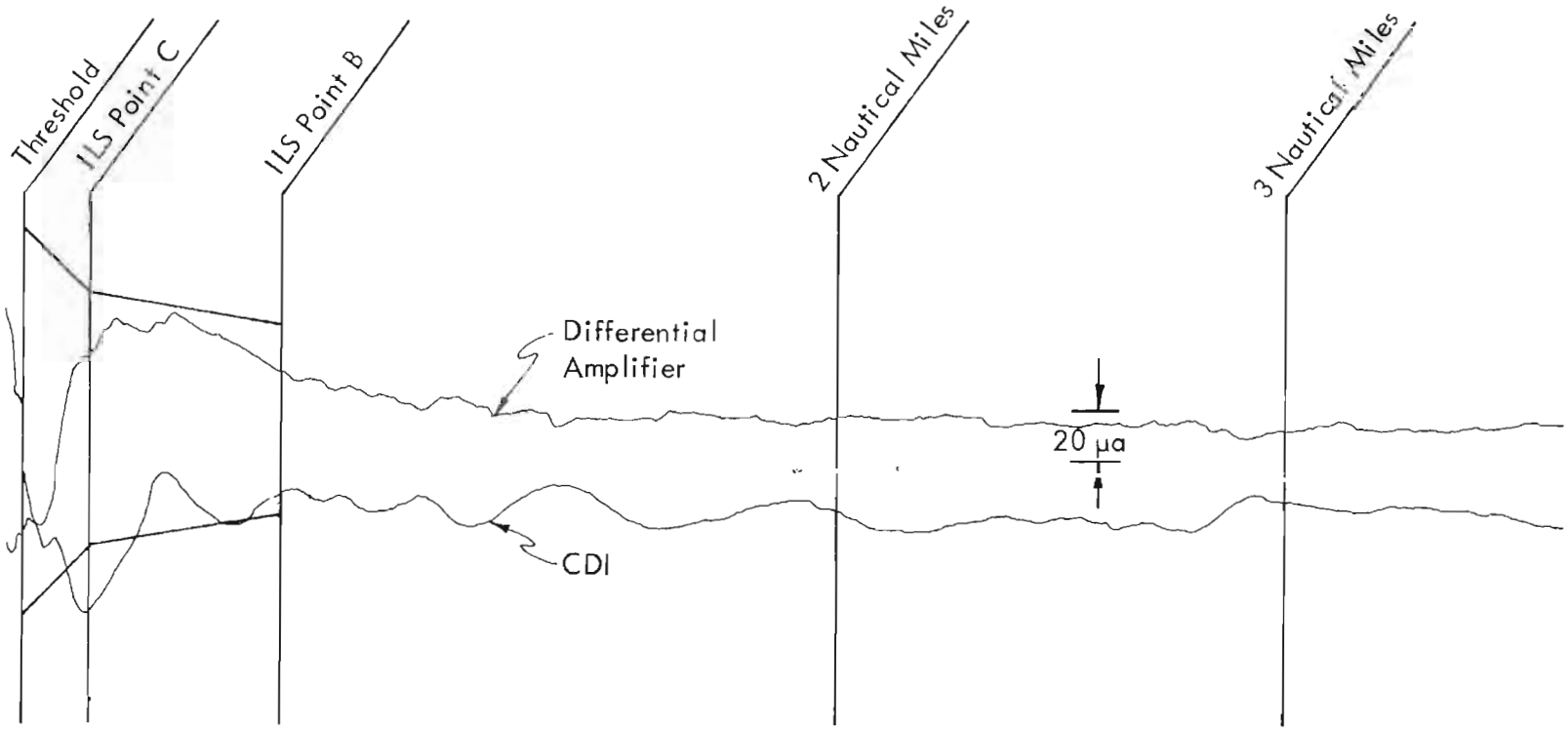

Figure 26. Typical Recording of Differential Amplifier and Course Deviation Indicator Values During Low Approach, Tamiami Airport, February 18, 1974, Antenna 5.

In general the path flew well in spite of the narrow azimuth width and undulations in the three-dimensional structure. Fortunately, signal strength drops off rapidly in azimuth so that flag is generally evident when outside the correct portion of the path. A turn-in for an approach at the intercept altitude beyond the outer marker allows the pilot to see fly-up command on the CDI once the flag has lifted. This would not be necessarily true if a close turn-in were made because increased signal strength on the fringe areas would allow the flag to lift while the CDI was oscillating between fly-up and fly-down commands. This would serve to distract the pilot, perhaps causing loss of confidence, but would not be dangerous since the information could not be flown due to the high frequency of the needle movement.

B. Staunton Tests. The second and final phase of the Watts glide-slope evaluation program involved installation of the Watts array at Shenandoah Valley Airport, Staunton (Weyers Cave), Virginia in March and April, 1974. This series of tests was undertaken (1) to evaluate the Watts system operational characteristics at a problem site where an image-type system had failed, (2) to assess the effects of an upslope on the Watts array, (3) to observe operation at another frequency in the glide-slope band, viz., 332.6 MHz, and (4) to provide FAA Flight Inspection the opportunity to compare the Watts array directly with a sideband reference system.

The site for Runway 6 at the Shenandoah Valley Airport, shown in Figure 27, is a typical capture-effect type site, with the terrain dropping off at the end of the runway and then rising to an elevation of 0.3 degree above the site just before the middle marker. See Figures 28 and 29. It was expected that this type of terrain would markedly affect the course structure; however, the goal was to realize a usable glide slope that would meet Category I requirements.

Setup of the array was a duplicate of Position 5 as used at Tamiami. The only change in the setup was to decrease the space between the front and rear antennas to 556 feet as opposed to 600 feet as used at Tamiami. See Figure 30. This was done to compensate for the change in transmitter frequency that was necessary at the Shenandoah site.

Two different sideband reference systems with antenna ratios of 2.5:1 and 3.5:1 were established for comparison to the Watts slotted-cable glide slope.

Figure 31 shows the results obtained from flight tests with the antenna array at Position 5. From this, it is obvious that there was an excessive flare in the path as the threshold was approached. Successive lateral movements of the rear antenna from 0 to 48 inches improved this condition but not sufficiently to produce an acceptable path. Figure 32 shows the typical flare characteristics experienced during the tests made with the antenna at Position 5.

Because of this, and at the suggestion of Watts Prototype Company personnel, the antenna array was moved to a new location denoted Position 6. The layout of this position is given in Figure 33. Again, several lateral movements of the rear antenna were

Figure 27. Aerial View of Glide-Slope Site at Shenandoah Valley Airport, Staunton, Virginia, March, 1974.

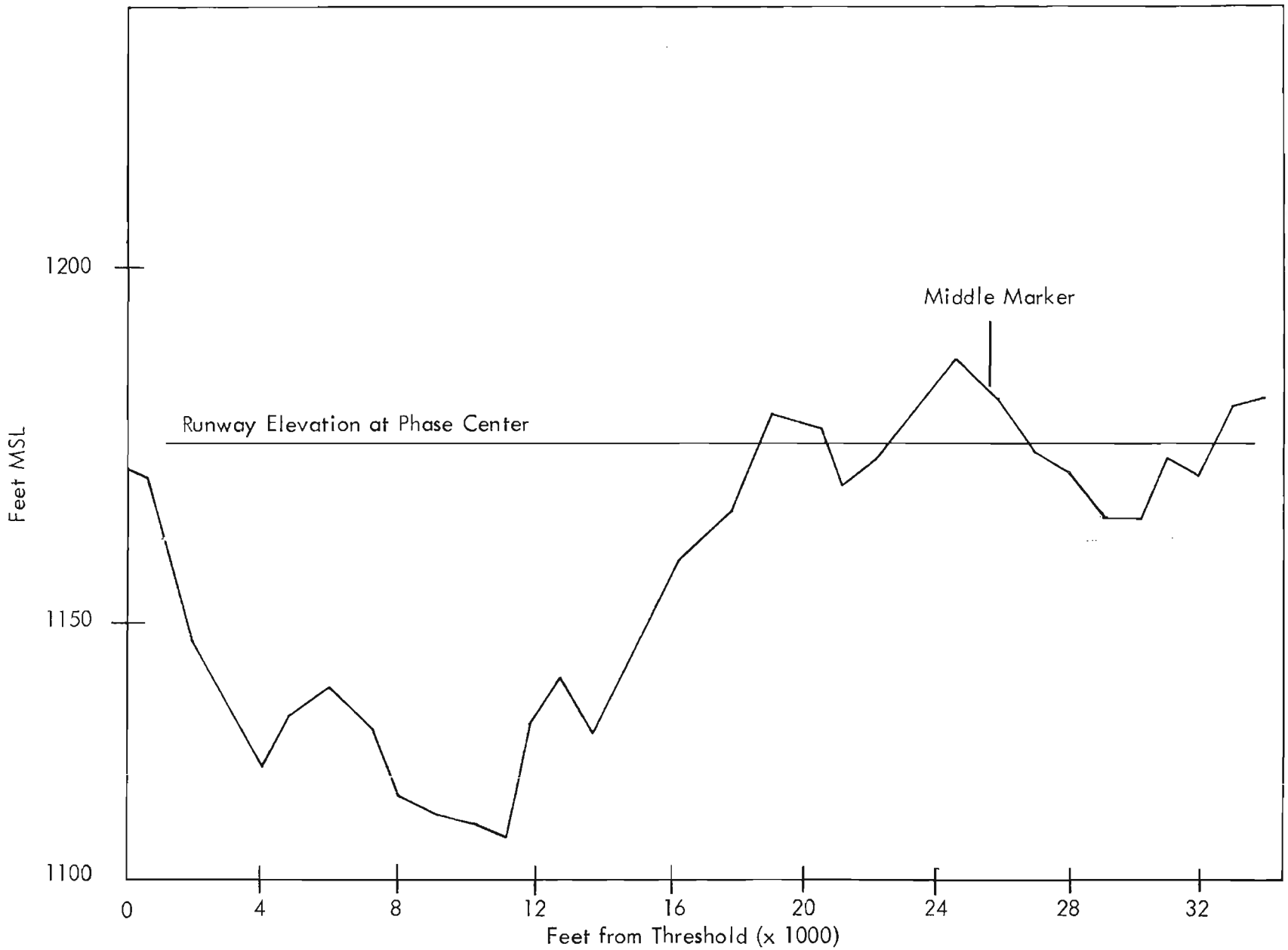

Figure 28. Extended Centerline Profile Runway 4 - Shenandoah Valley Airport.

Figure 29. View of the Upslope Area Looking Out Into the Approach Region for Runway 6 at the Shenandoah Valley Airport, Staunton, Virginia. The smooth hill is believed responsible for the major path perturbation experienced in particular with the image systems tested there.

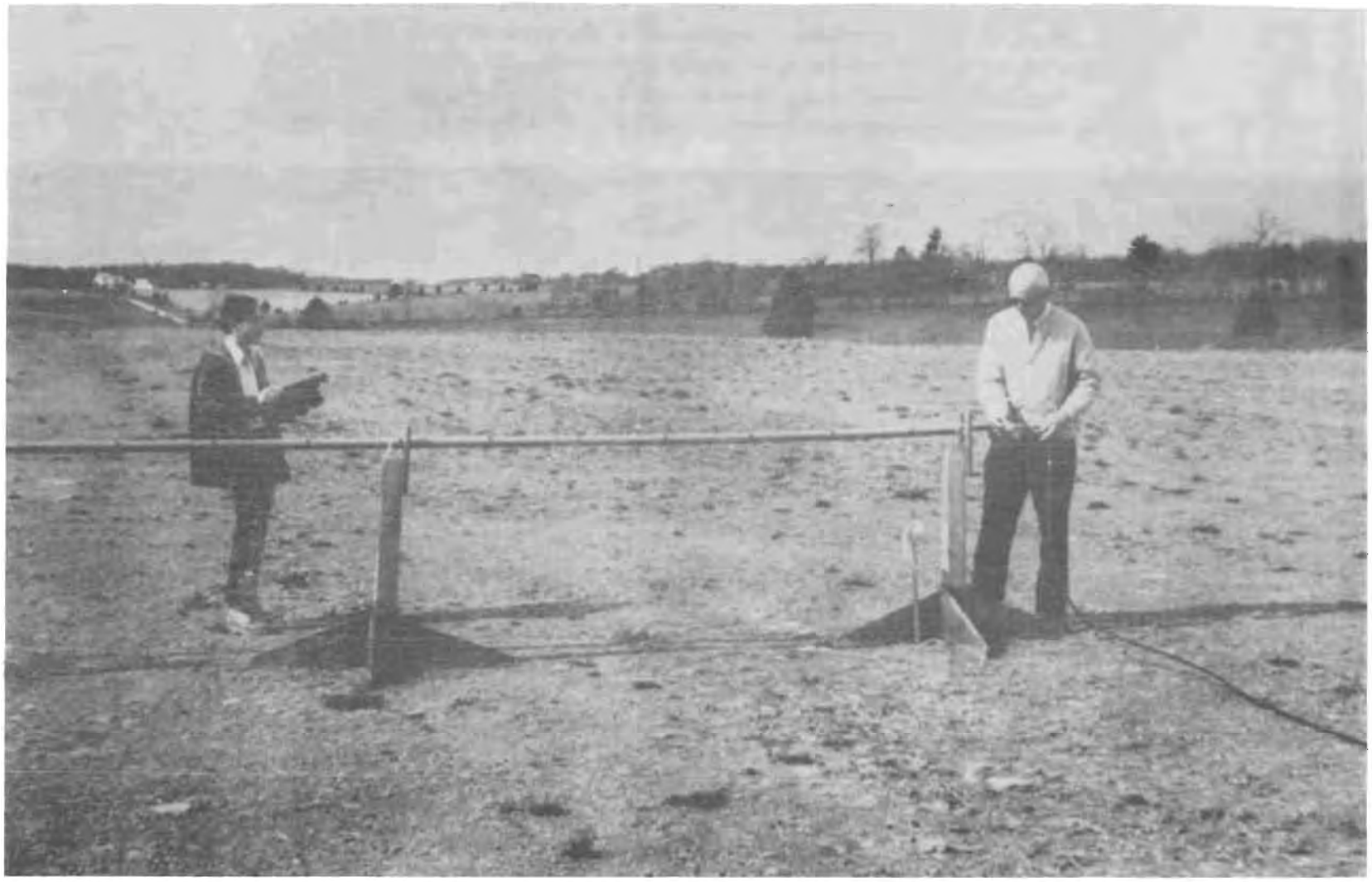

Figure 30. Mr. Ban Tran and Mr. Chester Watts in the Process of Collecting Data on the Forward Slotted-Cable Antenna Installed at the Shenandoah Valley Airport, Staunton, Virginia.

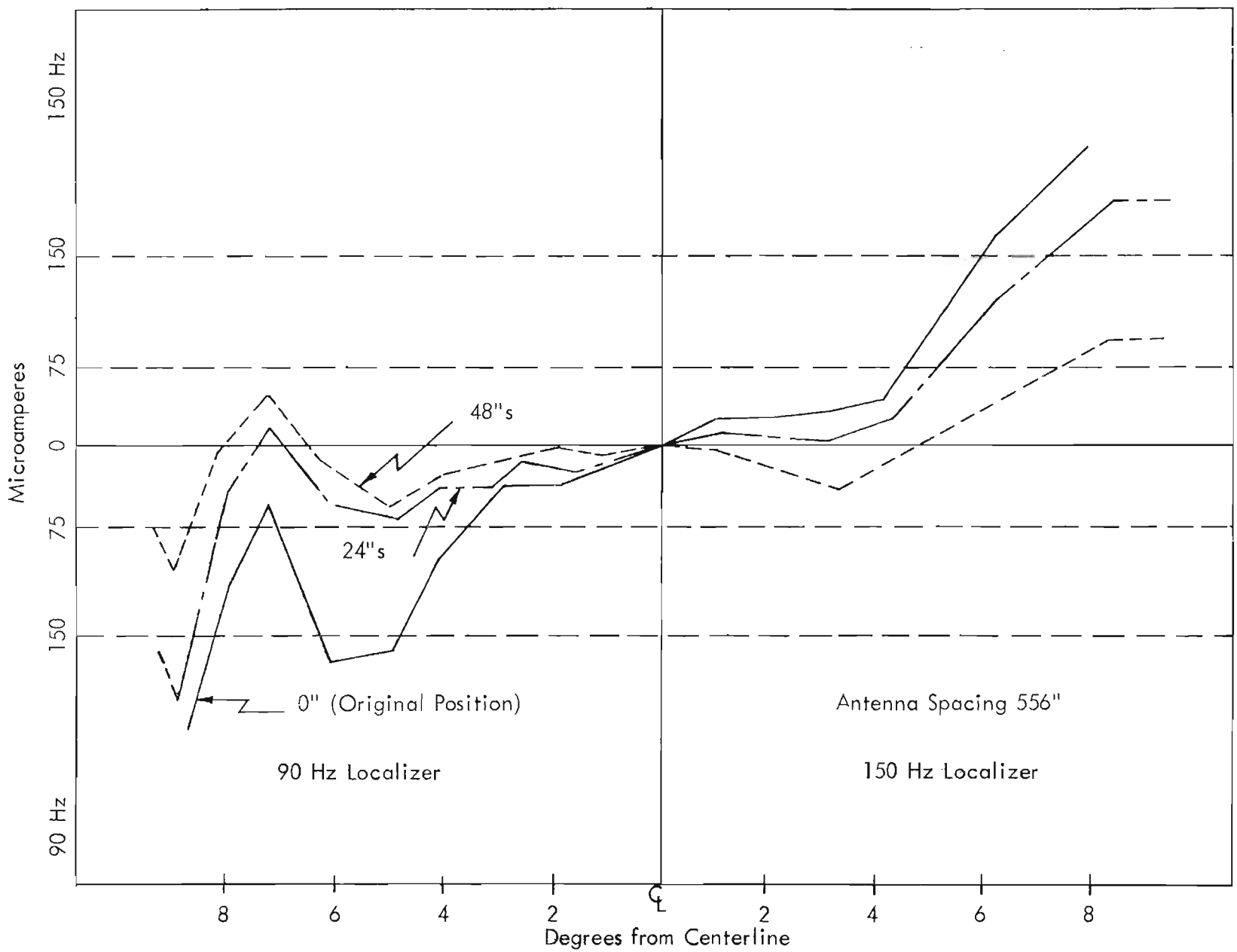

Figure 31. Watts Array - Position 5 - Effect of Lateral Offset of Rear Antenna, Perpendicular Cuts, March 25, 1974.

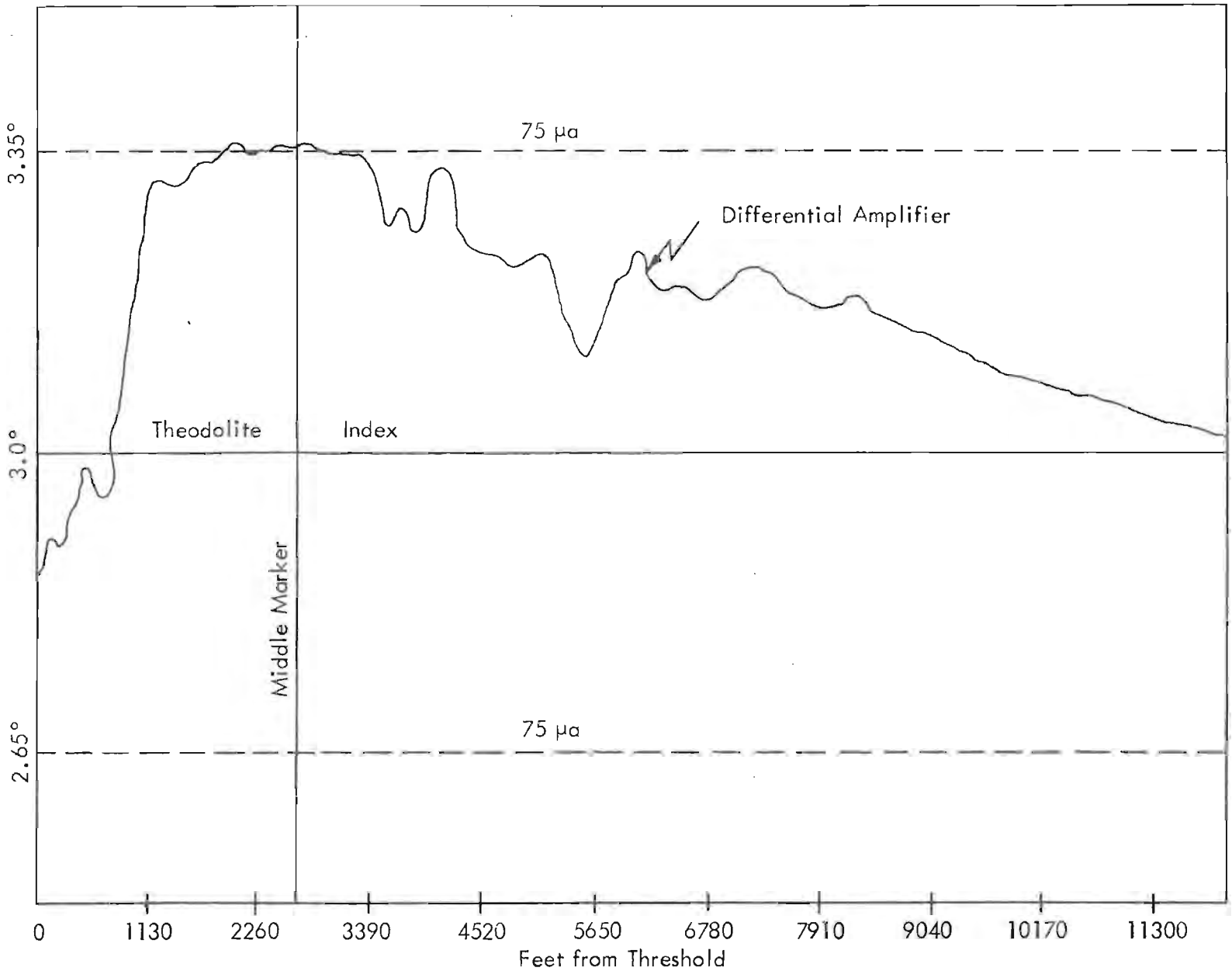

Figure 32. Watts Array - Position 5 - Approach on Path 48", Lateral Movement of Rear Antenna, March 25, 1974.

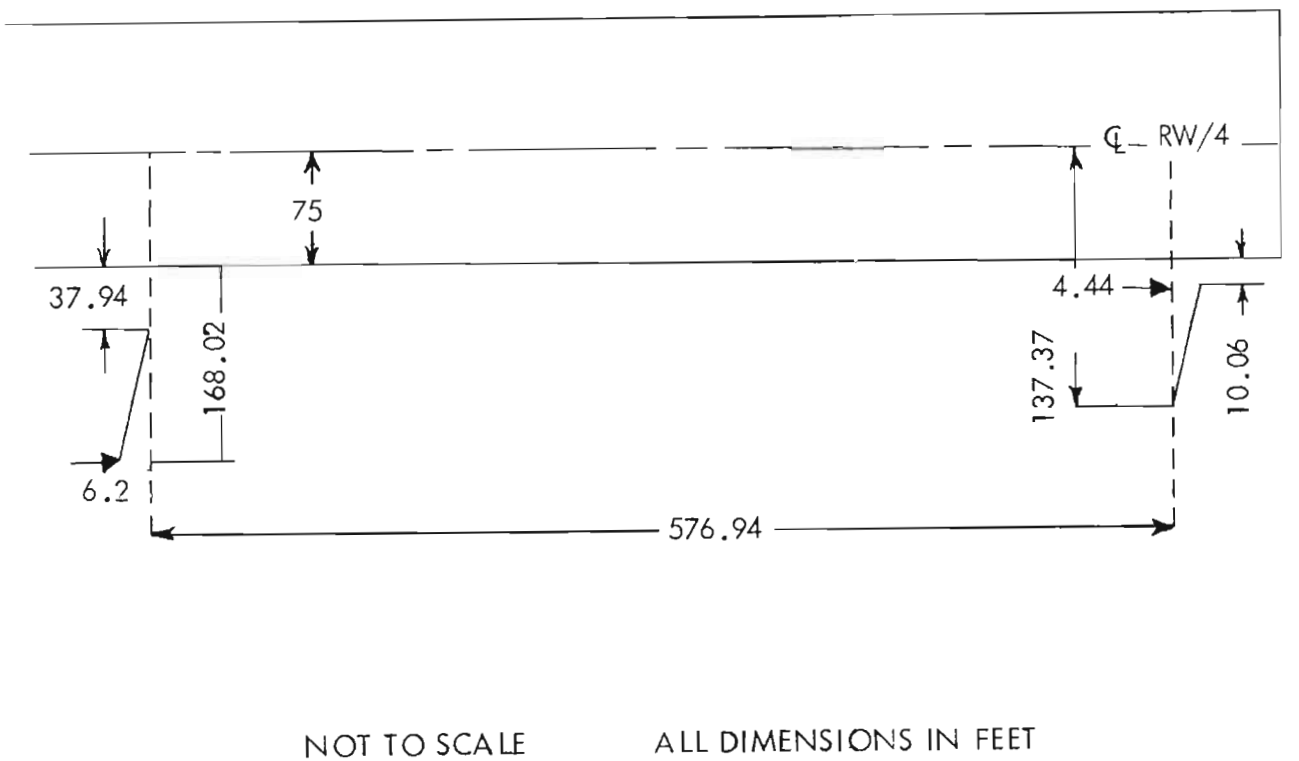

Figure 33. Watts Array Layout - Position 6 - Shenandoah Valley Airport, March 28, 1974.

necessary to optimize the flare characteristics at the threshold. Figure 34 shows the improvement obtained with these lateral movements and Figure 35 is included as a comparison to the Tamiami path structure with the antennas at Position 5. Comparison of these figures indicates that considerable improvement in the flare characteristic was obtained. The general upslope of the plot of the Shenandoah curve is probably due to the terrain which not only slopes upward forward of the antenna but also slopes on a line perpendicular to the extended runway centerline. Figure 36 compares on-path approaches for Positions 5 and 6 and demonstrates the change in the flare characteristics as can be predicted by the perpendicular cuts. Figure 37 shows a comparison of perpendicular cuts for Position 6 of the Watts array and the sideband reference system with a 3.5:1 antenna ratio. It should be noted that the same upward slope prevails.

Comparisons made against the sideband reference arrays showed a 35 percent improvement in roughness with the Watts array. The sideband reference system did not meet Category I tolerances of 30 μa at point B, and the 3.5:1 antenna ratio provided a better path structure than the 2.5:1 antenna ratio.

As an additional experiment, the Watts antenna array was lowered to a height of 15 inches above the ground to determine system performance. See Figure 38. At this height, the signal strength deteriorated to the point where the signal was unusable. Where previously with the 42-inch antenna height a signal of 200 microvolts was obtained, only 4 microvolts was obtained at the 15-inch height location. No improvement in course structure was noted.

From April 23 through April 25, 1974, the final series of tests was performed on the Watts array at the Shenandoah site. The unacceptable path symmetry that had been experienced was investigated during this test series. Included in this was orientation of the antenna array to serve Runway 22 with the phase center still about 700 feet from the threshold of Runway 4.

To determine the extent of path derogation caused by the uneven and sloping terrain existing between the threshold to beyond the middle marker, it was decided to reposition the antenna array at the same location to serve Runway 22 instead of Runway 4. In this manner the smooth, almost level runway area would replace the uneven terrain that existed to the middle marker.

Path symmetry at this site using Runway 4 was a particular problem due to terrain conditions. Figure 39 depicts the width measurements made at Tamiami (Position 5), Shenandoah (Position 6), and Shenandoah (Position 7). As can readily be seen, Position 7 and Position 5 are very much alike. This, of course, was expected since both are situated on fairly smooth terrain. Position 6, however, shows irregular structure and a large imbalance in path symmetry. The FAA Handbook OAP8 00.1 requires that the path be symmetrical within 40 to 60 percent above and below path for Category I operation and increases to 45 to 55 percent for Category II. Position 6 shows a symmetry of 31.7 percent 90 Hz and 68.3 percent 150 Hz and therefore falls outside even Category I tolerances.

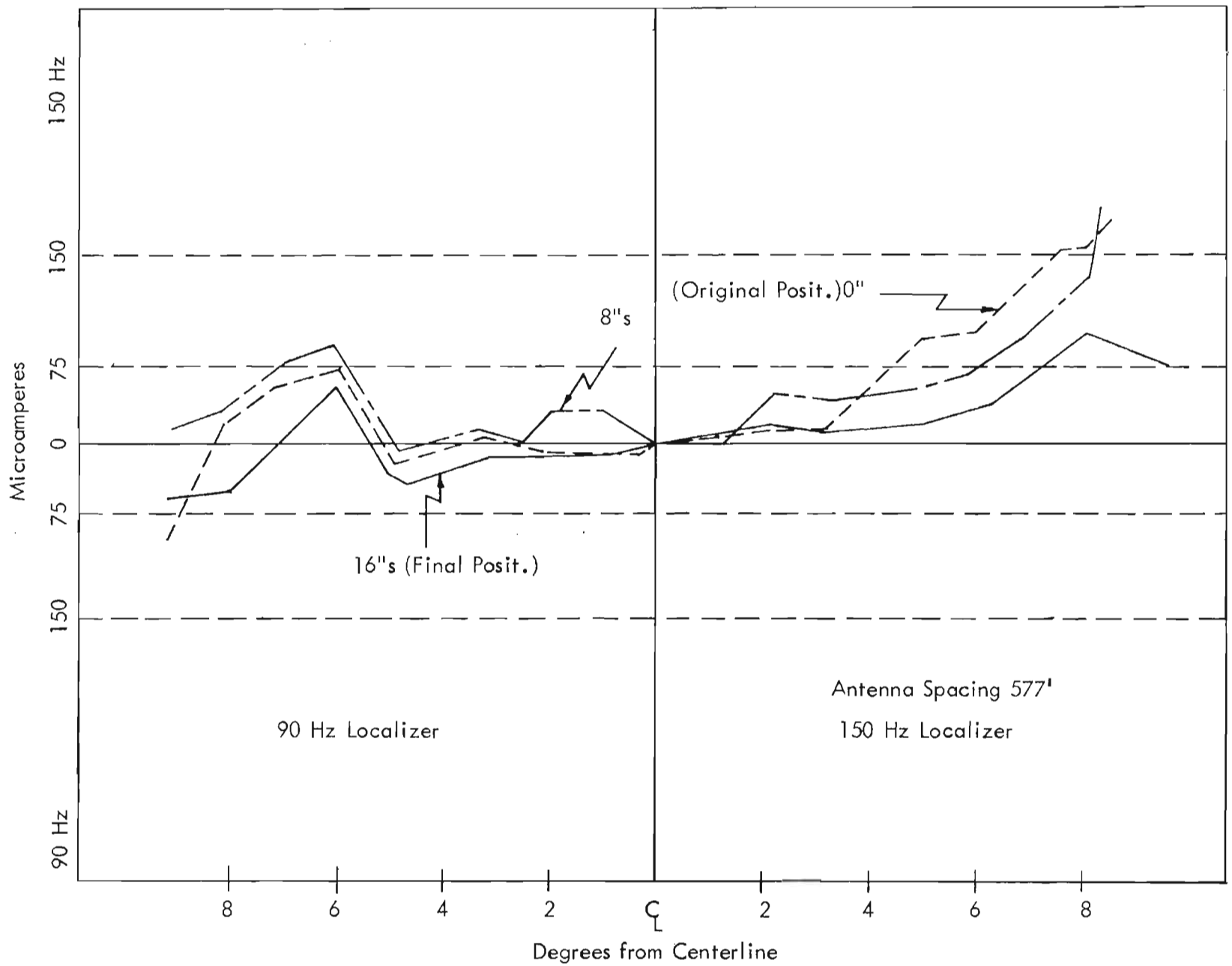

Figure 34. Watts Array - Position 6 - Effect of Lateral Offset of Rear Antenna, Perpendicular Cuts March 1, 1974.

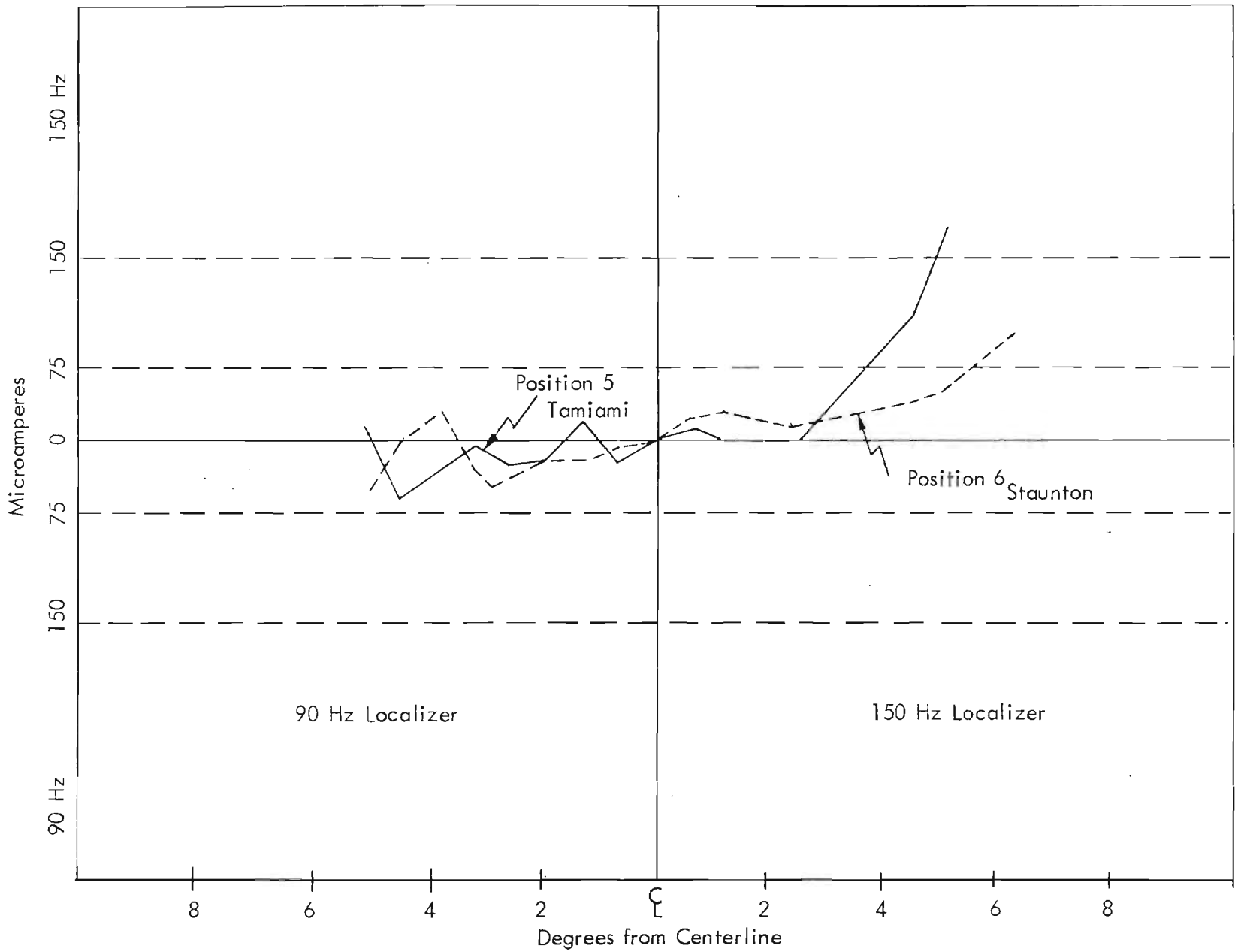

Figure 35. Perpendicular Cuts, Position 5 - Tamiami, Position 6 - Staunton.

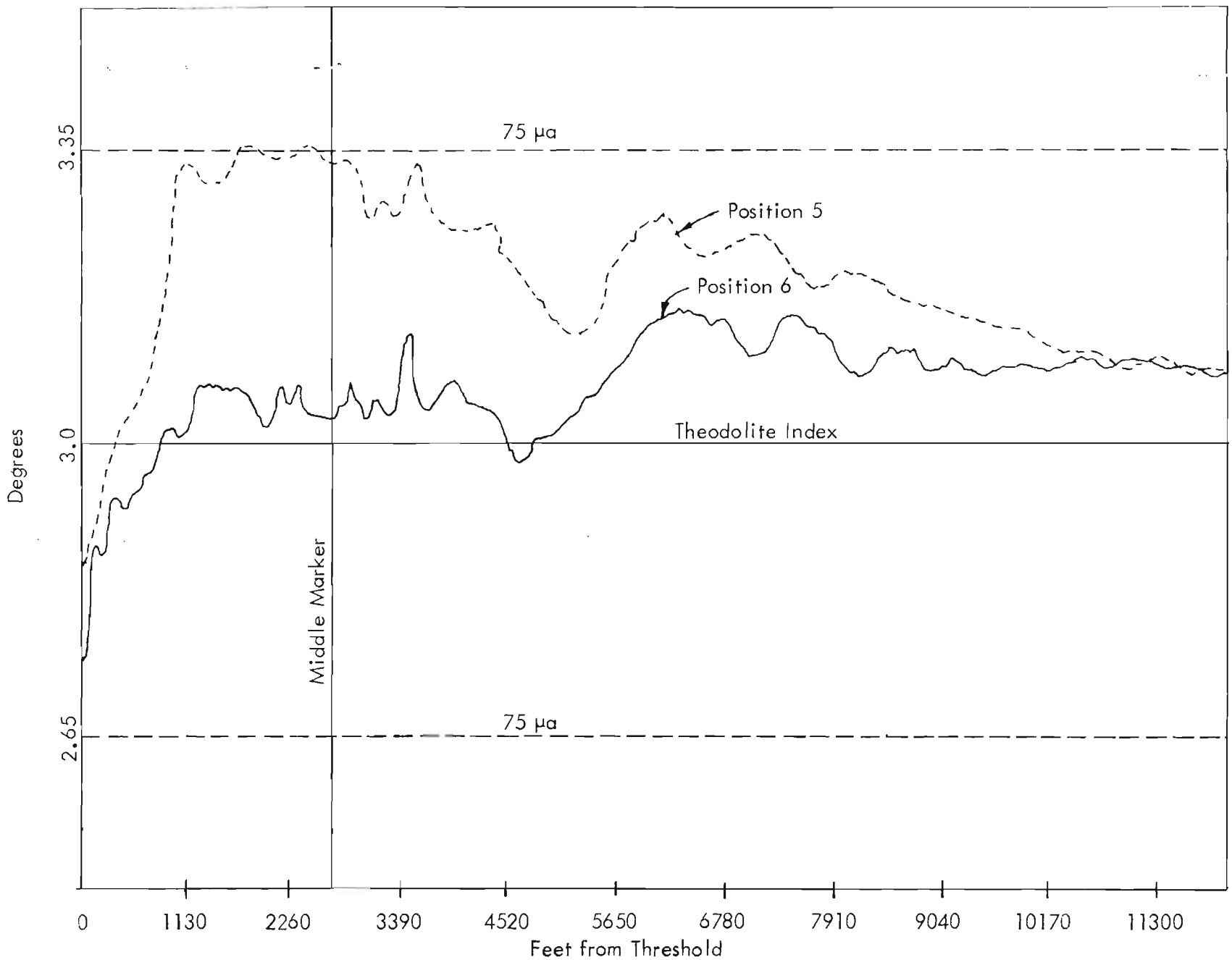

Figure 36. Approach on Path - Comparison Positions 5 and 6.

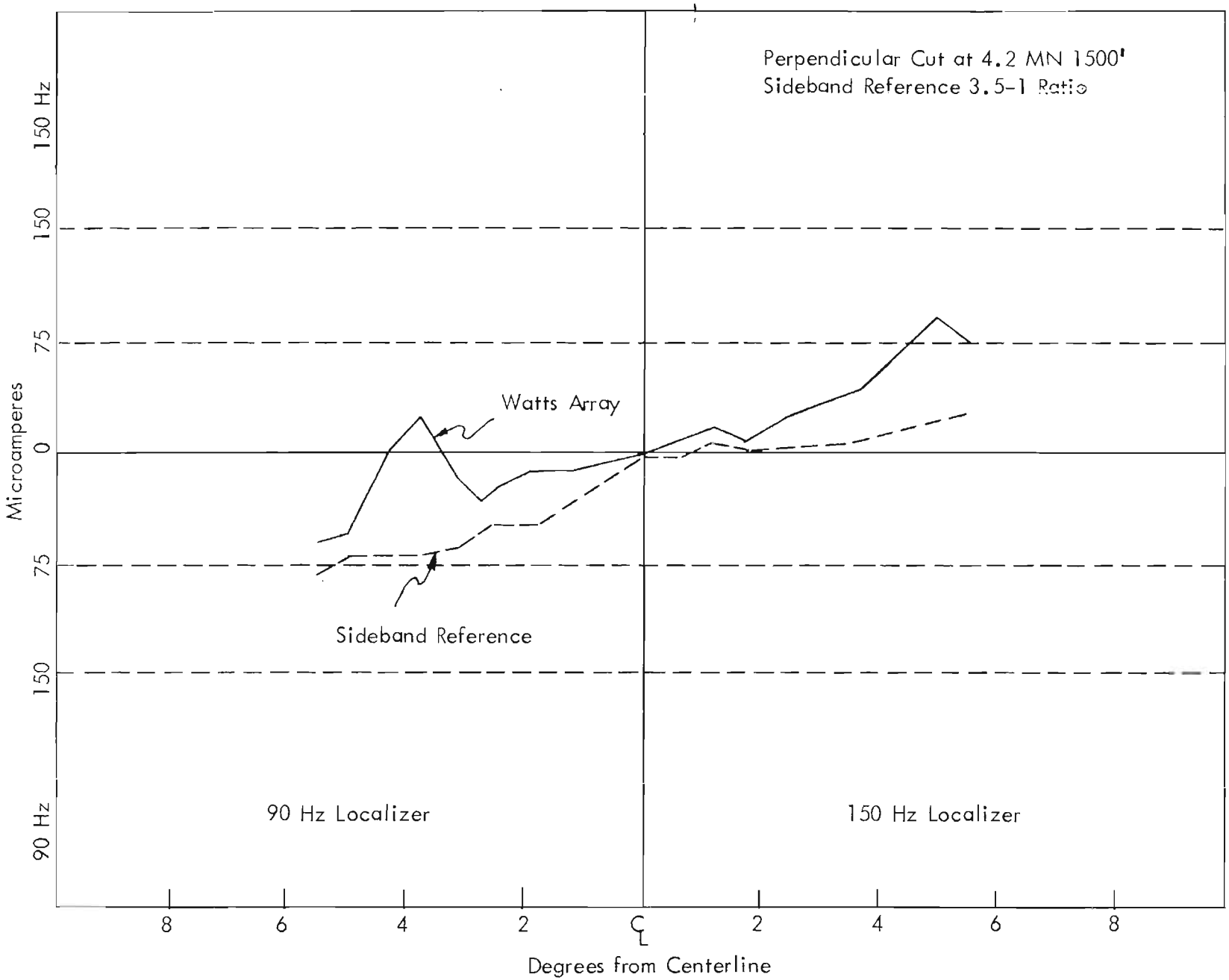

Figure 37. Comparison Watts Array versus Sideband Reference - Position 6 with Optimized Offset - April 11, 1974.

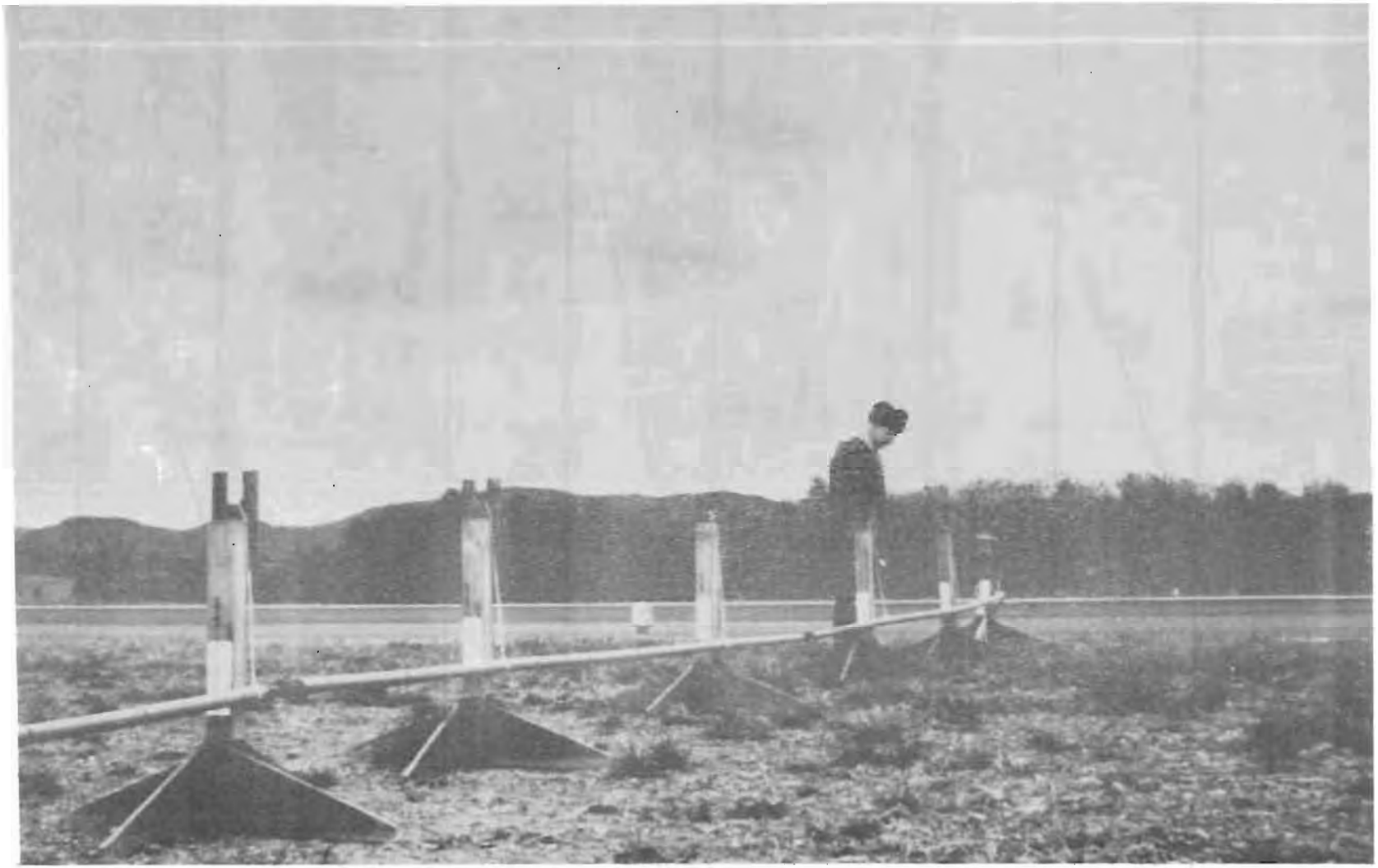

Figure 38. Slotted Cable at Reduced Height for Purposes of Evaluating Performance in This Configuration. In particular, consideration was given to the minimization of signal illuminating terrain upslope in the approach region. No significant improvement was obtained but the system did perform but with reduced signal strength available for the aircraft.

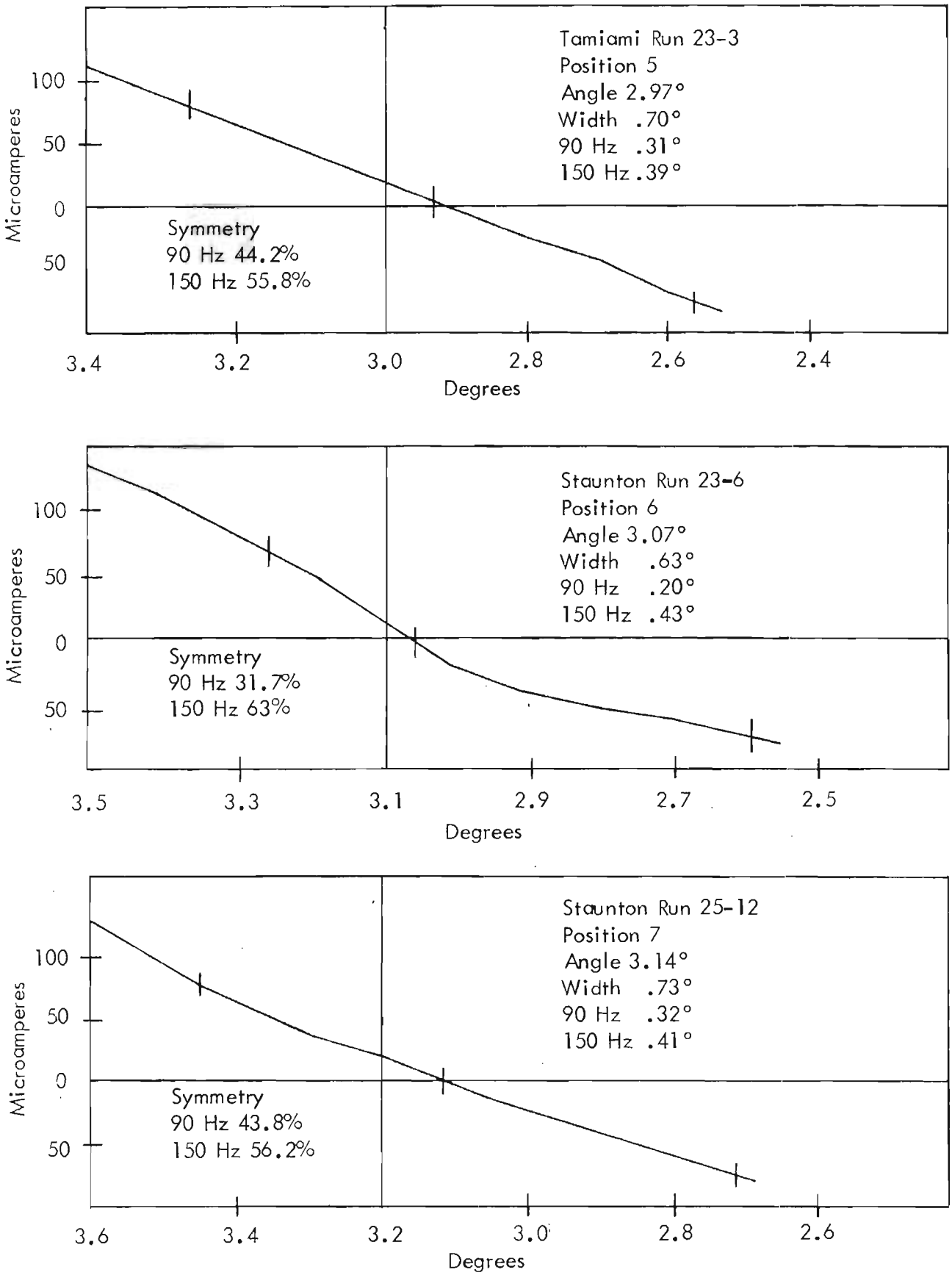

Figure 39. Width Measurements by Level Runs.

The large imbalance in path symmetry for Position 6 was due to a "flat" area occurring in the 150 Hz portion of the path as seen in the level run for Position 6 and it was felt that this particular measuring point was not indicative of the overall width envelope. To determine average width symmetry, RTT controlled approaches were conducted at the 75 μa displacement points above and below the path.

Figure 40 contains the differential amplifier trace (from point A to point B) for approaches 75 μa above and below the nominal path. Figure 41 shows the same differential amplifier traces replotted to the actual width envelope. The average values of the three traces are shown in Figure 41 and it is from these average values that final determination of angle, width, and symmetry are made.

Using the average value of 2.99 degrees path angle, 2.56 degrees at 75 μa below path, and 3.35 degrees at 75 μa above path, the half widths are found to be .79 degree. The 90 Hz portion was .36 degree and the 150 Hz portion was .43 degree. These values show a path symmetry of 45.8 percent in the 90 Hz and 54.2 in the 150 Hz which is within Category I tolerances. Figures 42 and 43 are similar to Figures 40 and 41 except for a broad width. Again path symmetry satisfies Category I tolerances.

Time did not allow for an optimum setup at Position 7. Figure 44 shows a perpendicular cut of the final adjustment made and predicts a large flare which starts about 11,000 feet from the antenna and increases to touchdown. An approach on path (Figure 45) shows the magnitude of the flare and the predicted flare from the perpendicular cut. While the actual flare is twice the magnitude of the predicted flare, the normal theoretical path producing a flat perpendicular cut does contain a built-in flare for the final 6000 feet. Figure 46 is used in conjunction with Figure 44 in predicting the flare magnitude.

One apparent problem encountered with the Watts glide slope at Staunton was the discrepancy between Ohio University and FAA signal strength quantitative flight-check data. This problem area is discussed in detail in Appendix A.

Inadequate signal strength was identified as a problem with the Watts glide slope especially when the system was used with a low power solid state transmitter. Because of this, the Watts Prototype Company has undertaken a redesign of the antenna array to provide a larger magnitude of signal in the glide-slope use area. When used with the solid state transmitter with a power output of less than 4 watts, the system is severely limited in signal strength in the use area. This is due to the relatively large spacing between the slotted-cable antenna elements that leads to the use of long transmission lines and is due to the low antenna heights used in the system.

The Watts slotted-cable antenna is quite directional in azimuth. This compensates substantially for the factors mentioned in the preceding paragraph and permits peak signal to be provided in the principal region for the user. However, it provides an amplitude taper toward the edges in azimuth, thus making the most critical signal strength region that of a 10-mile range at minimum intercept and at 8 degrees azimuth on the same side of the runway centerline as the array.

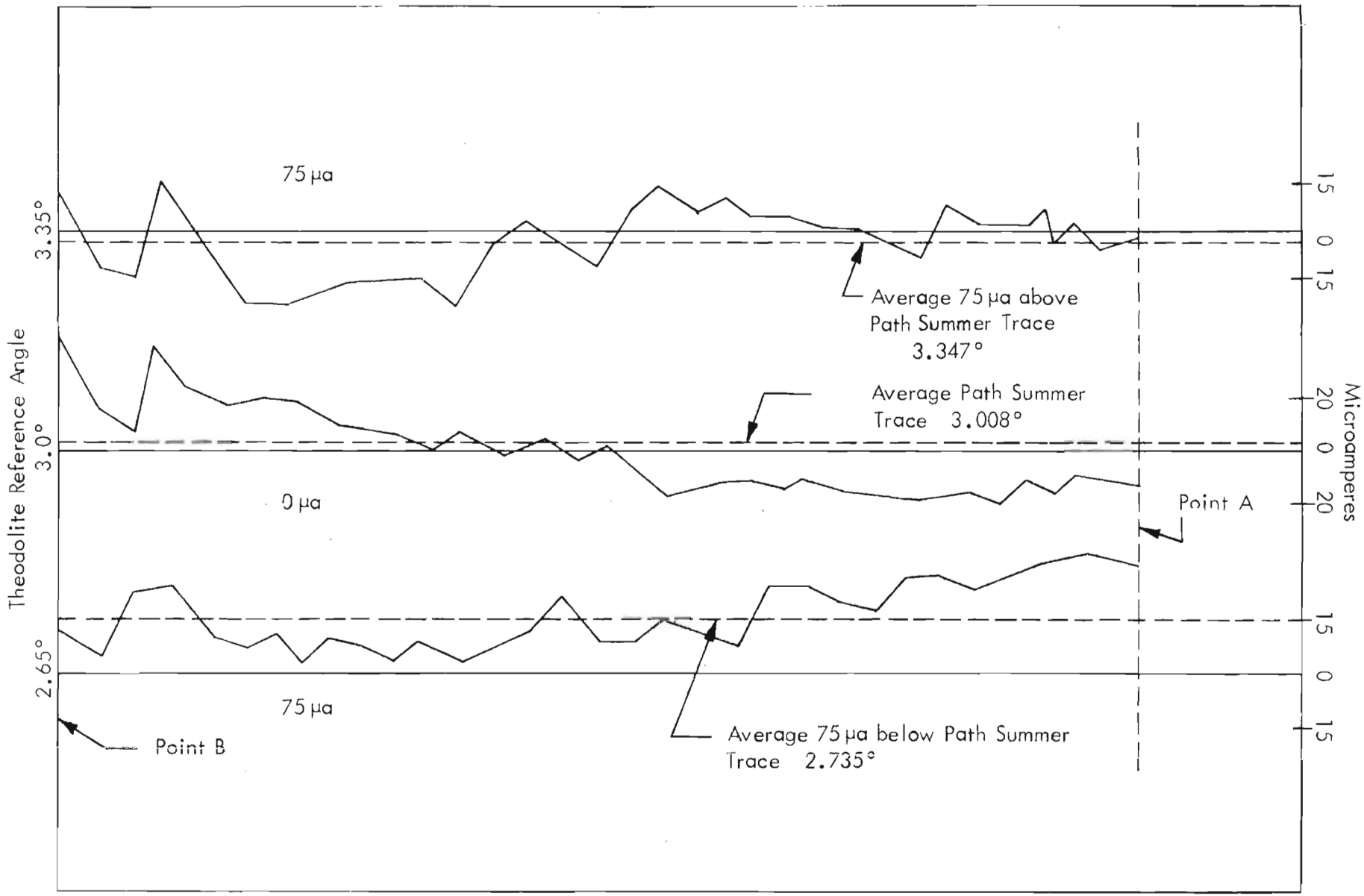

Figure 40. Differential Amplifier Recordings - Position 6 - Staunton, Virginia, April 23, 1974, Runs 23-12, 23-13, 23-14.

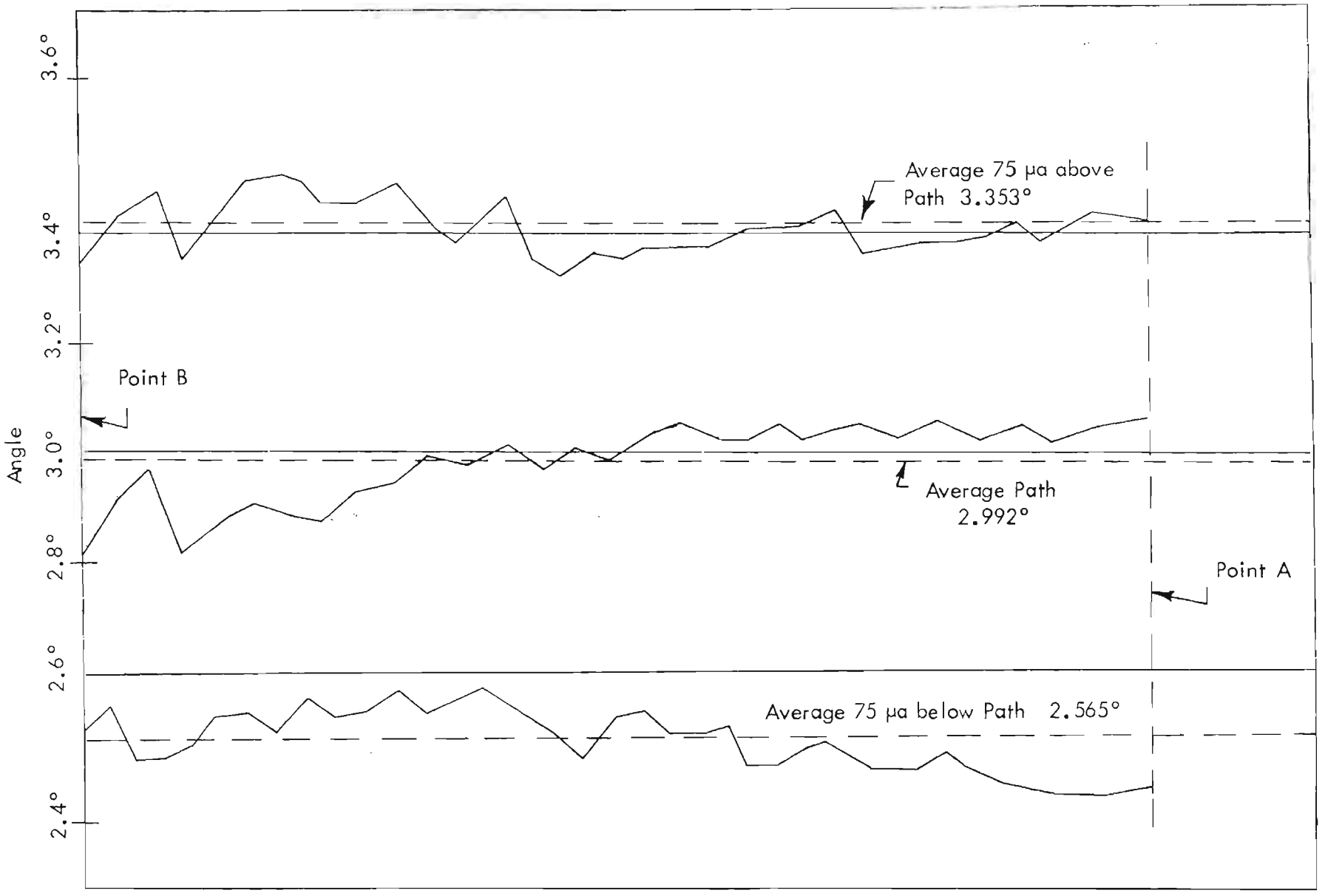

Figure 41. Width Envelope, Staunton, Virginia, Runs 23-12, 23-13, 23-14.

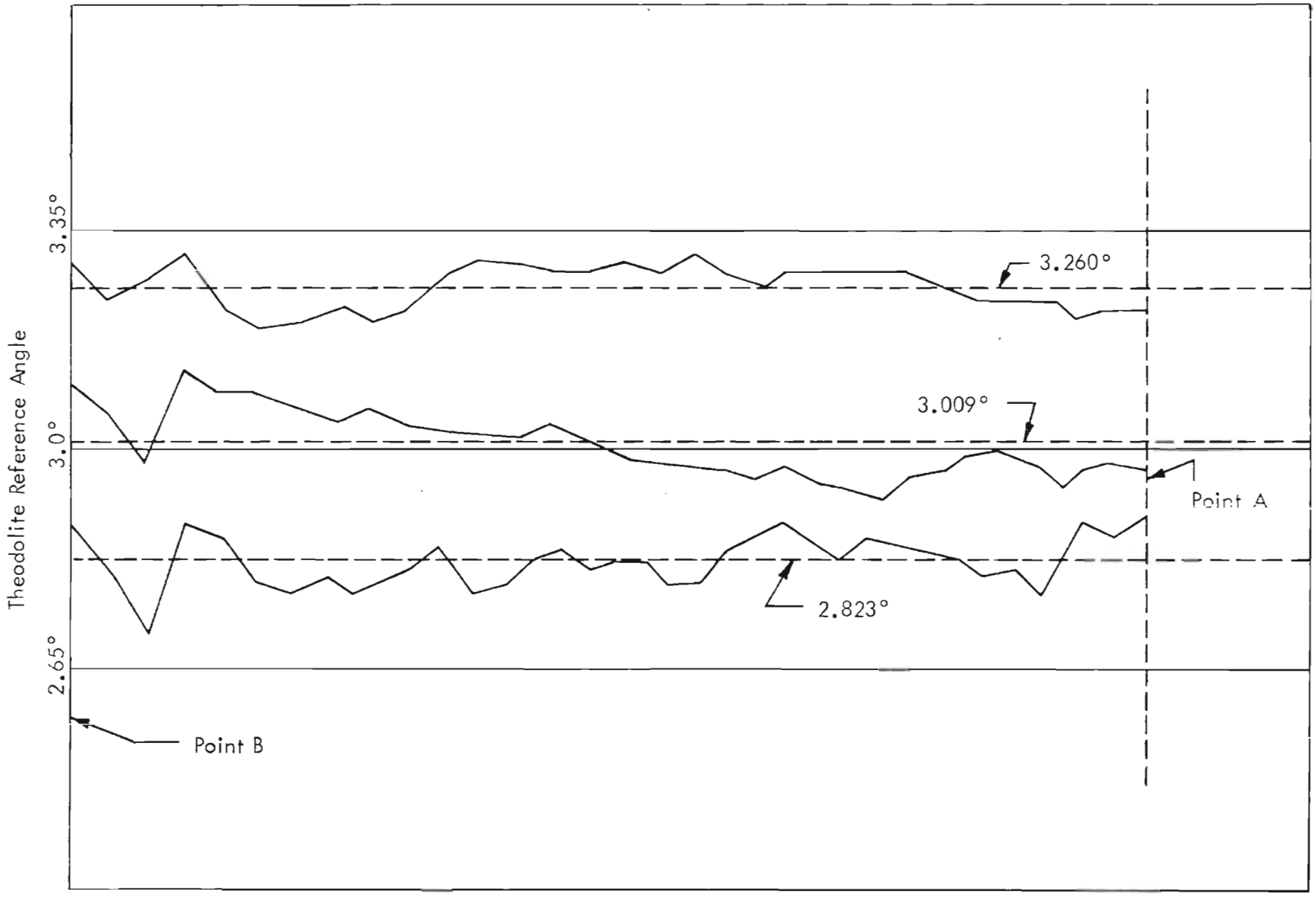

Figure 42. Differential Amplifier Recordings - Position 6 - Staunton, Virginia.

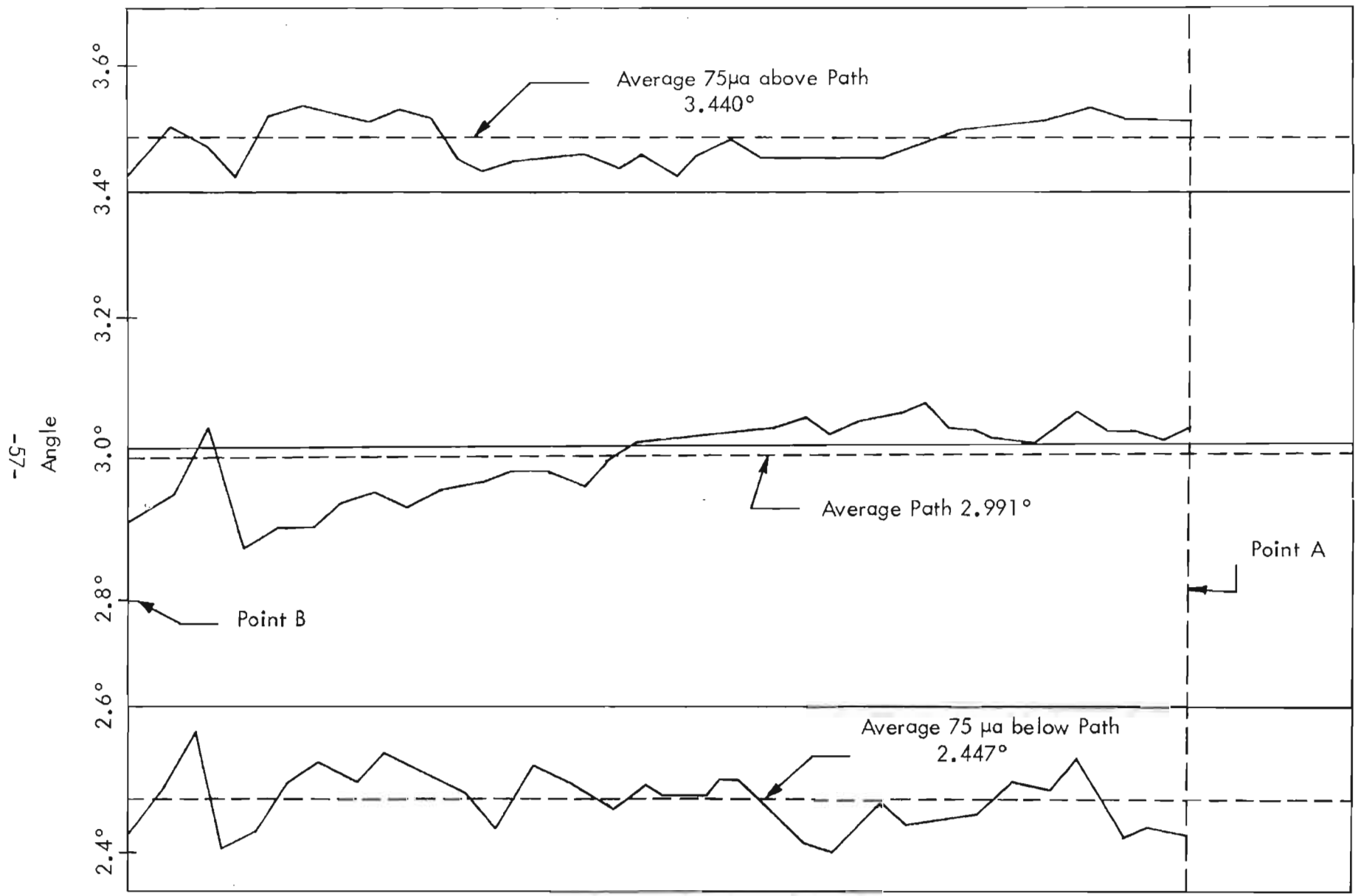

Figure 43. Width Envelope - Position 6 - Broad, Staunton, Virginia.

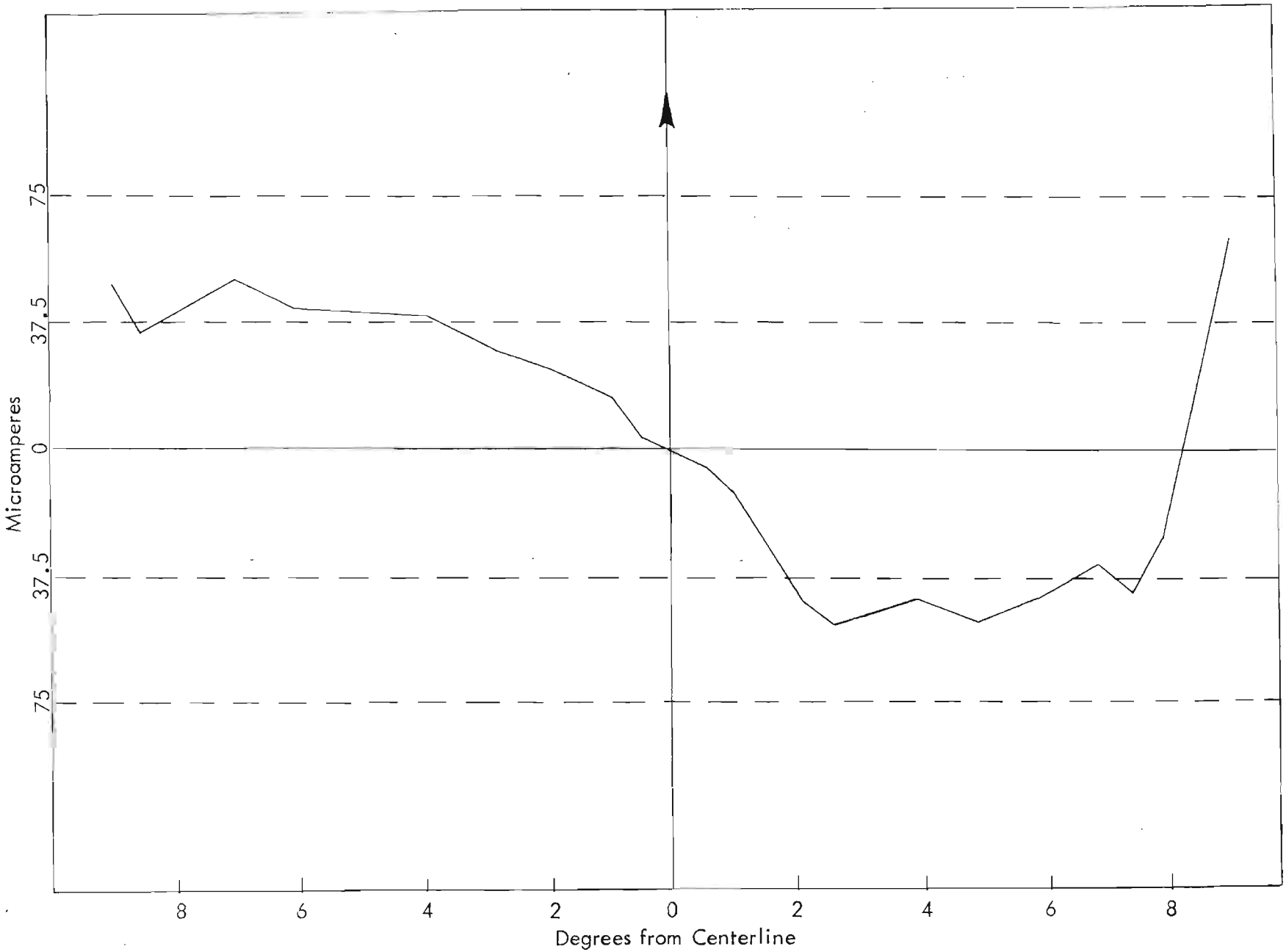

Figure 44. Perpendicular Cut, Watts Array - Position 7 - Staunton, Virginia, Run 25-15.

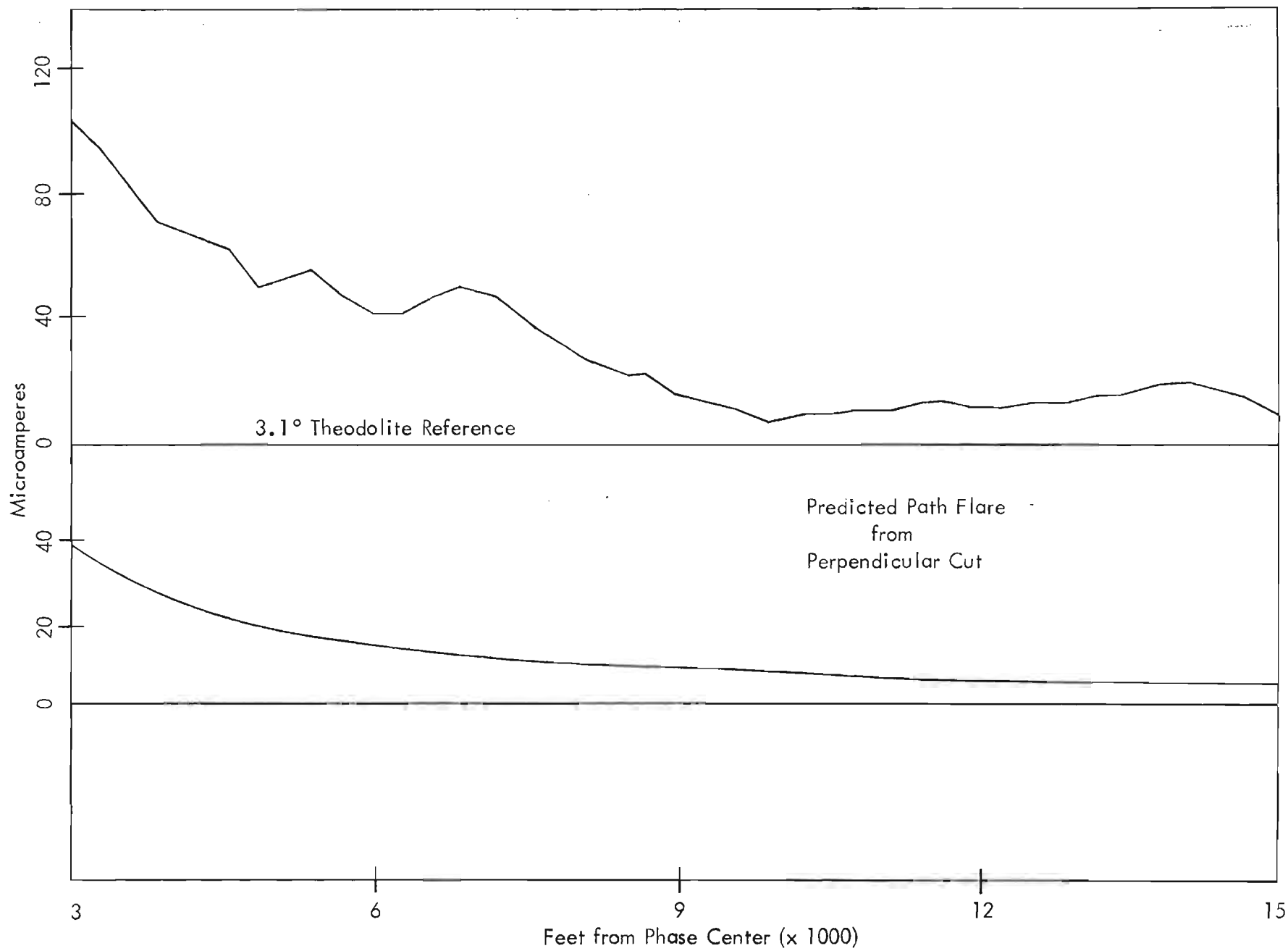

Figure 45. Approach on Path, Watts Array - Position 7 - Staunton, Virginia, Run 25-20.

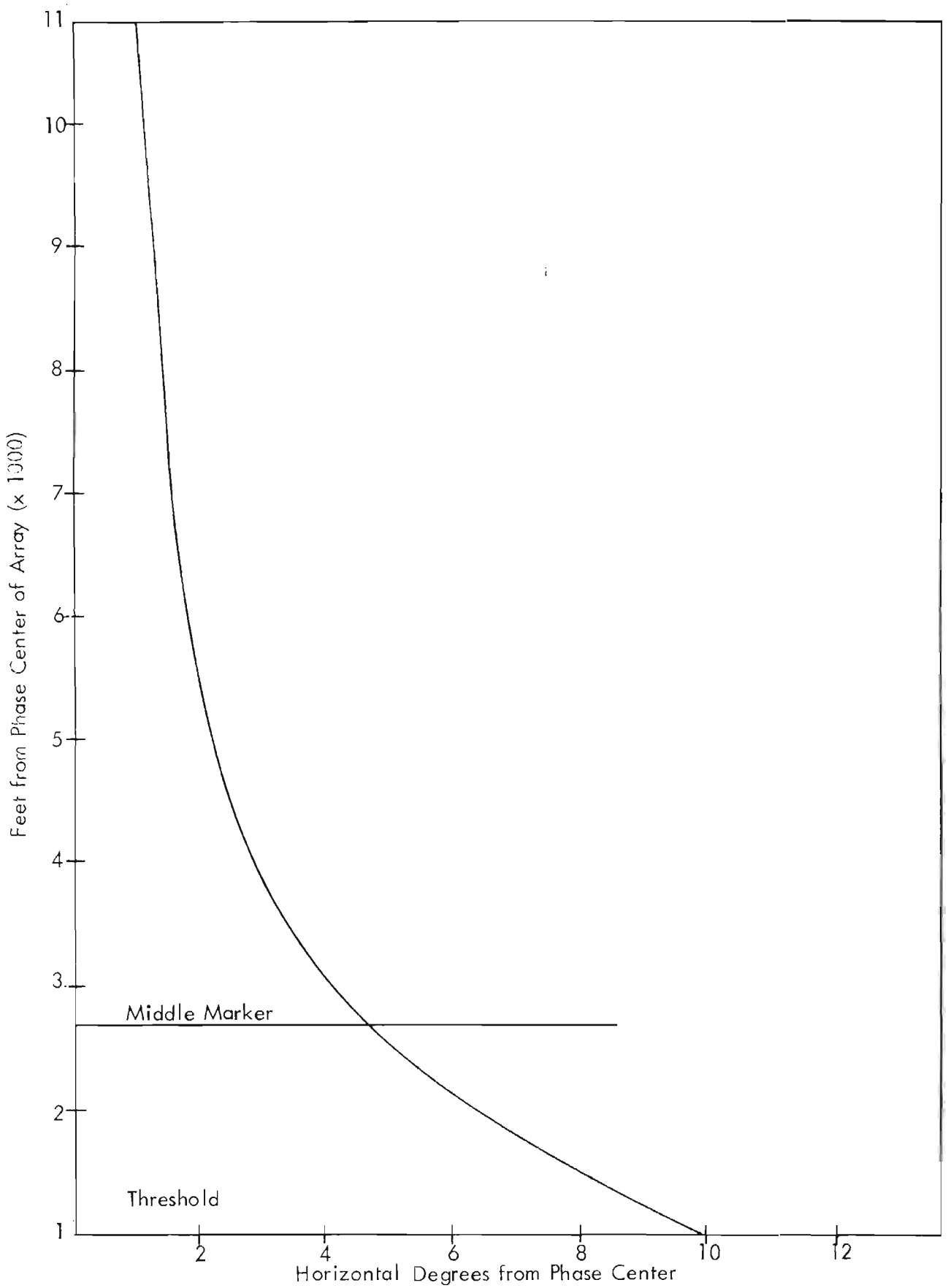

Figure 46. Approach Distance versus Horizontal Angle of Watts Array. Phase Center 169' from Centerline.

Early observations by Ohio University of signal strength with the Watts array powered by a TU-4 tube-type transmitter (7 watts), operating with a total of 1100 feet of 1/2-inch air-filled transmission line, some short jumpers of RG-244/U line, indicated that minimum signal level standards could not be met. Because of the availability of sensitive receiving equipment on board the Ohio University flight-check aircraft, successful path structure measurements were accomplished at Tamiami.

Flight check of the system by the FAA Orlando Flight Check Inspection DC-3 also showed deficient signal strength, but adequate to obtain values of path parameters.

The move of the system to Shenandoah Valley Airport, Staunton, Virginia, resulted in a different cabling configuration. Signal lost in the transmission was reduced since the transmitter building was near the center of the antenna array and total transmission line length was reduced by 600 feet. However, this gain was offset by the use of a solid state transmitter that was capable of delivering just under 4 watts and of some R6214/U solid dielectric feed cables from the sideband reference array. Flight-check measurements were accomplished at the Shenandoah site (as at Tamiami) even though the signal strength was below U. S. Flight Inspection requirements especially in off-centerline portions of the required region beyond the outer marker. It should be noted, however, that signal strength at the Shenandoah site was greater than at the Tamiami site.

In order to assess the performance of the slotted-cable antenna itself, ground-based, signal strength measurements were taken of the element operating alone and these were compared to values predicted by the Watts Prototype Company. Numerical values of the signal are provided in Table 3 which shows the antenna is performing as would be expected from the Watts design data.

C. Signal Strength Calibration and Rationalization. The FAA flight-check report of deficient signal prompted (1) a careful review of available data relating to Watts system signal strength, (2) a direct comparison between the Watts system and the image sideband reference system data, (3) special measurements on the Watts array using different types of equipment, and (4) a special calibration of the Ohio University airborne laboratory at an FAA facility so that Ohio University flight measurements could be directly related to the FAA standards.

Available signal strength data on the Watts array consists of the following:

1. Data taken with Ohio University aircraft, Tamiami site,

2. Data taken with FAA flight-check DC-3, Tamiami site,

3. Data taken with Ohio University aircraft, Staunton site,

4. Data taken with FAA flight-check DC-3, Staunton site,

Degree Azimuth	Ground Measurement dB	Calculated dB
-10	20.5	19
-8	11.5	9
-6	9.0	6.4
-4	5.0	3.4
-2	3.5	1
+0	0	0
+2	2.5	1.2
+4	5.0	1.3
+6	4.5	2.5
+8	3.0	2
+10	3.5	3.5
+12	5.5	5
+14	7.5	7.4
+16	12.5	14

Table 3. Comparison of Ground Measurement and Calculated Field Strength of Watts Array.

5. Data taken with Ohio University aircraft using Cardion Portable Field Detector, Staunton site,

6. Data taken on ground using Cardion Portable Field Detector, Staunton site.

Important relative values were obtained by connecting the transmitter to a dipole located on the tower at the height used for the sideband reference glide-slope system.

It is noteworthy that, based on special comparative measurements at the FAA calibration laboratory at NAFEC, the basic calibration difference observed between the Ohio University airborne electronic equipment and the FAA DC-3 flight inspection equipment amounted to only about one decibel. The confusion and problems which were evident when trying to reconcile the data taken by the two aircraft can be explained by two factors. First, FAA receivers are calibrated using a six dB pad between the receiver and the standard generator and the calibration values are taken at the generator-pad connection. This results in a voltage value (in "hard" microvolts) at the generator that is double that actually appearing at the receiver terminals. On the other hand, Ohio University receivers are calibrated with the voltage measured at the receiver-pad connection. Thus there is an immediate factor of 2 difference in voltage readings as obtained by Ohio University and the FAA flight inspection aircraft for the same signal strength values. A further difference of 3 dB was introduced by the FAA practice of injecting the calibration signal ahead of the splitter rather than after the splitter as done by Ohio University. See Appendix A. Thus, an Ohio University reading of 5.3 microvolts would be adequate to meet the Flight Inspection Manual criteria and would not imply that a 9 dB power increase is necessary. To reconcile Ohio University and the FAA reported microvolt readings, the Ohio University signal strength reading should be multiplied by 2.82 to give the FAA value. This is reasonably consistent with the 45 and 13 microvolt readings (ratio 3.46) of signal strength taken by the FAA and Ohio University, respectively, at the Staunton outer marker.

Further, it should be noted that the Ohio University equipment used for making the glide-slope measurements was 8 dB more sensitive than that used by the FAA, thus making it possible for Ohio University to collect data even though the signal levels were below those necessary to meet usable range requirements of the Flight Inspection Manual.

Based on reconciliation of the data, the FAA flight-check tests indicate that a usable distance of the Watts array at Tamiami is to be approximately 7 miles, and at Staunton approximately 6.5. Ohio University measurements indicate a usable distance of 7 miles at Tamiami and 7 miles at Staunton.

Some consideration as to the significance of the relative values of signal should also be given, especially those referenced to the sideband reference system which is accepted as providing adequate signal levels in space. This adequacy is based on

solid state transmitting equipment but with directional antennas, rather than the standard dipole used in the measurements at Staunton. If the reported difference of 4 dB between the directional antenna and the dipole is assumed, then the measurements made at Staunton by the FAA aircraft indicate that the Watts system is 13.2 dB below the sideband reference standard. Ohio University measurements indicate that the Watts array is 14.2 dB down.

Special measurements were made at Tamiami in October, 1974, when the array was reestablished for further testing. For these measurements a new, production, directional glide-slope antenna was used as a reference. The antenna, shown in Figure 47 , obtains its gain by use of a corner reflector and three collinear dipole elements.

Airborne measurements showed the Watts system to be 18.8 dB below the sideband reference at 10 miles and 20.7 dB lower at 5 miles. Calculations of a power budget given in Appendix A, Section IV, reveal that an additional 20.5 dB can be expected from modifications to the Watts system. These modifications include the use of larger diameter (7/8") air dielectric coaxial cables, relocation of the transmitter nearer to the center of the array to give shorter cable runs, closer (400') spacing of antenna elements to allow shorter feed cables, and installation of corner reflectors with the slotted cable. Signal levels comparable to the sideband reference system can thus be anticipated. Calculated patterns show azimuth tapers for both the sideband reference directional antennas and the new Watts model antenna are nearly the same to establish further compatibility between the two systems.

D. Conclusions Concerning Performance of the Watts End-Fire Glide-Slope Array. The following conclusions are based principally on the analysis of over 400 flight records with reference to the criteria of the U. S. Flight Inspection Handbook.

1. The glide-slope surface provided by the Watts system is acceptably smooth even when operating at a site where terrain prevents satisfactory operation of a null-reference or sideband-reference system.

2. The performance of the glide slope is quite predictable. Measurements made of the glide slope compare closely with calculations made by the Watts Prototype Company. Other work at Ohio University gives indications that effects of specific terrain can be predicted also.

3. The three-dimensional path structure is relatively complicated when compared to the conventional image systems such as the null reference. This requires measurement of several characteristics not usually made. As presently configured, the Watts array, at best, just barely meets the ICAO azimuth requirements. Satisfactory command information, however, is available for normal turn-in and approach. The path is satisfactory in coverage only to ILS point C because of deficient and unsatisfactory path information on the side of the localizer opposite the antennas (150 Hz side at Tamiami and Staunton) inside point C.

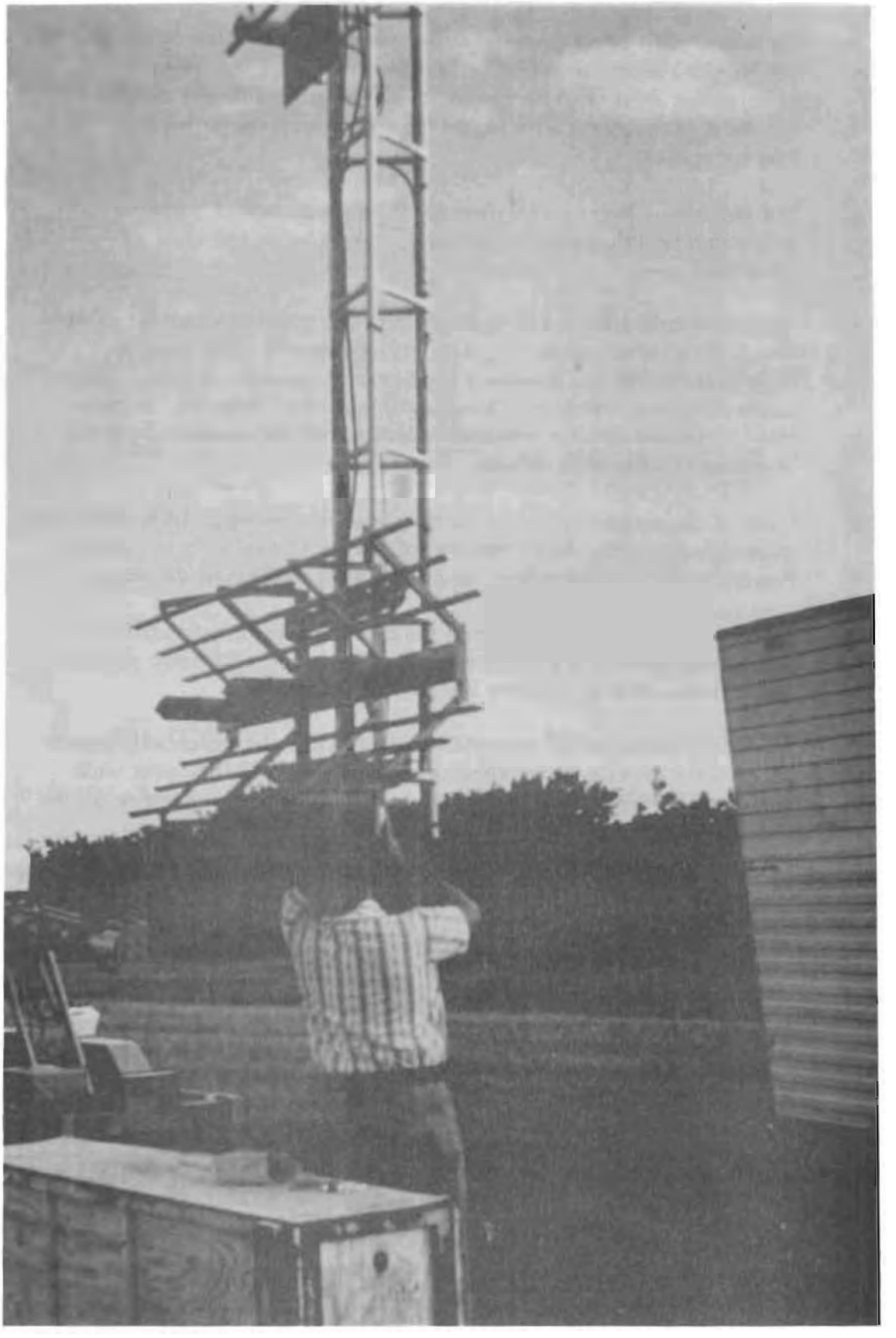

Figure 47. Directional Glide-Slope Antenna.

Deficiencies in coverage exist on the antenna side of the localizer (90 Hz side) when operating beyond the outer marker. These deficiencies exist because the basic cone produced by the array is skewed 3 to 5 degrees with respect to the runway centerline to give best coverage.

4. The path shape is critically dependent on placement of antennas. Tolerances on lateral placement will have to be on the order of ± one inch.

5. Path width and clearance characteristics are good on localizer centerline. With certain antenna configurations certain weak spots in clearance appear and these are predictable from calculations. Path width and angle values will vary as a function of azimuth. A carefully optimized array is required to insure that the variations are not in excess of allowable values.

6. Gain of the present system is not adequate to provide sufficient usable distance when using contemporary solid state transmitting equipment. Provisions for increasing gain and decreasing losses must be made.

7. Evidence acquired indicates that the system needs to be modified to broaden the path and coverage in azimuth, to make antenna placement less critical, and to increase the gain of the system.

8. Sufficient experimental evidence does not yet exist which will permit conclusions concerning monitoring capabilities, stability over wide temperature ranges, and performance capability over the entire glideslope band.

V. FABRICATION OF AN AUTOMATIC TRACKING RADIO THEODOLITE SYSTEM

During the past several years research has been under way at Ohio University for the purpose of developing an automatic radio telemetering theodolite (ARTT) to track flight inspection aircraft and to telemeter to the aircraft their angular position. This would, in effect, eliminate the man in the tracking loop and permit acquisition of more repeatable records.

Previous results may be found in FAA reports RD 73-137 and RD 74-214[5]. Several models have been investigated including in part construction of a model and execution of some tests.

For convenience these have been labeled the static tracker, the dynamic tracker and the video tracker. The static tracker makes use of a fixed position of the optical device with the light target moving about on the photocell to give an error signal. The dynamic tracker provides drive motors to position the optical device to place the light target on center. The video tracker provides gating and a readout of the frame where the target is located. All information concerning position of the target is then encoded in a form to be telemetered to the aircraft with conventional FAA flight-check telemetry equipment.

The first two trackers listed make use of a solid state device as the optical receiver. Two penalties are incurred with this approach, these being that no discrimination is possible when multiple targets are present and no direct monitoring is possible to ascertain if there are multiple targets actually involved or if there is a boresight error present. Two approaches were implemented to overcome these deficiencies so that fabrication of a practical model would be possible for this contract work.

To provide for monitoring, a video technique was investigated. This permits a direct and continuous capability for the operator to observe the tracking operation through the same optics that are being used to process the tracking data. This processor writes on the TV screen the location of the aircraft light target by showing an intersection of two light bars, one vertical, the other horizontal. The light target is shown directly on the screen in the form of a white dot. If the dot falls at the intersection of the two light bars then the system can be considered to be tracking properly.

The second of the systems considered for this fabrication requirement used a solid state detector but provided for a signature on the target so that it was recognizable against a background or in the presence of other light targets. The objective was to provide for greater utilization making operation feasible regardless of the lighting conditions.

As a part of this work effort a telemetry interface unit was designed, built and tested to provide for practical operation of the ARTT.

A careful investigation of both the dynamic tracker, working with a modulated light source, and a video system was conducted. Both offered advantages, and tradeoffs at this point of development were required. The video tracker is considered the most viable at this point in time and it was fabricated for use with this project. Its principal limitation is its requirement for a dark background for the light source. This means, at this time, tracking is essentially limited to nighttime conditions. Manual acquisition is quite practical and is considered acceptable. Discussions of the two primary tracking systems follow.

A. Video System. The video system achieves the tracking function through use of conventional closed-circuit television. This approach offers several advantages:

1. Much greater sensitivity than with the solid-state detector is achieved. On one test a tracking range in excess of nine miles was obtained with two 450-watt landing lights as sources. Typically, the solid-state detector gave 3-4 miles under the same conditions.

2. The operator sees on a TV monitor exactly the pattern of information that is being processed by the target position circuitry so that any errors or malfunctions are immediately apparent.

3. The scanning raster format converts positional differences to time differences so that electronic gating may be used to eliminate any unwanted portion of the video picture from that which is processed by the target position circuitry. This allows the exclusion of multiple spurious targets.

4. No additional lights are required on the flight-check aircraft since standard 450-watt landing lights are sufficient to obtain the desired ranges.

Two penalties exist with the video tracking, viz., an apparent substantial increase in the target size that is caused by excessive light as the target comes closer to the theodolite and persistence of the vidicon surface that causes smearing of the target when high sensitivity is required. These problems when they occur are immediately apparent, by means of the TV monitor, and are correctable.

It is well known that television displays are composed of lines of information with each line varying in brightness in direct proportion to a voltage that represents that line of information. In the tracking problem, assuming a black background, the target aircraft would appear as a voltage spike on the line of information that corresponds to the aircraft position. Since there are a precise number of lines that compose the picture, it is easy simply to count the lines as they occur until the line containing the target is encountered so that the elevation of the target is determined, modulo 1 line time. Since

the time interval of each line is precisely known, it is a simple task to determine its azimuth coordinate on the TV screen by means of determining the length of time between the start of the line that contains the target spike and the spike itself.

In this simple form, video tracking would not appear to present much of an engineering problem. However, several real-world complications appear that provide difficulties. First, backgrounds, even at night, are not a continuous black. They may contain varying shades of gray or undesired bright regions. Because of this the tracker must allow the operator the flexibility of working a single target and insure that the tracker will continuously stay locked onto that target and ignore all others, whether they be lumped or distributed light spots. Second, the target is usually of sufficient size that it extends over two or more lines of the video display even at long tracking distances. As the aircraft approaches the theodolite, this problem obviously becomes worse. Thus it becomes necessary for the processor circuitry to be somewhat selective as to which line of information will be used for the determination of target location. For instance, the choice must be made, after engineering evaluation, as to whether the processor should use the first line, the last line, or the line with greatest signal amplitude in determining the target location. Finally, during a tracking run, the target intensity may briefly fall below the minimum required because of yawing of the aircraft. In this case it is necessary that the processor recognize the situation and that it hold the last known valid position until the target intensity returns to a sufficient level. With these problems in mind the ARTT system, whose block diagram is shown in Figure 48, was fabricated.

As was noted earlier, one major drawback of the solid-state detector ARTT's was the lack of monitor capability of the operator on the system's health. Therefore, in the video ARTT complete instantaneous information on the tracker operation is provided on the video screen. This was accomplished by using the position voltages that the processor generated (these are necessary for telemetry to the flight aircraft anyway) to generate internally cursors on the video monitor screen. A typical display that the operator may see is given in Figure 49. As the vertical and horizontal cursors are generated, their intersection is used to define the target being tracked. The positions of the vertical and horizontal cursors are directly proportional to the vertical and horizontal position voltages. Thus, tracking lag, lost target, or false target occurrences are immediately apparent to the operator. One further advantage accrues from this in that the voltages that are used to generate the cursors can also be used to gate the video signals so that only the portion that lies within the section formed by the intersection of the cursors is processed by the target position circuitry. This effectively gates the video information. Thus the targets designated A and C in Figure 49 are ignored by the processing circuitry because they lie outside the mutual area of the cursors.

Figure 50 shows a functional block diagram of the cursor generating circuitry. When the target is centered on the vertical and horizontal axes of the display, coincidence will occur in the two comparators about 7 1/2 percent of a line or frame period before mid-screen, and the one-shot multivibrator then goes high until the spot has moved to 7 1/2 percent beyond the target location. As the target moves about in the TV field, coincidence of the comparators occurs earlier or later and the bright-bar cursors and video gates move in accordance with the new gate position.

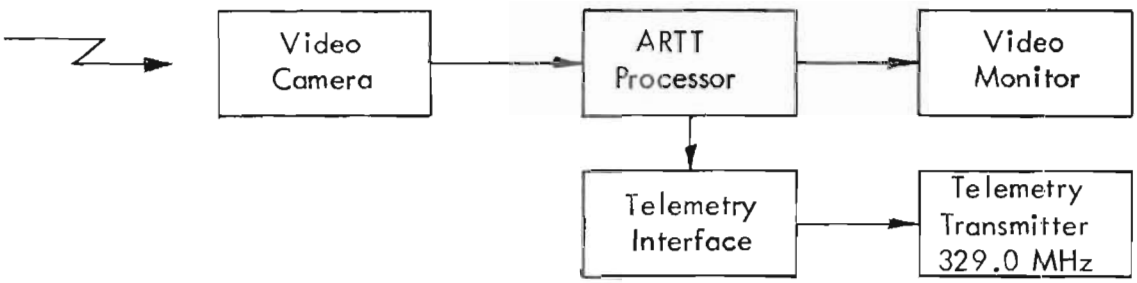

Figure 48. Block Diagram of Video ARTT System.

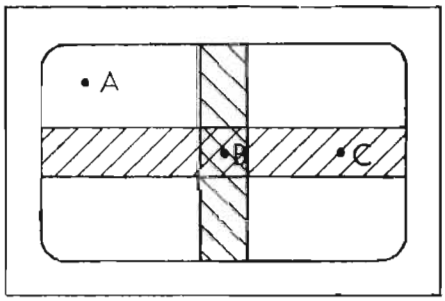

Figure 49. Display on Operator's Monitor After Cursors Are Generated. Display shows desired target B being tracked while the undesired targets A and C are excluded.

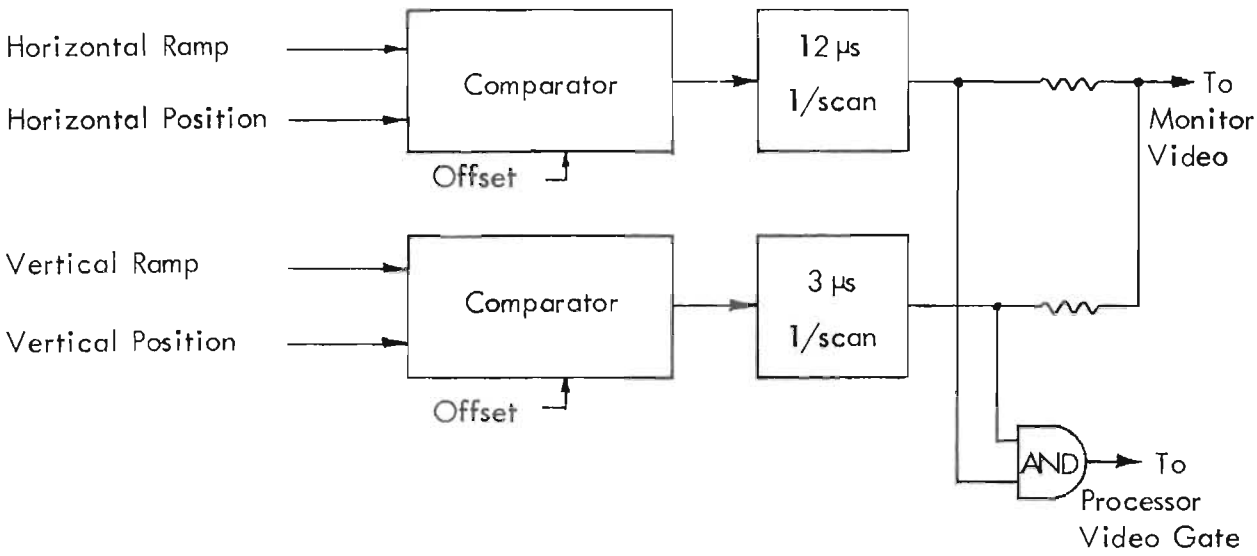

Figure 50. Functional Diagram of Cursor Generator, Video Brightening, and Rating Circuits.

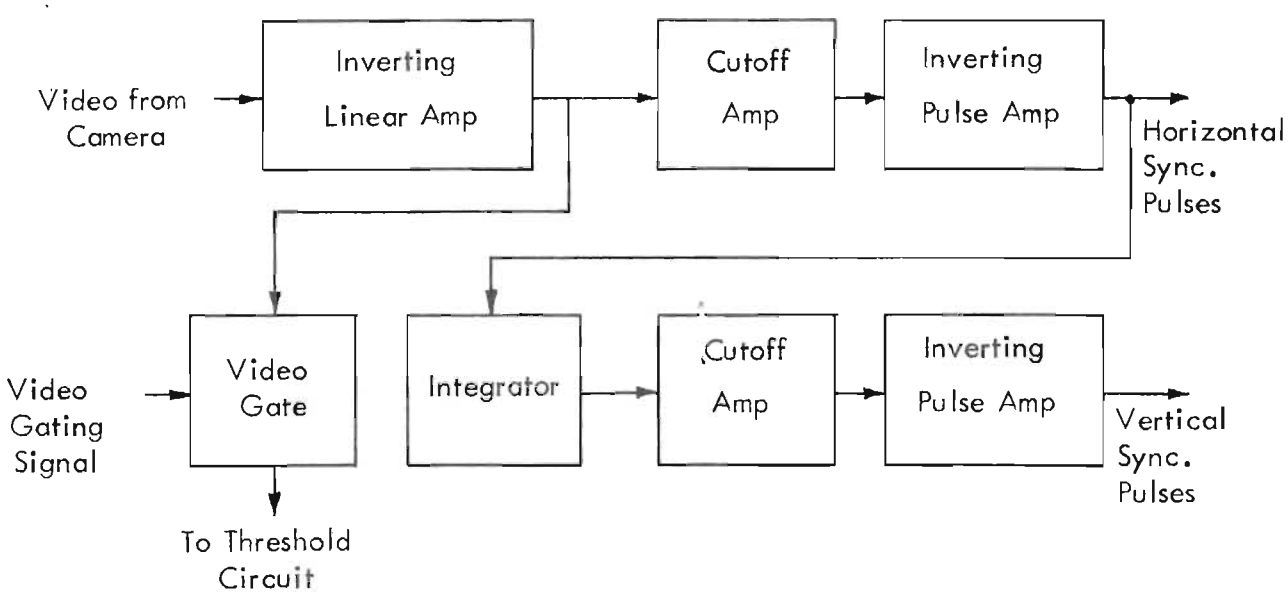

Figure 51. Block Diagram of Sync. Extraction Circuit.

Because the gate will tend to remain at the last valid target location during a "drop-out" condition, a kind of track will be maintained even if the target produces valid position information only every third or fifth TV field. The position voltages obtained under these conditions are not current and hence are somewhat inaccurate. They precede a complete lost target condition so that the operator should be alerted to such conditions so that he can take corrective action. The target one-shot multivibrator provides a convenient circuit location for making such a test. The target one-shot output is applied to a missing pulse detector which has zero output if there is at least one target pulse during each field. Should a field occur with no target pulse, the missing pulse detector output goes high and this condition is indicated on a milliammeter, alerting the operator.

Initial acquisition of the target is achieved by a pair of "slew" potentiometers. When the tracker is in the slew mode, the bright-bar cursors and the video gate are positioned on the screen by the vertical and horizontal position voltages, as in Figure 49. Instead of these voltages, the comparators of Figure 49 are provided with voltages developed by the vertical and horizontal slew potentiometers. By rotating these potentiometers, the cursors and the gate may be "steered" or positioned at any location on the video field. When the cursors are placed over a target which exceeds the set threshold, and the mode switch is changed from SLEW to TRACK, the cursors then lock onto the target they cover and remain on that target as it moves about in the TV field.

The first step in the video signal processing is the extraction of the video synchronization pulses from the video signal. It is these pulses that establish the entire timing of the system. The video signal direct from the camera is passed through an inverting FET amplifier. The resulting positive-going sync pulses are first applied to an NPN transistor at cutoff to obtain negative going sync pulses that are then inverted to positive-going 5-microsecond pulses of 10-volt amplitude for further use in the tracker. The horizontal sync pulses are also applied through a 3-stage integrator and a further cutoff amplifier and inverter to produce vertical sync pulses, 10 volts, positive-going, 1 millisecond duration. Figure 51 is a block diagram showing these circuit functions.

After the inverting input amplifier mentioned above, the video brightening signals are now negative-going. The video signal is now applied to the cathode of a fast diode whose anode is returned to an adjustable negative threshold voltage through a load resistor. Thus, when the video signal is more negative than the threshold voltage, a target pip (negative-going) is developed across the load resistor. Since the duration of these pips varies in accordance with the apparent target width, it is necessary to apply these pips to a one-shot multivibrator which generates a uniform 3-microsecond pulse for each target pip regardless of duration.

The missing pulse detector circuit described earlier also serves a function in setting the threshold voltage. It is used to reset the threshold level automatically. When the automatic threshold control (ATC) circuit is on, a field which contains no target pulse causes the threshold to be lowered by approximately 1/4 volt on the next field scan. Thus, a target whose intensity is fluctuating will continue to be tracked with reasonable accuracy.

The target location circuitry incorporates two ramp generators, one running in coincidence with the horizontal sweep and the other running in coincidence with the vertical sweep. An analog gate allows samples of these ramp voltages to be passed on to holding circuits consisting of capacitors followed by MOSFET source followers and voltage followers. The gates are enabled by the 3-microsecond pulses from the target one-shot multivibrator. Note that from the previous discussion, the only target that will trigger the target one-shot multivibrator is a target that is contained in the mutual area of the cursors. In the case of target dropout, no new information is applied to the holding circuit on that sweep so that it continues to retain the voltage corresponding to the last valid target position. Figure 52 is a block diagram of the target location circuitry and the target threshold circuitry.

Detailed circuit diagrams for the video ARTT processor may be found in Appendix B.

The video ARTT has been successfully tested both in the laboratory and with actual ILS flight checks. In laboratory tests, the system exhibited perfect repeatability and showed no degradation due to video persistence. What video persistence that was present was strictly in the CCTV monitor and not the ARTT processing circuitry. Several ILS flight checks have been accomplished using the video ARTT both at Port Columbus, Columbus, Ohio and Wood County Airport, Parkersburg, West Virginia. The results of these tests have steadily improved as experience with the system has increased and as the system itself evolved into a more optimum form. Figure 53 shows the differential amplifier output for two glide-slope approaches at Parkersburg, West Virginia. The runs show good repeatability. Tracking range for these tests had been purposely reduced by use of a 3x teleconverter in the lens system and tracking ranges in excess of 5 miles are regularly achieved when the teleconverter is omitted.

No equipment was purchased in the pursuance of this design project. Instead, video equipment already on hand at Ohio University was utilized. The following price estimates are included to provide an idea of total system cost:

1.	Camera	$300
2.	Monitor	150
3.	Lens	150
4.	Mount	150
5.	Electronics	100
		$850

B. ARTT with Modulated Light Source. Another ARTT system was investigated that had the advantage over the video tracker of not requiring nighttime conditions. This ARTT system used a solid-state detector with a modulated light source on the flight-check aircraft so that the desired target could be discriminated from any ambient background condition that occurred. This permitted exclusion of undesired targets and the

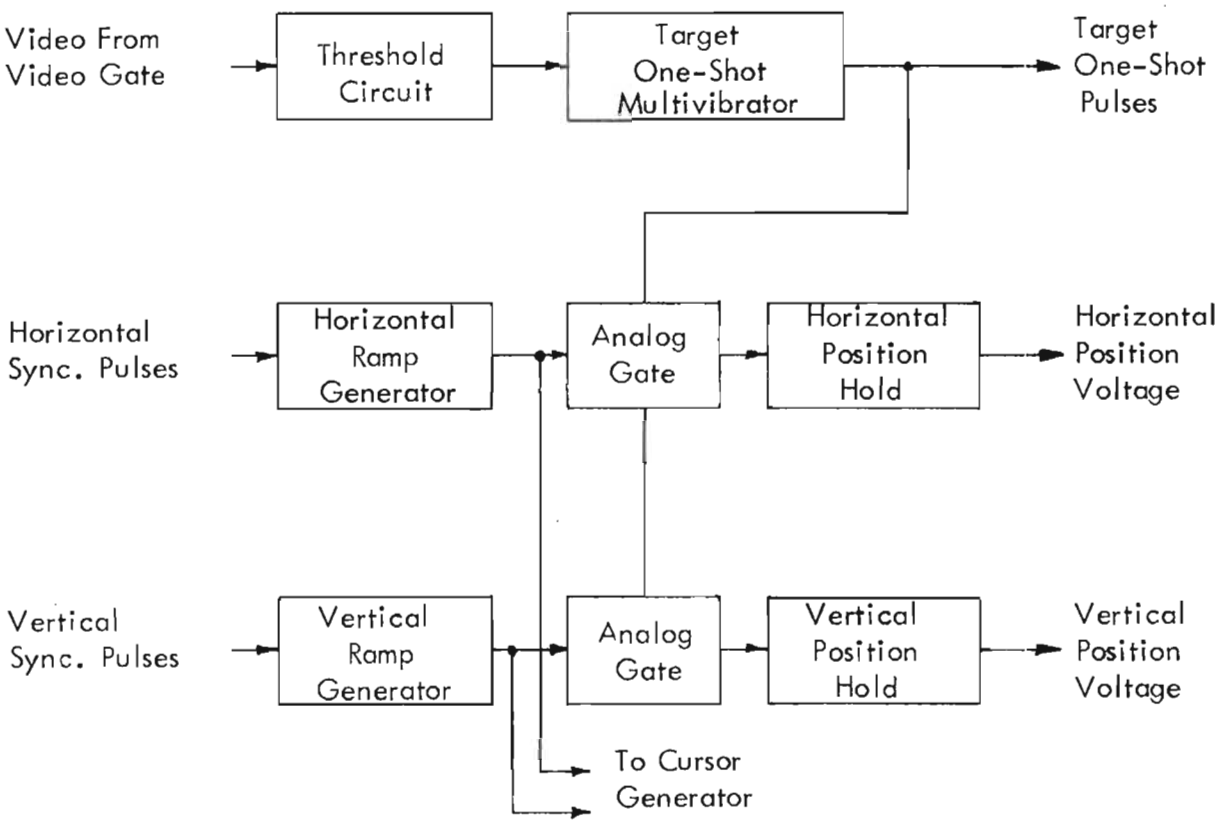

Figure 52. Block Diagram of Target Threshold and Target Location Circuitry.

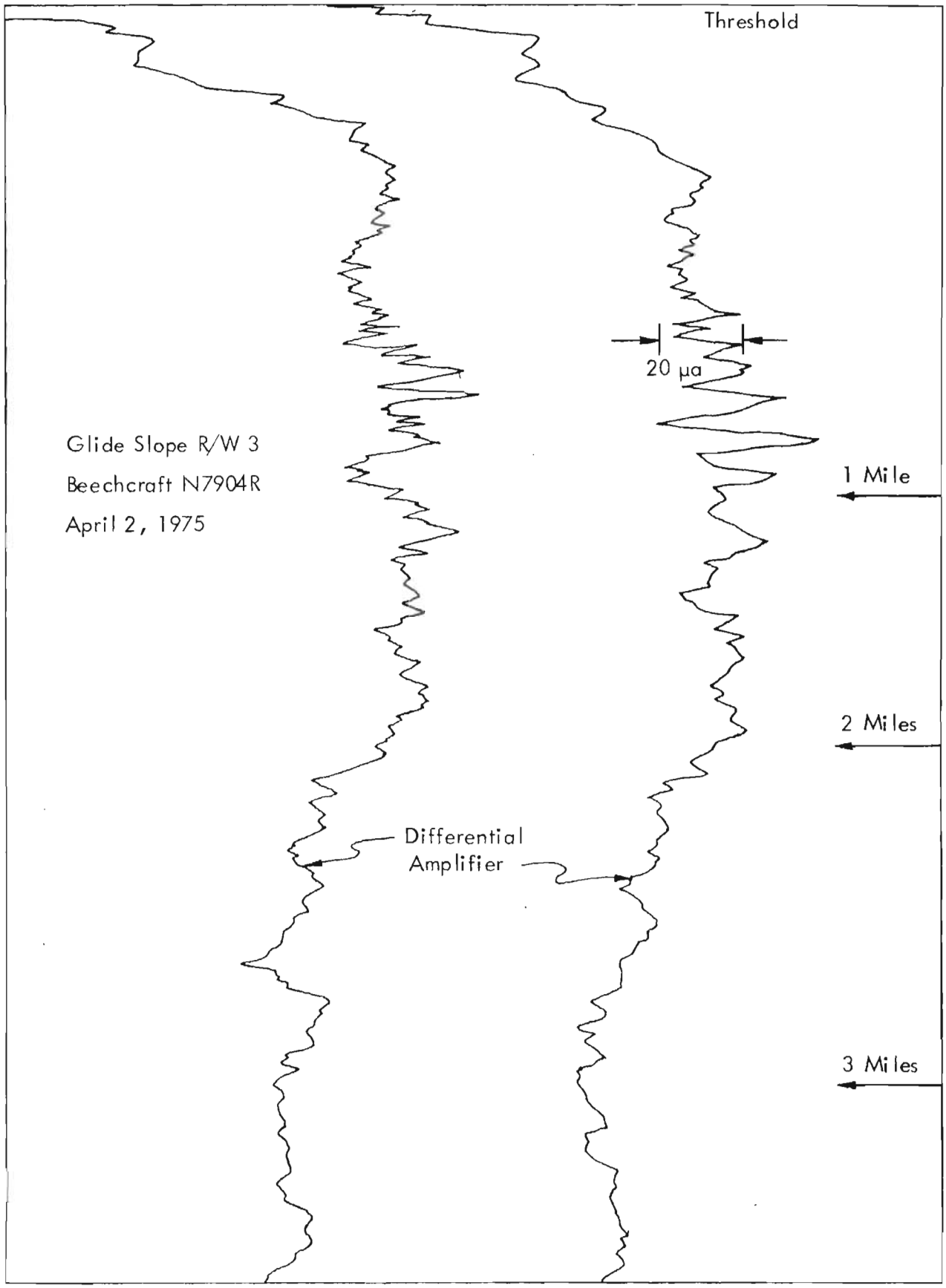

Figure 53. Video ARTT - Two Consecutive Runs Overlaid, April 2, 1975.

exclusion of a bright sunlight background from the signal that the ARTT system processed. The best source found for use on the aircraft that provided the modulated light was a Gallium-Arsenide coherent light emitting diode (LED). Some of these devices are capable of peak intensity outputs in excess of 1000 watts. However, in the ARTT application, the design challenge came because of a limit of a 0.02 percent duty cycle.

The LED ARTT system is designed as a dynamic tracker. That is, servo-motors were added to the vertical and horizontal axes of a standard Warren-Knight theodolite so that the position signal of the tracker processor could be used to maintain the target on the theodolite cross-hairs. Because of this, the receiving telescope does not require a large look angle so that large optical gains can be achieved.

1. LED Range Calculations and Experiments. Assuming a 350-watt LED with half beam-width angle of 10° and a variable pulse width, the following range calculations are made for the receiver preamplifier of Figure 54.

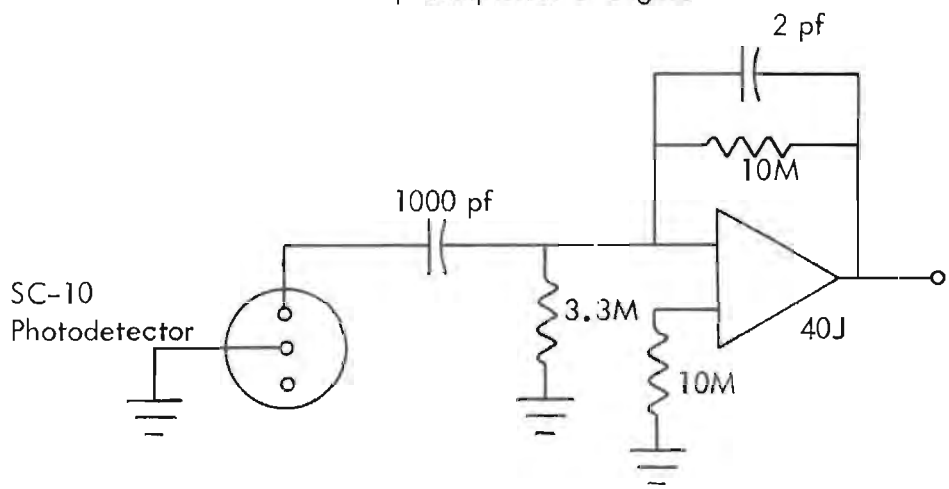

Figure 54. Preamplifier Circuit for SC-10.

The equivalent circuit for the SC-10 photocell is given in Figure 55. (See Section 3 for more detailed description.)

Utilizing the equivalent circuit for the SC-10, then an overall block diagram is derived and is shown in Figure 56.

Where

$$i = \frac{\gamma P_t A_r T_t}{\pi R^2 \tan^2\theta} e^{-\sigma \frac{R}{1000}}$$

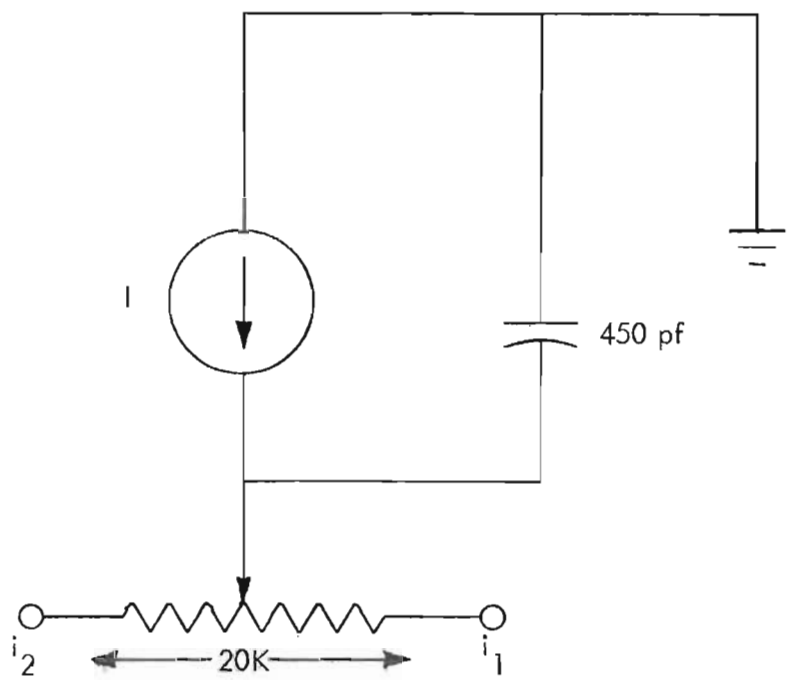

Figure 55. Equivalent Circuit for SC-10 Photocell.

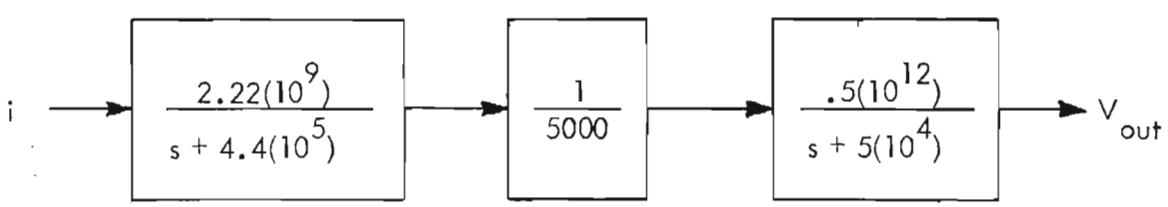

Figure 56. SC-10 and Preamplifier Circuit Shown in Transfer Function Form.

P_t = Peak transmitted power

A_r = Area of receiving electronics

R = Range

θ = Laser half beam width

σ = Atmospheric attenuation constant

γ = Photocell sensitivity

T_t = Attenuation constant of optics

So that

$$V_{out}(s) = \frac{2.22(10^{17})\ (1 - e^{\tau s})\ i}{s[s + 4.4(10^5)]\ [s + 5(10^4)]}$$

Where

τ = Pulse width

Separating by partial fraction expansion and taking the inverse Laplace transform,

$$V_{out}(t) = (1.01 - 1.14e^{-5(10^4)\,t} + .129e^{-4.4(10^5)t})\ 10^7\ i\ u(t)$$

$$- (1.01 - 1.14e^{-5(10^4)\,(t-\tau)} + .129e^{-4.4(10^4)\,(t-\tau)})\ 10^7\ i\ u(t-\tau)$$

The normalized pulse response of the circuit is calculated and is given in Figure 57, i.e., Figure 57 is a plot of

$$v'(t) = (1.01 - 1.14e^{-5(10^4)t} + .129e^{-4.4(10^5)t})\ u(t)$$

$$- (1.01 - 1.14e^{-5(10^4)\,(t-\tau)} + .129e^{-4.4(10^5)\,(t-\tau)})\ u(t-\tau)$$

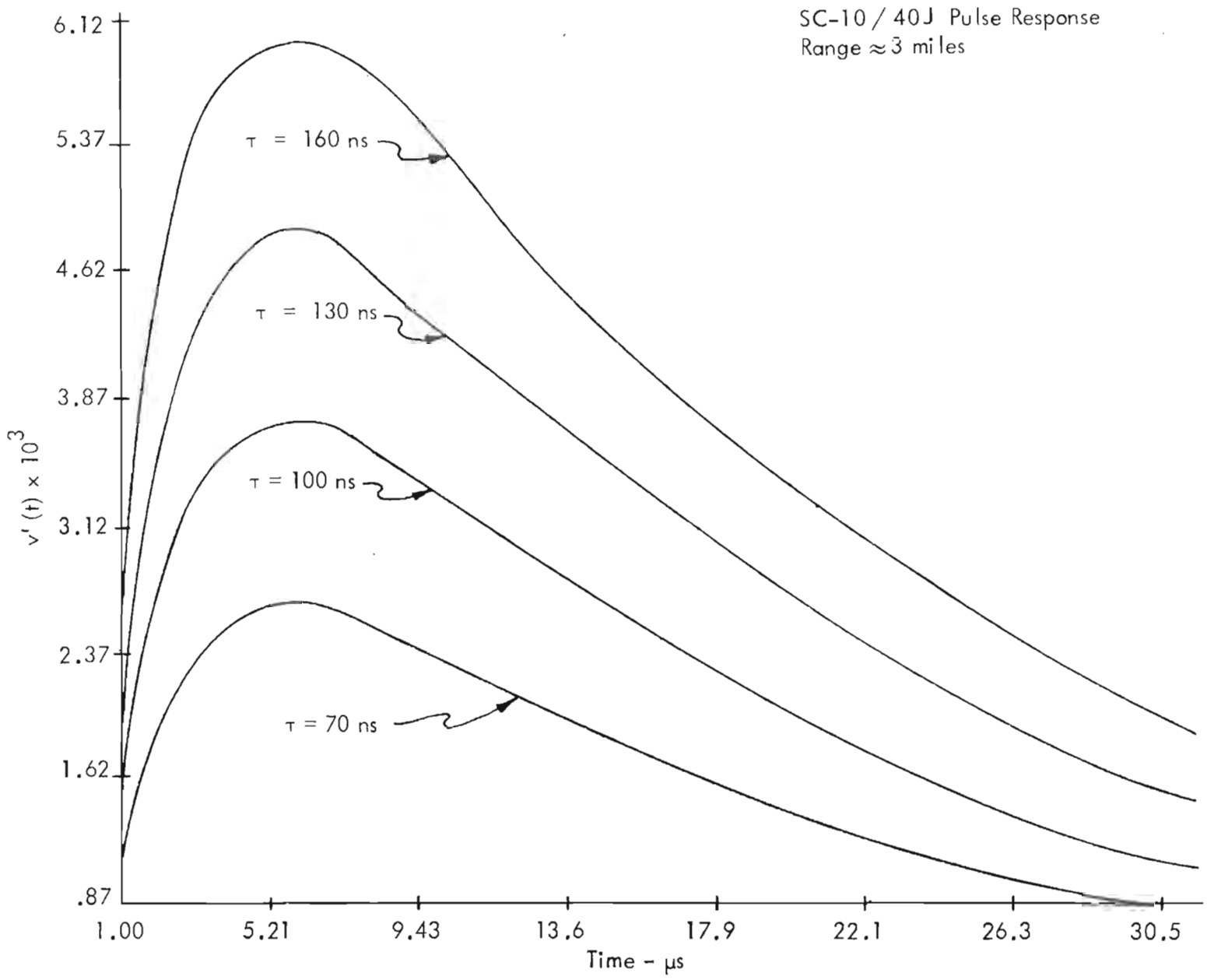

Figure 57. Circuit Response for Varying Pulse Widths.

From the peak values of Figure 57, the peak V_{out} is then plotted in Figure 58 over the anticipated range requirements with the constants assigned the following values.

$A_r = 0.0127\ m^2$

$\sigma = .3$ (Corresponds to ~ 6 miles visibility)

$\theta = 10°$

$T_t = 1$

$\gamma = .3\ a/w$

$P_t = 350\ w$

So that

$$i = 13.65 \frac{e^{-.3 \frac{R}{1000}}}{R^2}$$

Thus as can be seen from Figure 58, a signal level of just under 10 mV is expected at a range of 3 miles and will increase to an amplitude of ~ 8 V at the minimum range of 1000 feet.

Utilizing the receiver circuit of Figure 54, experiments were performed using a 4-watt GaAs laser with a 70 ns pulse width. Assuming the following constants, the theoretical and experimental results are tabulated below.

$A_r = 0.0127\ m^2$

$\sigma = .3$

$\theta = 20°$

$T_t = 1$

$\gamma = .3\ a/w$

$P_t = 4\ w$

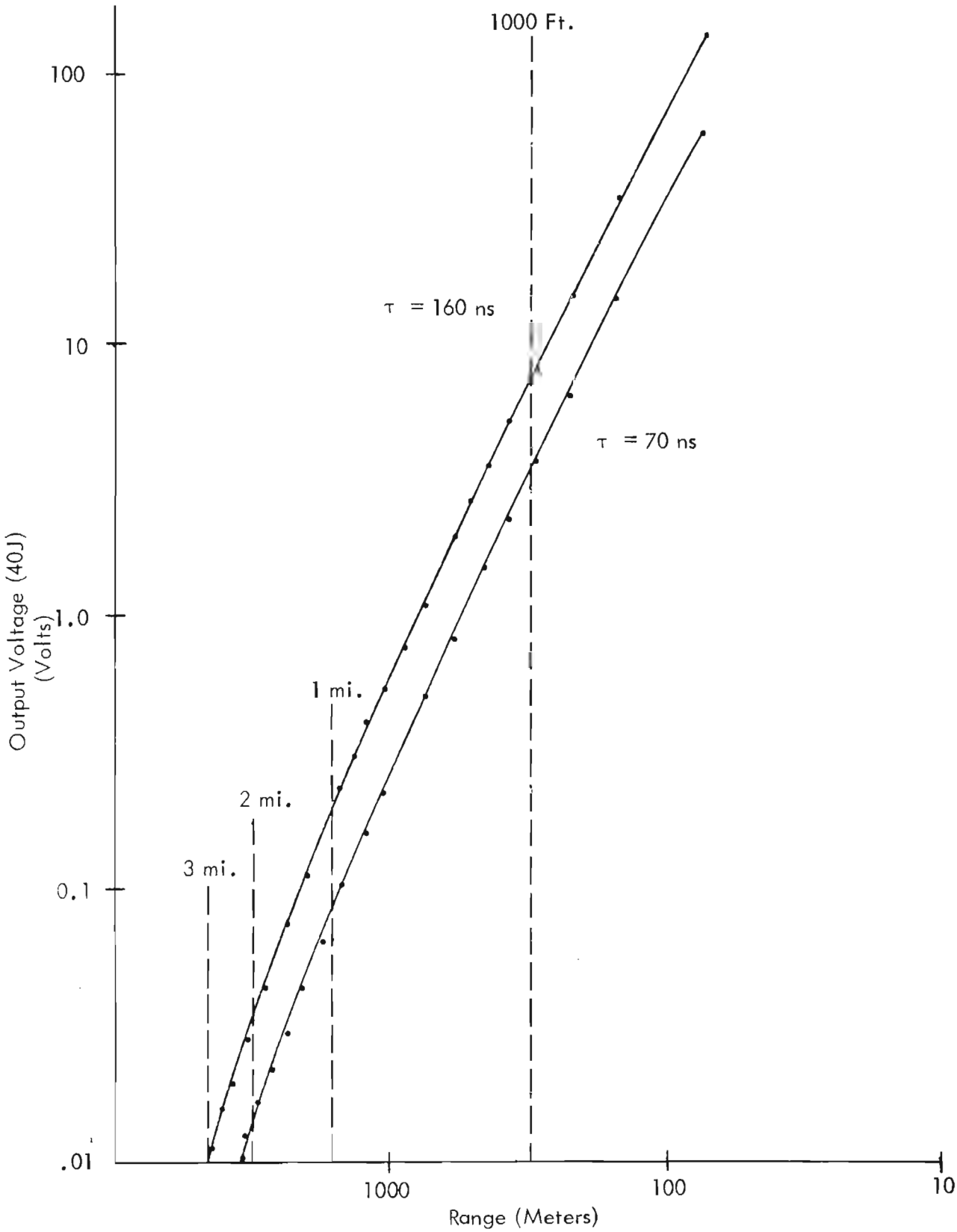

Figure 58. Output Voltage Amplitude of Preamp for Varying Range in Pulse Width.

Range	V_{out} Theoretical	V_{out} Experimental
123 m	0.064 V	0.07 V
164 m	0.036 V	0.05 V
201 m	0.023 V	0.03 V
283 m	0.012 V	0.02 V

A favorable comparison is shown between the calculated and experimental results.

2. LED Control Design. The source chosen for the LED ARTT system was the LD 235 Gallium-Arsenide diode manufactured by Laser Diode Laboratories. The LD 235 is a series-strung collection of 48 separate diodes and has a peak output power of 390 watts at a wavelength of 9025 angstroms, ± 25 angstroms. Following the procedure of Section V, B-1, the maximum range expected from this source when used with the SC-10 cell was approximately 3 miles. Due to power dissipation factors, the LD 235 can only be used in a pulsed mode of operation with a maximum repetition rate of 1000 pulses per second and a maximum pulse width of 200 nano seconds. A current pulse of 11 amperes minimum and 40 amperes maximum is needed to cause the diode to emit radiation.

The LED control circuitry is contained in two separate units. (See Figure 60 for photograph.) One unit is located in the cockpit and contains all of the operator switches and indicators. The other unit is mounted on the wing of the flight-test aircraft and contains the LED itself. The circuitry contained in these two units can be broken down into five subfunctions as indicated in Figure 59. These subfunctions are described in detail in the following paragraphs.

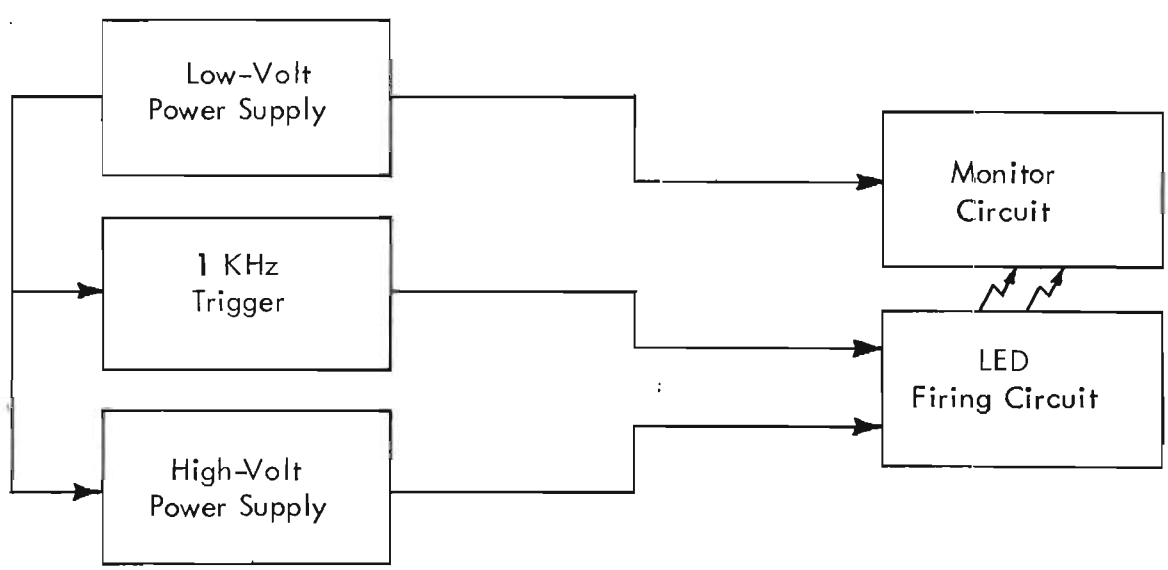

Figure 59. LED Control Block Diagram.

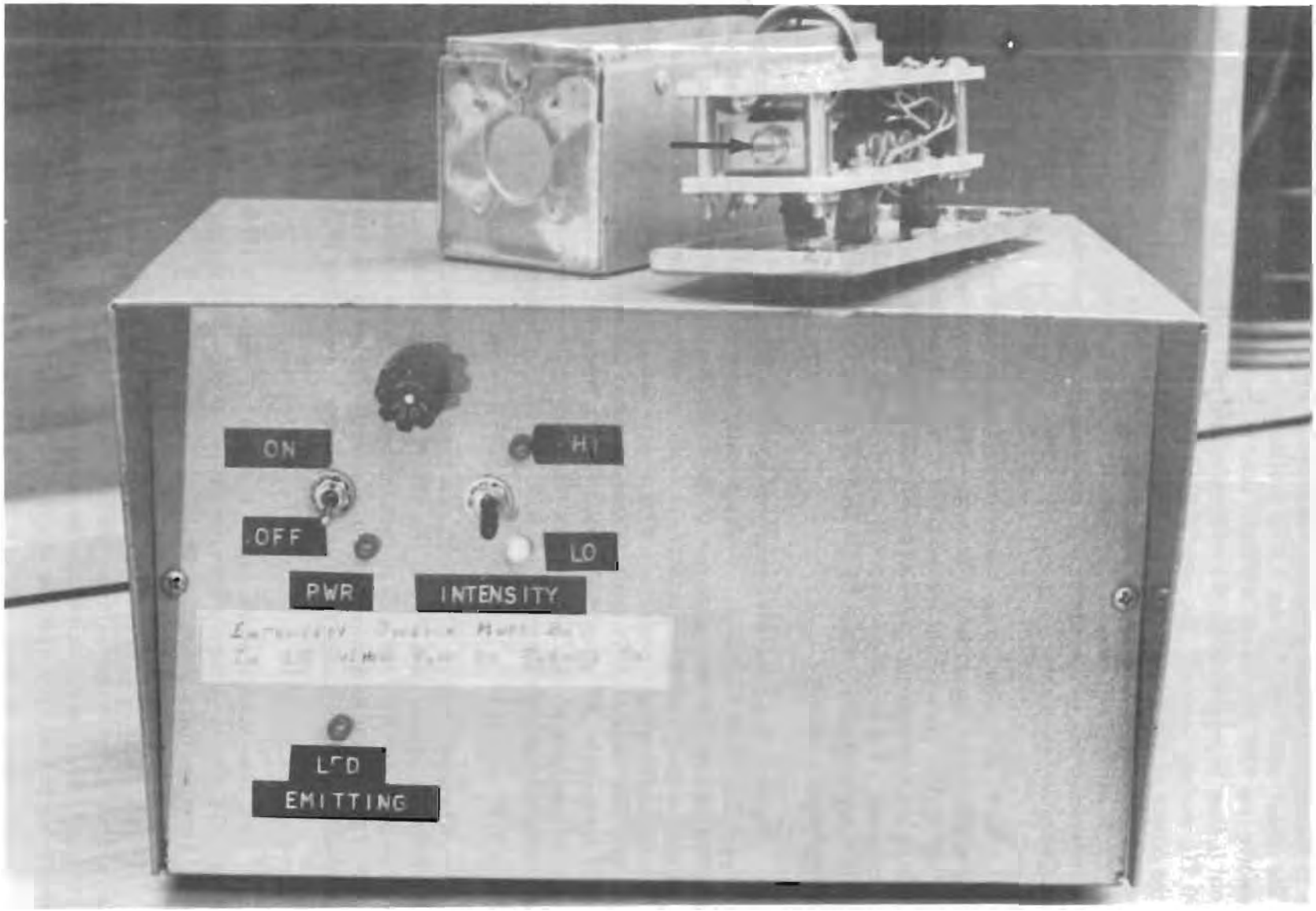

Figure 60. Light Emitting Diode Wing Unit and Control Box. Arrow designates LD 235 light emitting diode.

A crystal-controlled oscillator was required to establish the firing rate of the LED due to the high-Q filtering used in the receiver electronics, as will be discussed later. The circuit schematic for the 1 KHz oscillator is shown in Figure 61. Evident in the schematic is a 100 KHz Clapp oscillator used to derive a stable frequency source. This signal is then level shifted by Q1 to develop a signal suitable for TTL logic. Utilizing two 7490 TTL decade counters, the level shifted 100 KHz signal is divided by 10 twice so that at the output of the second 7490 is a 1 KHz pulse train. A 9602 one shot multivibrator is then used to achieve the required 200 ns pulse width. These 200 ns pulses are then level shifted to 13.7 volts by high-speed transistors Q2 and Q3. The final stage of the trigger circuit is located in the wing-mounted unit and consists of an emitter follower (Q4) for impedance matching purposes.

The high voltage power supply (Figure 62) is required to supply the charge stored in the LED firing capacitor. This high voltage is obtained from a standard DC-DC converter which utilizes a center tapped 6.3V filament transformer for voltage step-up. Two output voltage values are provided so that the LED may be used with either high or low output power. The high/low output is controlled by varying the regulated supply voltage to the astable multivibrator formed by Q1 and Q2. A μ723 IC regulator is used to provide the regulated supply voltage.

The high level current pulses that actually cause the LED to radiate are generated by the firing circuitry of Figure 63. In this circuit, transistors Q1 and Q2 are used to charge the capacitors rapidly and thus allow use of the firing circuitry at frequencies much higher than is possible with the standard resistive charging circuit. After the capacitors are charged to the high-voltage level the 1 KHz trigger signal then turns the SCR ON so that the capacitors discharge through the LED causing it to emit radiation. At the same time, Q1 and Q2 are turned OFF since the current flowing through CR1 and CR2 causes a one diode drop reverse bias on Q2. As long as the steady state current at the SCR anode from R_3 is less than the holding current of the SCR, the SCR will turn OFF as soon as the capacitors have discharged.

A monitor circuit, Figure 64, has been included so that a positive indication is provided in the flight-test aircraft that the LED is radiating. Phototransistor, Q1, receives back-scatter radiation from the LED so that the phototransistor is pulsed ON and OFF. This signal is then input to a monostable multivibrator which is used to stretch the pulses. This stretched pulse then is used to drive an indicator lamp on the LED control unit in the cockpit.

The low-voltage power supply is shown in Figure 65. This circuit develops the required 13V regulated supply from the 11-14V unregulated supply available on the Beechcraft Bonanza flight-check aircraft.

3. LED ARTT Receiver. The LED ARTT receiver is an optoelectronic receiver/processor and is used with a modified Warren-Knight Model 83 theodolite. The modifications to the theodolite include the addition of a 5-inch lens diameter Celestron reflecting telescope and the addition of slip-clutched servo-motors to both the vertical and

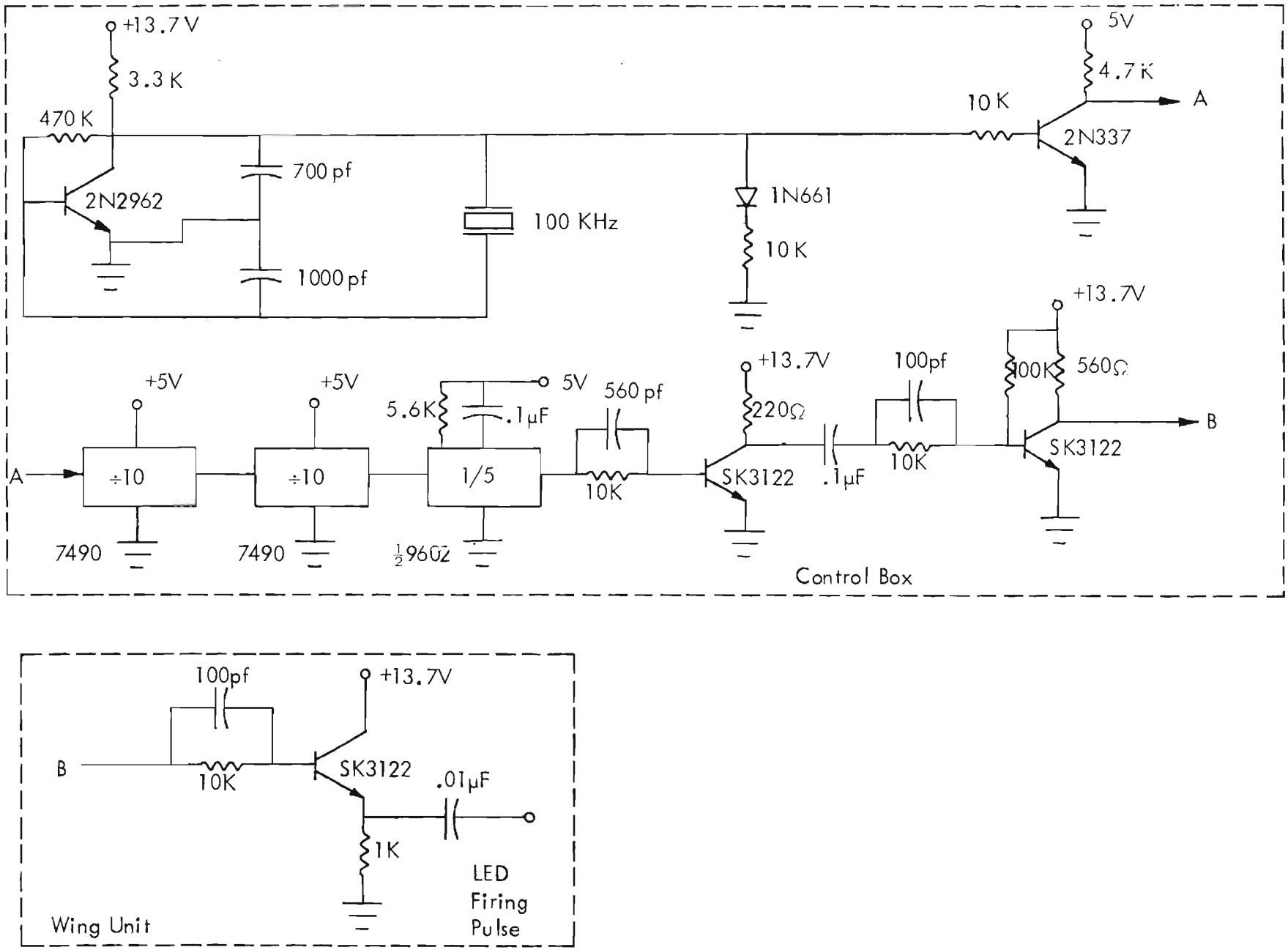

Figure 61. 1 KHz Trigger Circuit.

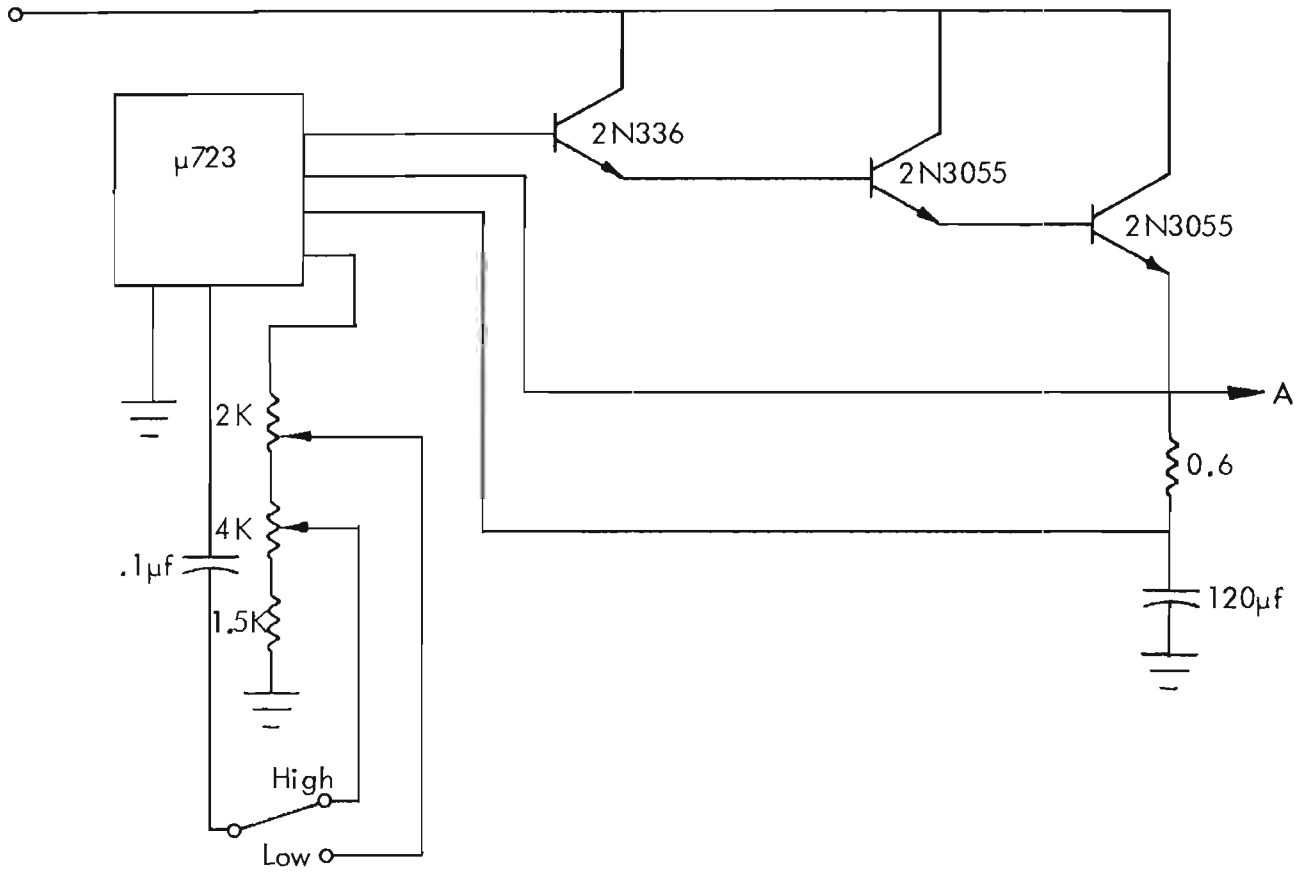

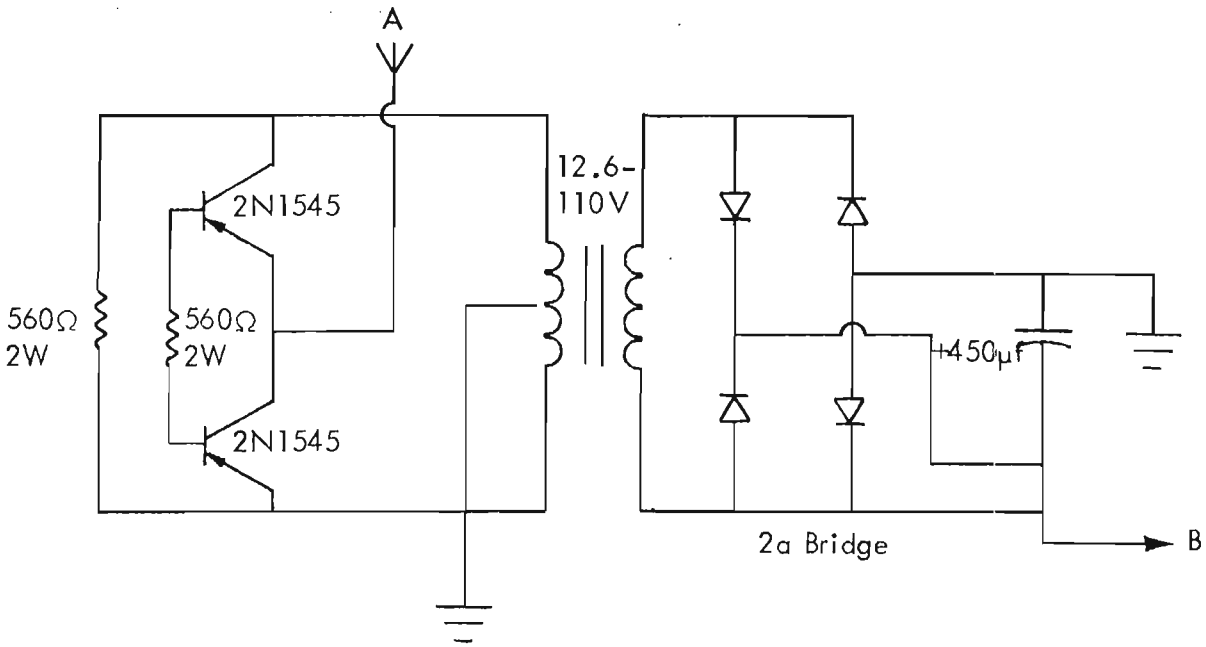

Figure 62. High Voltage Power Supply.

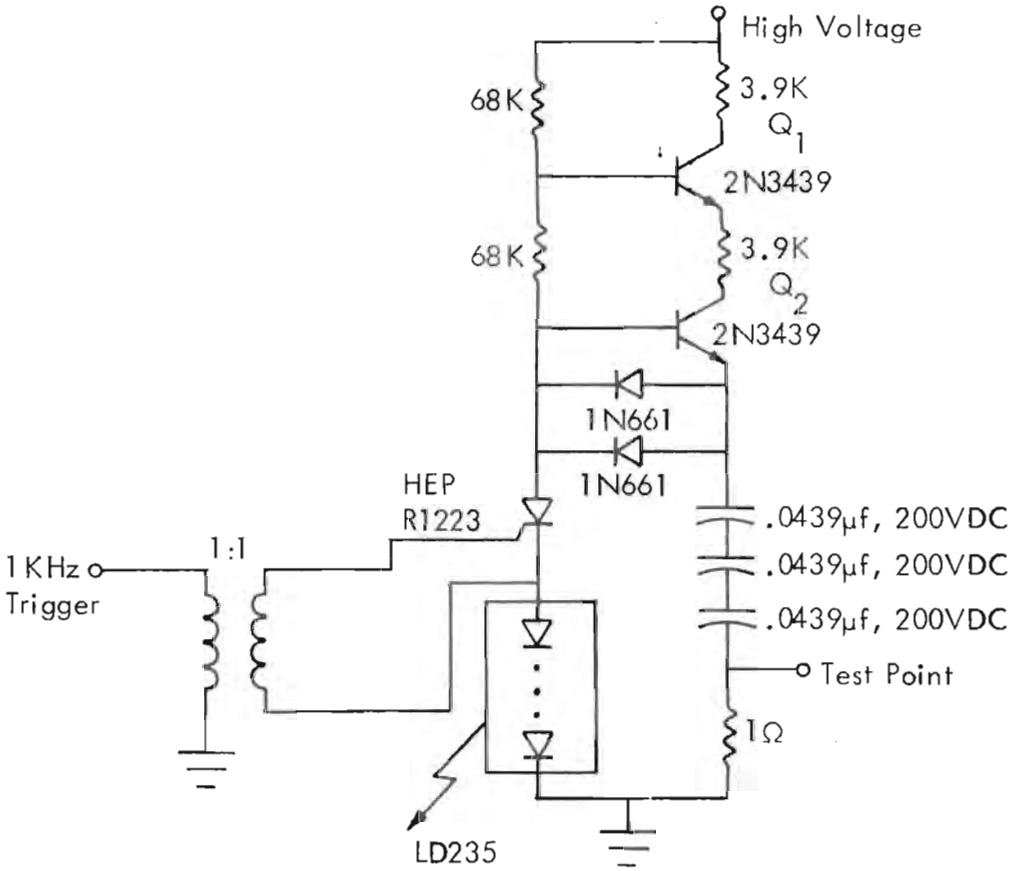

Figure 63. LED Firing Circuit.

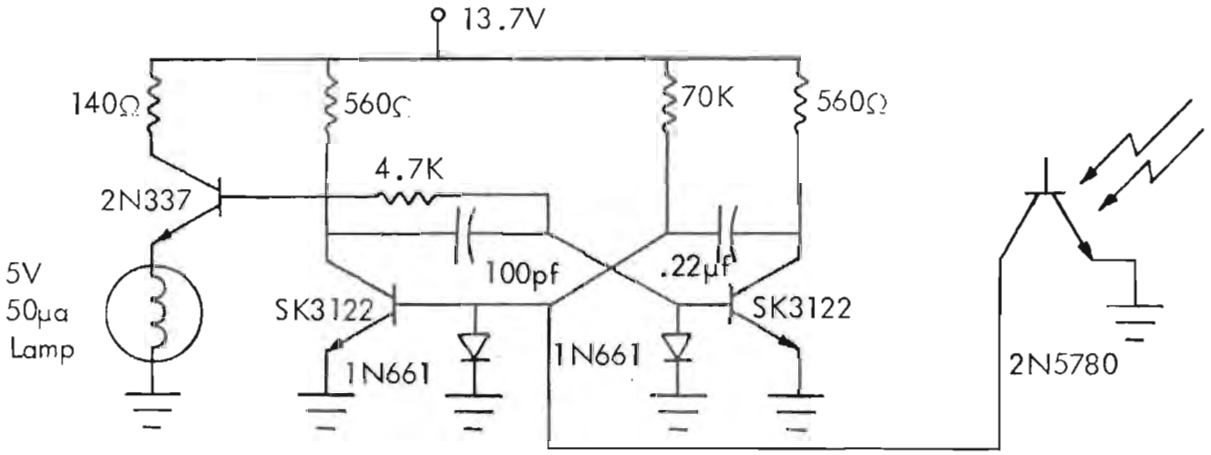

Figure 64. LED Monitor Circuit.

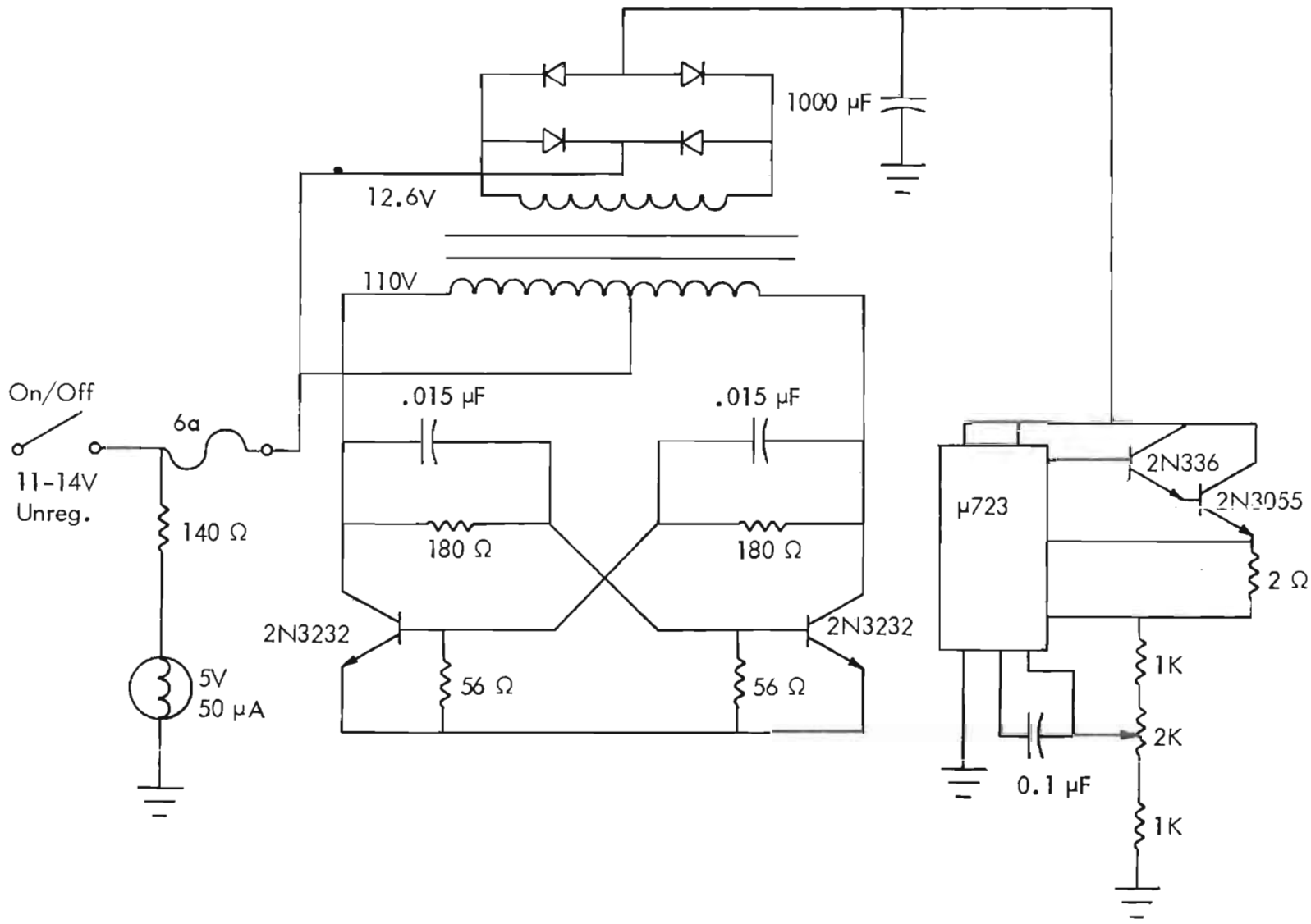

Figure 65. Low-Voltage Power Supply.

horizontal theodolite axes. The Celestron telescope, together with a United Detector Technology SC-10 photodetector, comprises the optical receiver portion of the system. Two electronic modules, one a high gain amplifier unit and the other a signal processor unit, are required to generate the servo-control signals. The detailed design of the LED ARTT receiver along with some preliminary analysis is discussed in the following paragraphs (See Figure 66).

The SC-10 photodetector is essentially the heart of the ARTT system and is a PIN photodiode with a 1.0 cm^2 sensing area. It provides positional information, in two axes, of the centroid of the light spot on the cell. An equivalent circuit for the SC-10 (one axis only) is given in Figure 67. The magnitude of current I_s is determined by the intensity of the light on the cell and I_1 and I_2 are determined by the position of the centroid of the light spot on the cell. In the configuration used in the ARTT design (See Figure 69) the equivalent circuit of the SC-10 with the light spot centered becomes that of Figure 68. Typical values are $R_s = 20\ K\Omega$ and $C_D = 400$ pf so that the cutoff of the cell is 80 KHz. Some decrease in junction capacitance C_D is obtained by back-biasing the photodiode. This also has the added advantage of doubling the light sensitivity of the diode. Use of the Celestron telescope with the diode provides an optical gain of approximately 126. A data sheet for the SC-10 is included in Appendix C.

The receiver preamp unit is a dual-channel, high-gain amplifier unit mounted on the theodolite tripod to reduce lead length between the preamp and the SC-10 photocell, hence reducing stray capacitance. The schematic for the preamp is given in Figure 69. The first stage amplifier is an FET input Analog Devices AD40J used in a current-to-voltage converter configuration. The amplifier is cut off at 800 KHz, which is an order of magnitude greater than the cutoff of the SC-10 so that the total circuit response is determined by the physical characteristics of the SC-10. The second stage of the preamp is an Analog Devices AD528J amplifier. This stage is a threshold amplifier which limits the shot noise produced by the cell. At the input of this amplifier the noise has a higher 1 KHz component than the signal due to the small duty cycle of the signal. With the threshold adjustment set just above the average peak noise voltage, the only noise passing through the amplifier will be that riding on top of the short signal pulse. The 1 KHz component of this noise is much smaller than that of the signal. The total preamp gain from the cell to the output of the noise threshold circuit is $2(10^7)$. This brings the level of the signal up to where it can be processed by the rest of the circuitry.

The pulse signal out of the preamp is then fed to the processor unit. Figure 70 shows one channel (typical) of the processor unit's bandpass filter and precision rectifier circuits. Amplifiers A1-A3 form a second-order state-variable bandpass filter with a center frequency of 1 KHz and a Q of 25. This filter is used to remove all but the first harmonic from the input signal. The state-variable bandpass-filter configuration was chosen for several reasons. First, neither the center frequency nor the Q drift significantly with temperature or amplifier gain. This is very important. If the center frequency were to change, the processor would not produce the proper control voltage. Second, the adjustments for center frequency and Q can be made independent, thus allowing for easy tuning of the bandpass filters. The amplitude of the sine wave output of the filters is proportional to the magnitude of the current out of the SC-10. This 1 KHz sine wave is

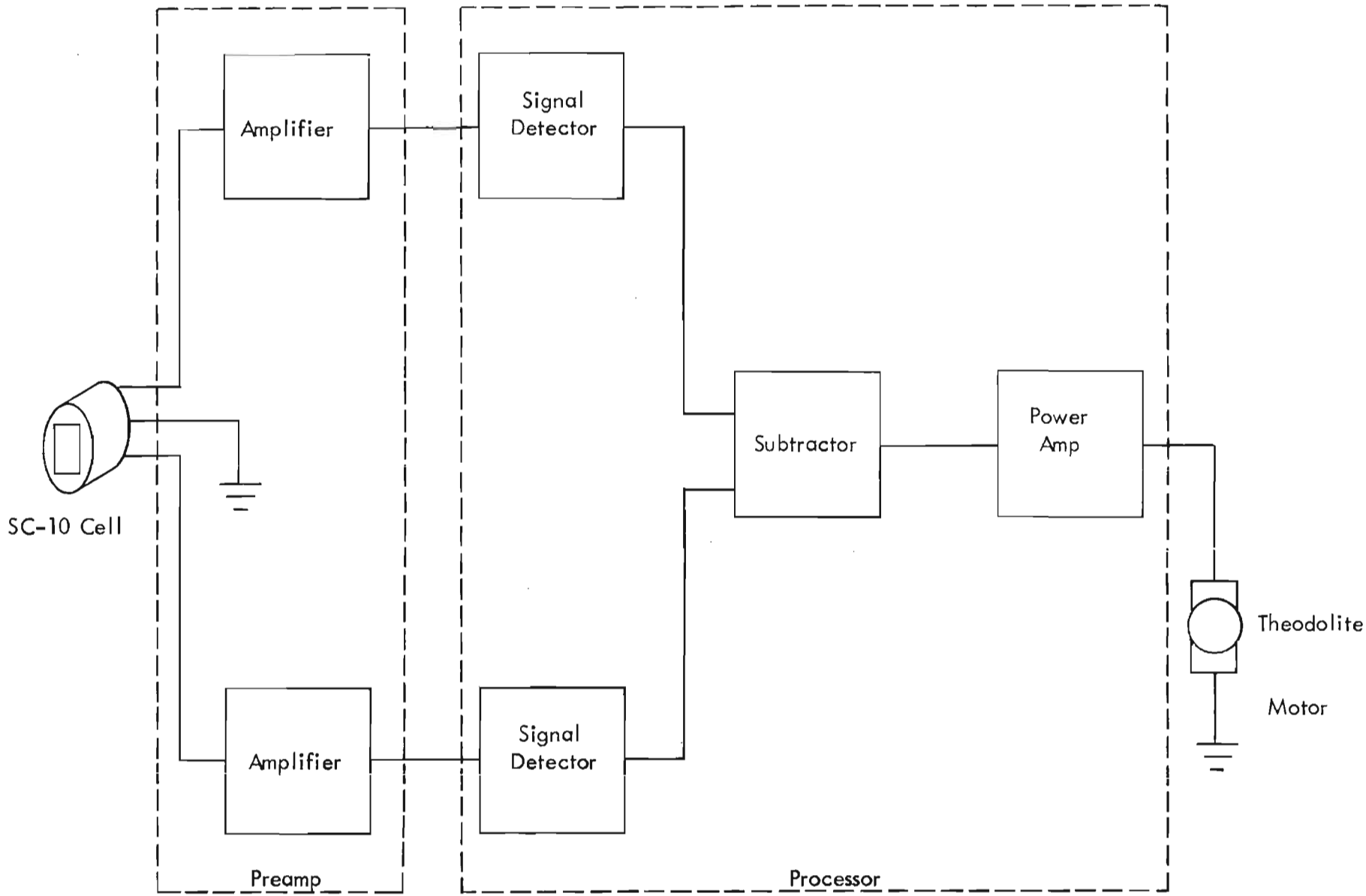

Figure 66. LED Receiver Block Diagram.

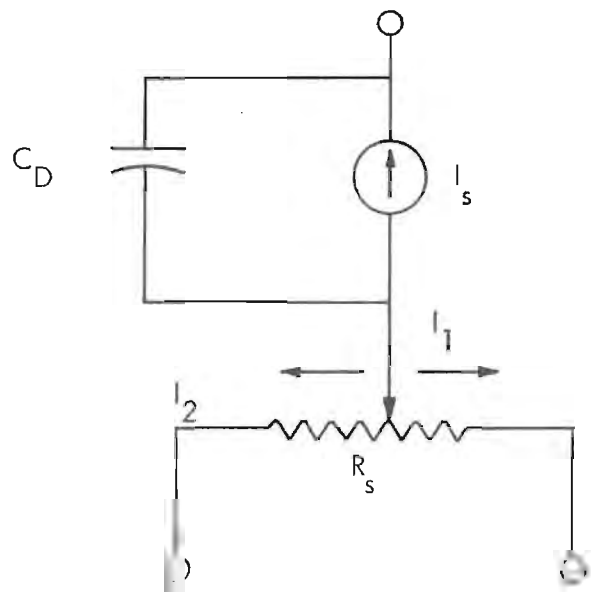

Figure 67. SC-10 Photodetector Equivalent Circuit.

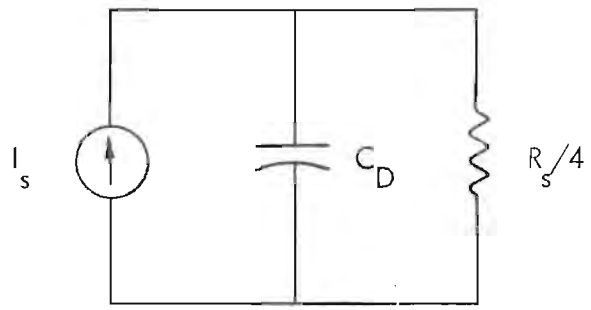

Figure 68. SC-10 Photodetector Utilization.

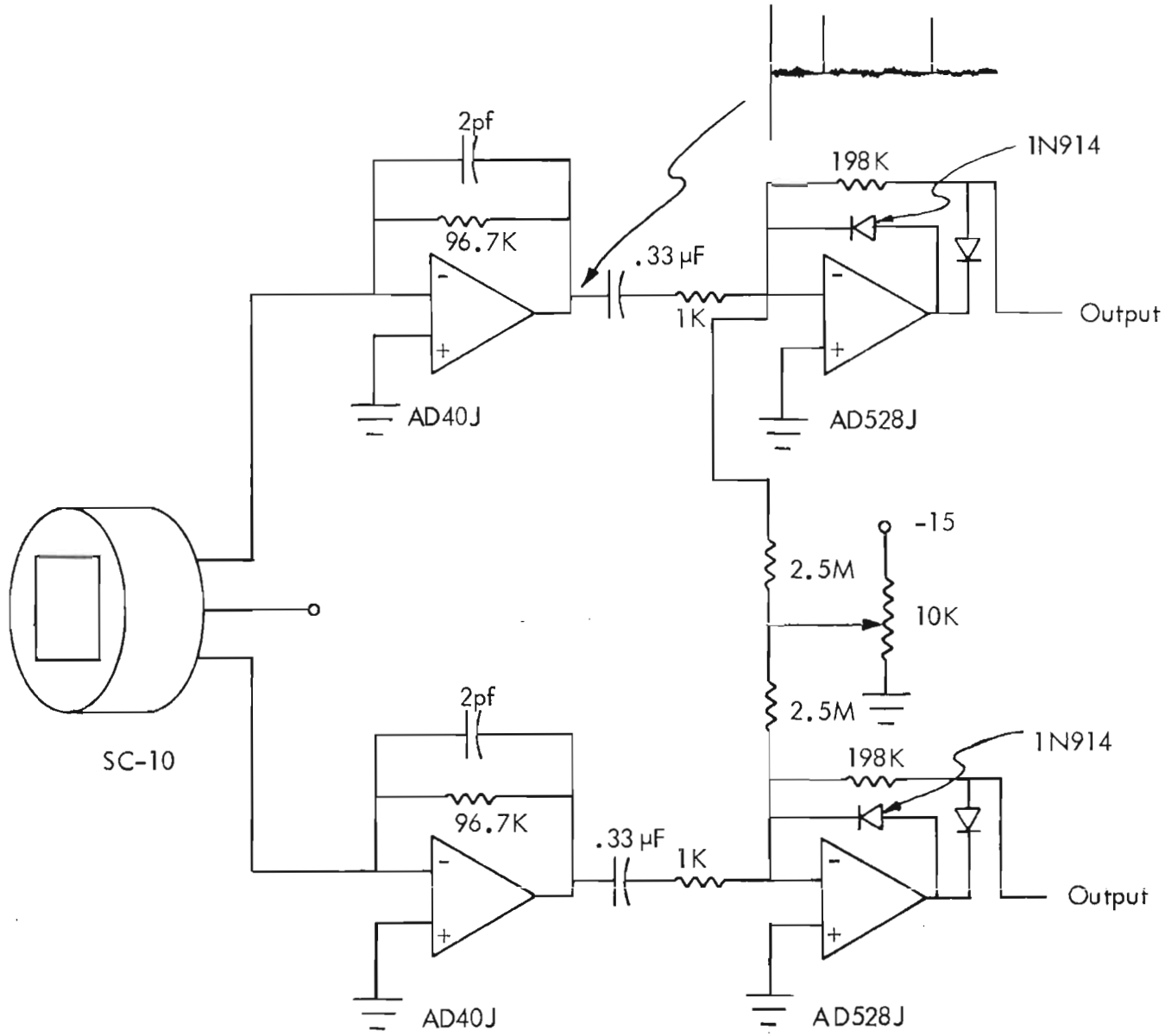

Figure 69. ARTT Preamp.

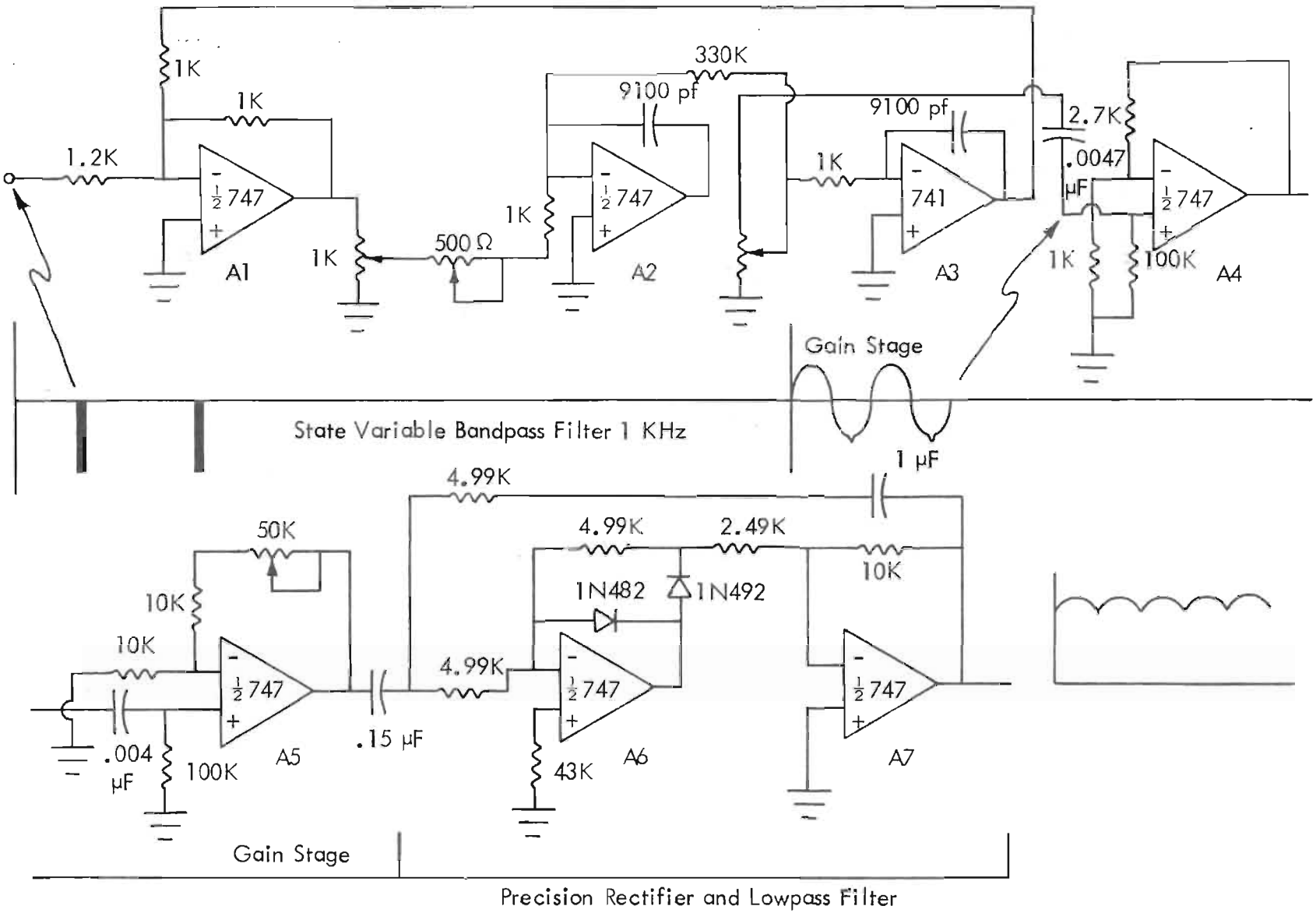

Figure 70. ARTT Amplifier and Bandpass Filter (One Channel).

then amplified by A4 and A5 and then rectified and filtered by A6 and A7. The result is a DC voltage which is proportional to the magnitude of the current out of the SC-10.

The final section of the receiver/processor is the DC processor as given in Figure 71. The outputs of the two rectifier/filters are input to the differential amplifier formed by A1. The signal out of A1 then is the error signal; i.e., the signal out is proportional to the amount of displacement of the light spot on the cell in relation to the center of the cell. The signal is then amplified by A2 and A3. The gain of A2 is variable via a front panel control and A3 is a power amplifier suitable for driving the theodolite motors. Meter M1 is provided as a front panel monitor on the error signal.

The circuit for the receiver power supply is shown in Figure 72. This provides the four voltage levels required for the operation of the receiver. The ± 24 volt supplies are used to power the final amplifier and the theodolite motors while the ± 15 volt supplies are used by the rest of the circuitry.

Chassis ground potentials of the preamp and processing unit differ by 15 volts. The reason for this is to provide an easy method for back-biasing the cell. The two chassis must therefore be insulated from each other. The power supplies are current limited so that no permanent damage will result if the insulation fails; but the unit, of course, will not operate properly.

C. Telemetry Interface. In the course of testing tracking equipment developed under the automatic radio telemetering theodolite (ARTT) program, it is necessary to provide angle output information in the form of a potentiometer setting for operation of the video ARTT and the static ARTT, the latter described in FAA RD-74-214. The potentiometer replaces the one normally located on the Warren-Knight Model 83 theodolite, which determines the relative 90/150 Hz modulation components produced in the telemetry transmitter. However, with the video and static tracker, the target aircraft angular information is in the form of a voltage; thus, there is a need for a converter unit.

The converter unit designed for the ARTT accepts angle information in the form of voltages from tracking devices, and provides outputs in the form of potentiometer settings suitable for use with telemetry transmitters. A second function has been incorporated into the converter, namely a complete, low-sensitivity receiver which monitors the output of the telemetry transmitter and provides an accurate check of the telemetered information on a large panel meter displaying conventional course deviation indicator (CDI) current values. This inclusion provides the opportunity for additional monitoring of the telemetry transmitter, as will be described later.

1. Operating Considerations and Functional Design. The angle input voltages to be handled by the converter may have ranges of ± 1 volt up to ± 5 volts, centered approximately at ground or at + 15 volts. Thus, stepped and variable input offset and variable gain are provided by the input signal conditioning section. The full-scale output of this section is ±5 volts, ground-referenced, for all input signals.

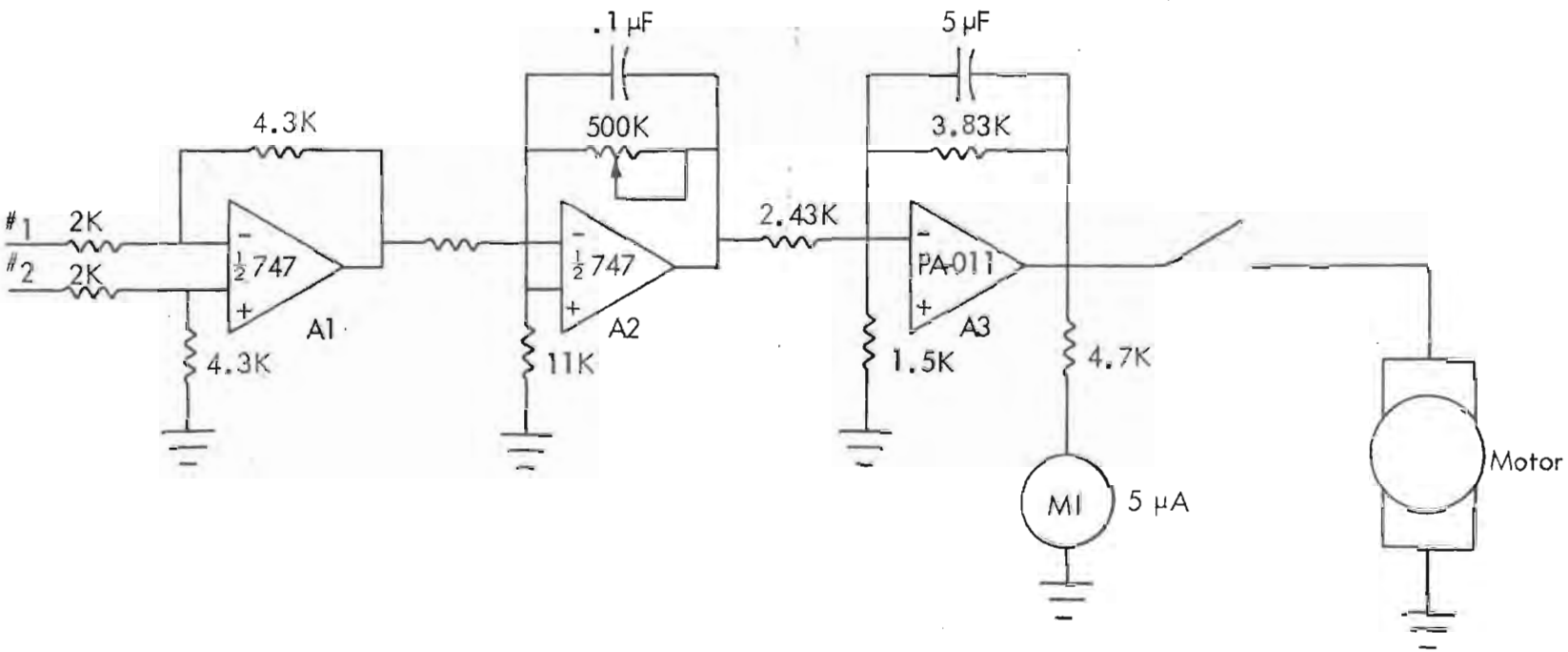

Figure 71. DC Processor Circuit.

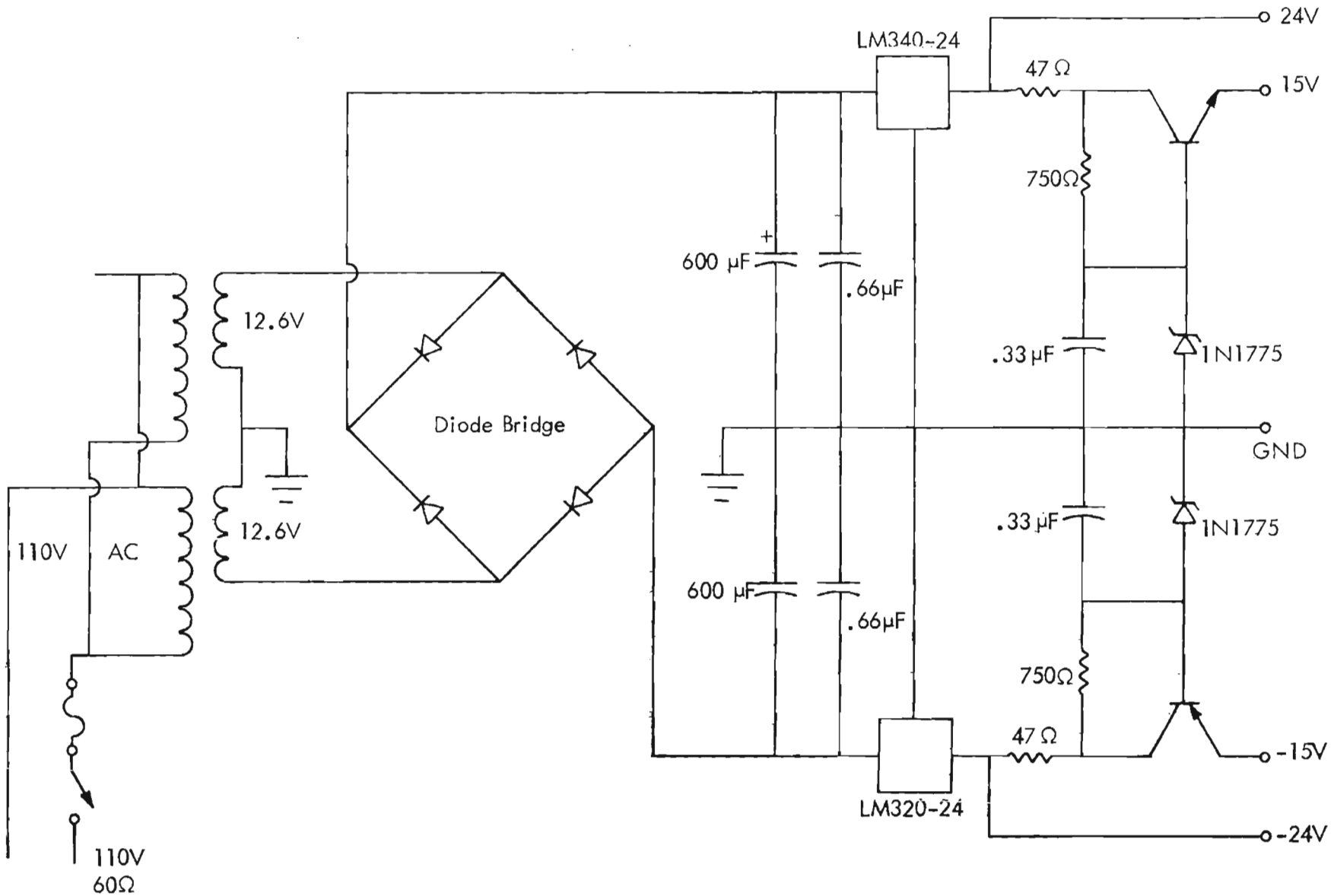

Figure 72. Receiver Power Supplies.

The voltages from the input signal conditioning section are passed on to an electromechanical servo-system which performs the conversion of voltages to potentiometer settings. The loop contains two ganged potentiometers driven by a small DC motor through an appropriate reduction gear. Variable gain and damping controls were considered desirable to permit optimizing the servo to each specific input device.

The tone receiver is merely an untuned diode detector which rectifies a small portion of the telemetry transmitter power. The detector is followed by a 90/150 Hz tone decoder board which is a slight modification of the high-linearity decoder developed earlier in this program for flight checking the Warts slotted-cable glide slope. The modification provides an increased CDI output voltage level for compatibility with the servo-loop portion of this interface unit. With this modification, the CDI output of the tone decoder board may be selected as the "position" feedback voltage to the servo-system. This option is discussed more fully in Sections 2b and 2d.

A block diagram of the converter/receiver unit is shown in Figure 73.

2. Detailed Circuit Description.

a. Signal Conditioning Section. Figure 74 shows a detailed circuit diagram of the signal conditioning section. The input high signal is on the innermost conductor of the three-circuit jack, and any accompanying reference is on the next outer conductor. The outermost conductor is the common ground. The INPUT jack levels are repeated on a RECORDER jack so that recordings may be made at this circuit location if desired. A gross offset of +15 volts is subtracted from the input signal by a zener diode if the OFFSET switch is in the 15 volt position. In addition, offsets of up to ±3.5 volts can be nulled out by use of the CENTERING control. The second 741 amplifier, in addition to providing the continuous offset range, provides also a variable gain function of 0.5 to 4, determined by the setting of the SCALE control. The purpose of the above is to provide a standard output of ±5V full-scale for the various input signals. A zero-center meter indicates the output of this second 741 and facilitates setup adjustments. A decoupling filter is used to isolate this section from the ±15 volt supply which powers the remainder of the unit.

b. Servo-Loop. Figure 75 shows the circuit details of the servo-loop. The ±5V full-scale input is compared to the position feedback voltage and the difference drives the first 741 amplifier. This stage provides a voltage gain of fifteen, and is cornered at about 0.75 Hz to reduce noise band width. Following a screwdriver-adjust GAIN control, a second 741 serves as the power amplifier for the DC motor which drives the potentiometers. The DC motor is a miniature Swiss unit identical to those used to drive the two axes of the modified Warren-Knight Model 83 Theodolite (See SRDS Report RD 73-137) in the dynamic ARTT program. Its loaded current is a modest 10 milliamperes (mA), which is easily provided by the 741. A third 741 is used as a differentiator to provide the rate input to the power amplifier. This input may be adjusted with the RATE control.

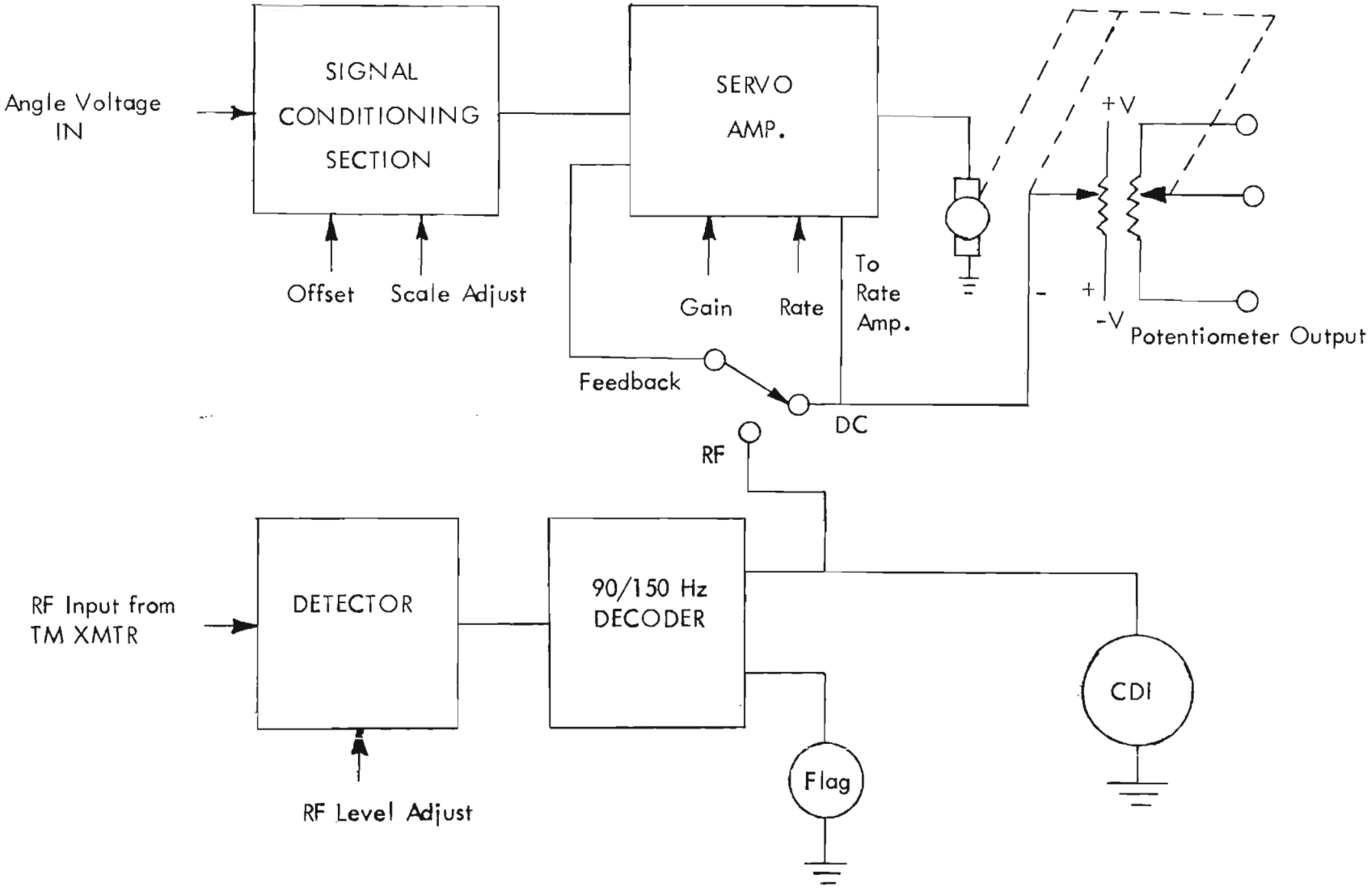

Figure 73. Block Diagram of the Converter/Receiver.

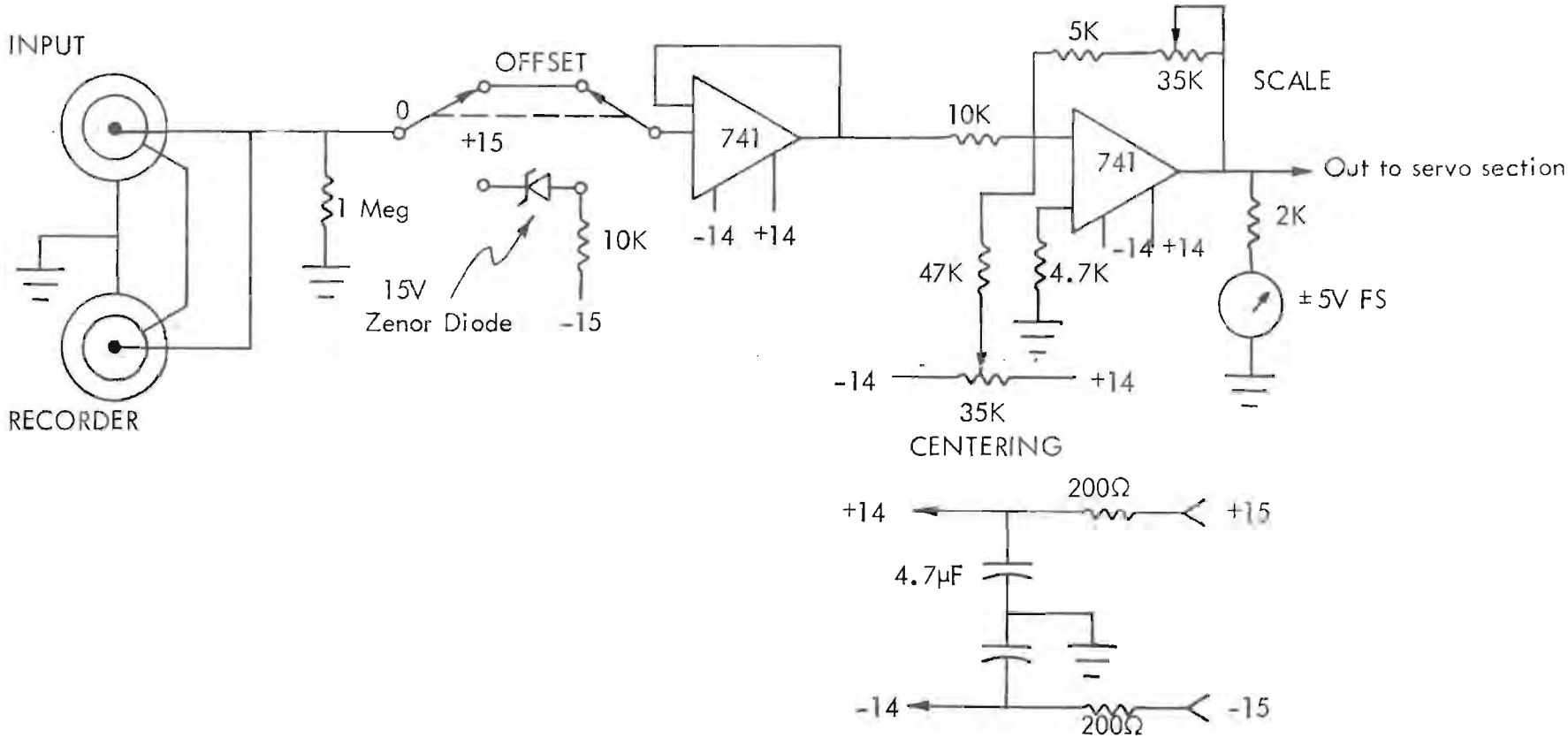

Figure 74. Signal Conditioning Section Circuit Diagram.

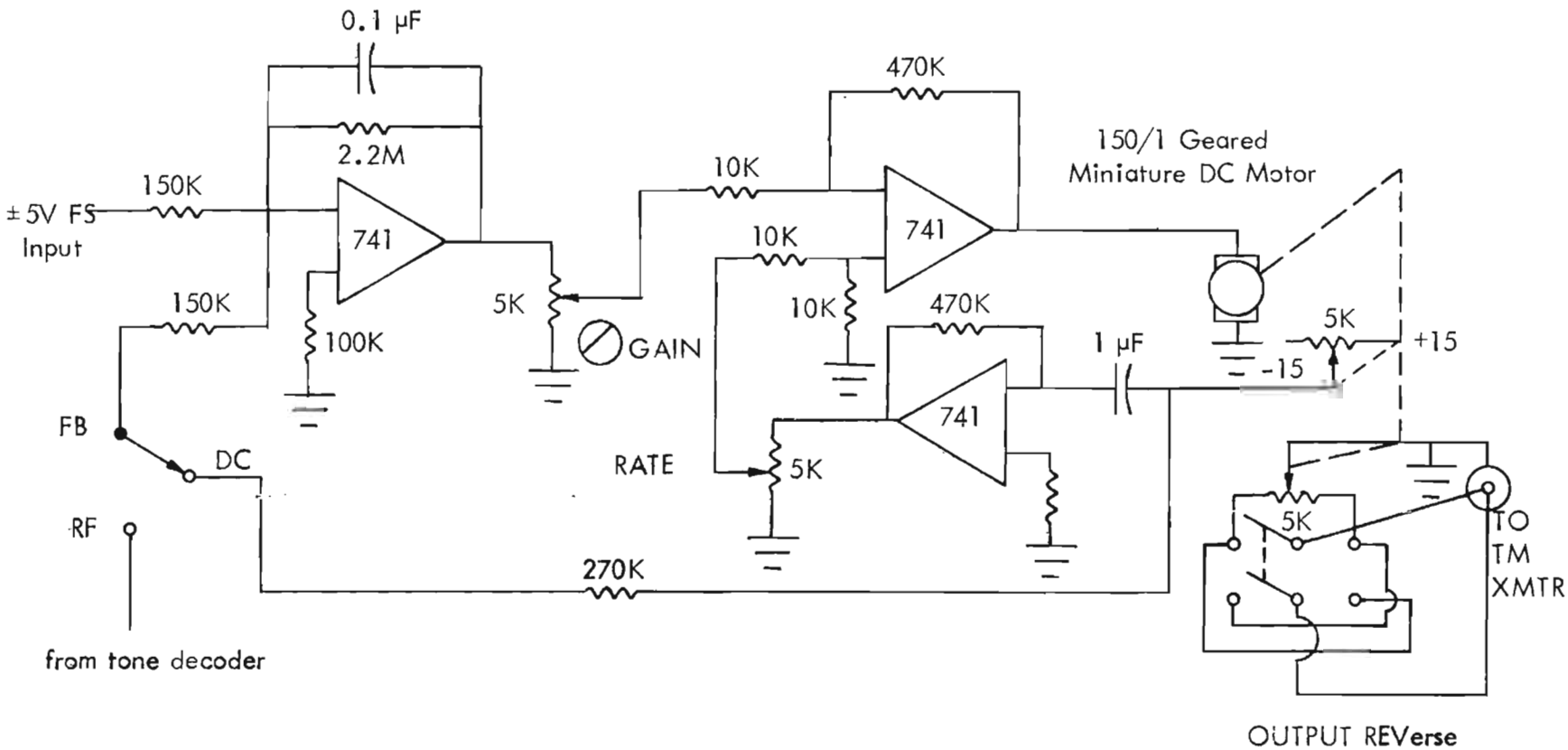

Figure 75. Servo-Loop Circuit Diagram.

The motor drives a 150:1 speed reducer, which in turn drives two 5K precision linear potentiometers. The first of these is used as a position follower from which rate information is derived, and is also the usual source of position feedback voltage. A switch permits the operator to choose between this position voltage and the output of the tone decoder as the feedback voltage returned to the servo input for comparison. The second potentiometer goes to the TO TM XMTR jack through the OUTPUT REVerse switch which enables reversal of the sense of potentiometer rotation.

c. Receiver. Figure 76 shows the receiver circuit diagram. The receiver section is coupled to the telemetry transmitter RF output by means of a 20 dB directional coupler. Its sensitivity is intentionally very low, so that other local RF signals in the 330 MHz range will produce no spurious responses. This is necessary because the equipment normally operates within a few dozen feet of the glide-slope transmitter site. After entering at the RF INput jack, the RF is applied to an untuned diode detector. The detector output passes through an RF filter and on to the SENSitivity potentiometer, thence to the tone decoder board.

d. Tone Decoder. The tone decoder, shown in Figure 77, is a minor modification of a design developed earlier at the Avionics Engineering Center. This design uses all active filters to recover the 90 Hz and 150 Hz tones, avoiding the use of iron-core inductances and their associated problems. The particular version for this application provides ± 5V output levels corresponding to 0.175 DDM, thus providing compatibility with the output of the signal conditioning section. Therefore, the actual DDM output from the tone decoder may be used as the feedback voltage to the servo-loop if desired. This option is available through the DC-FB-RF switch shown in Figure 75. When the CDI voltage is used to provide position feedback information to the servo-loop, the telemetry transmitter becomes a part of the servo-loop, and the loop drives the potentiometer to produce a specific output from the tone decoder, thus eliminating any non-linearities which may arise in the modulation and characteristic of the telemetry transmitter.

e. Power Supply. A packaged power supply (Analog Devices 902) provides regulated ± 15 volts at 100 mA for operation of the entire converter/display unit. The complete circuit diagram is shown in Figure 78.

3. Laboratory Tests. The converter/display unit was tested using the setup shown in Figure 79. The digital power supply was used to provide input signals from zero to ± 5.000 volts, equivalent to the maximum expected range of input signals. The Reaction Instruments Model 6050 Telemetry Transmitter is the one currently in use in the field by the FAA. The potentiometer output of the converter establishes DDM in the telemetry transmitter. Fifty milliwatts of modulated RF is coupled from the transmitter output to drive the receiver.

Data was taken for ± 5V input ranges using the DC feedback available internally in the converter/display unit. Table 4 presents this data. The central 40 percent of the range is error-free, and the extremities reveal an error of approximately 2 percent. This data is also plotted in Figure 80.

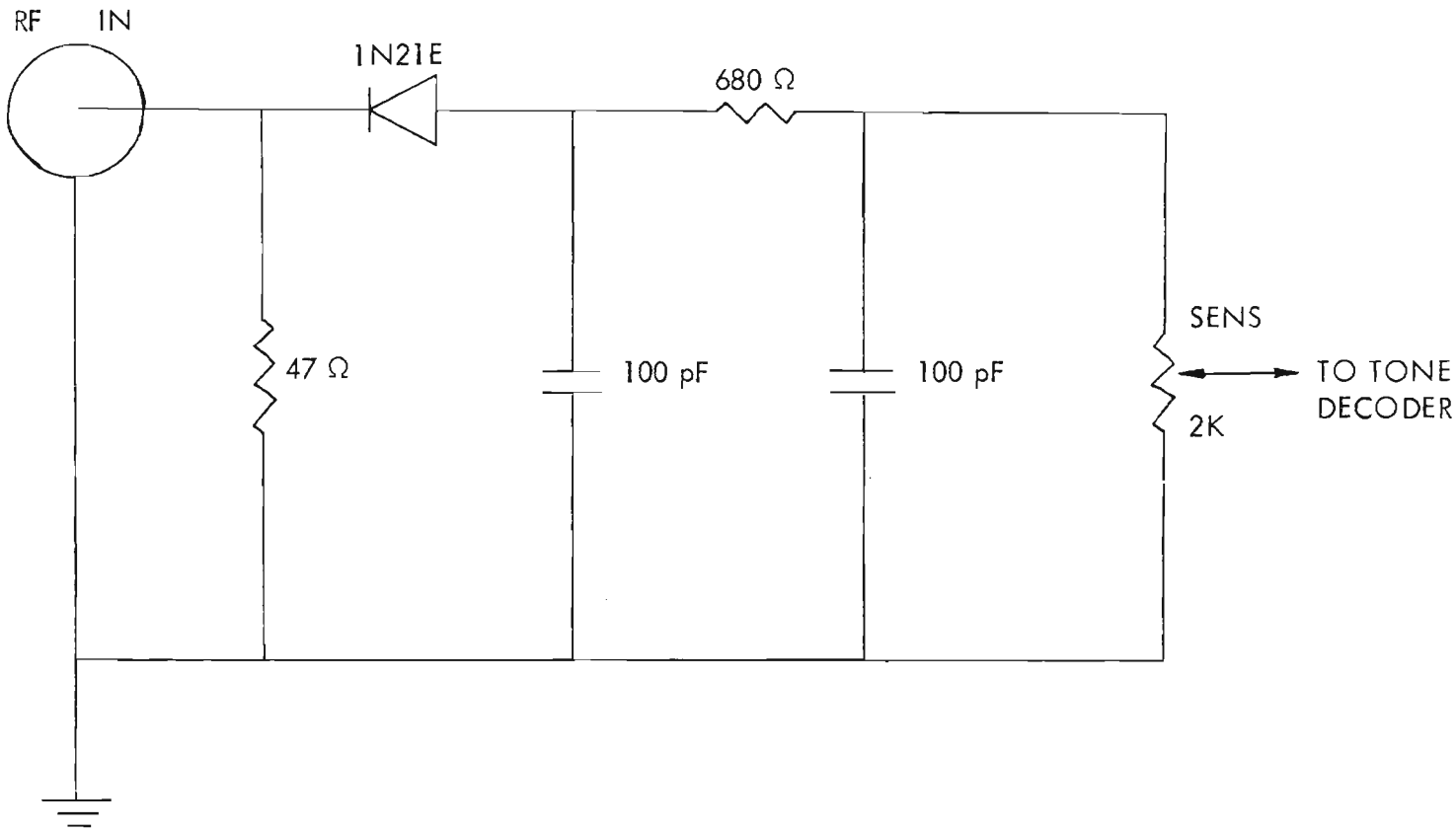

Figure 76. Receiver Circuit Diagram.

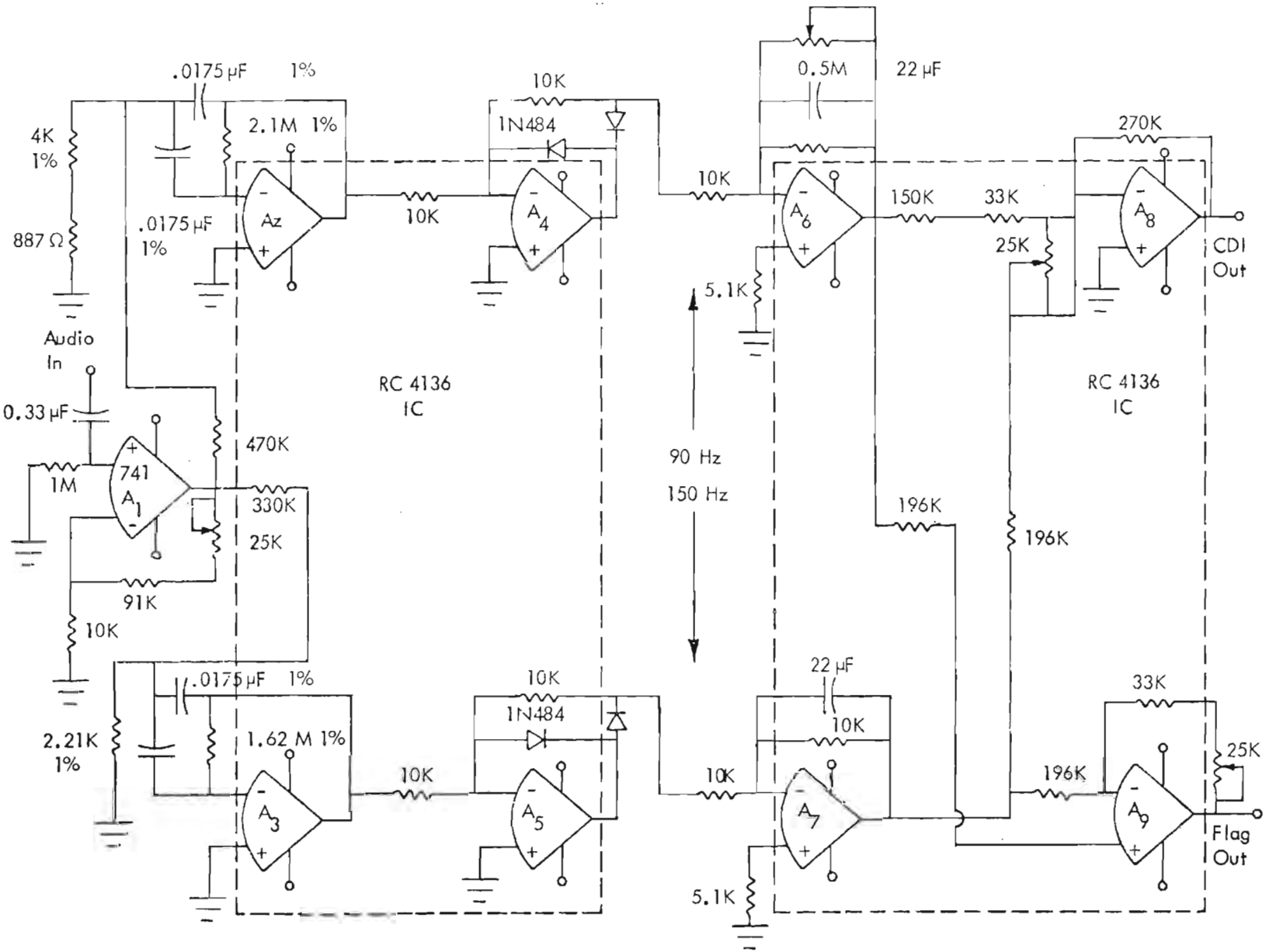

Figure 77. Tone Decoder Circuit Diagram.

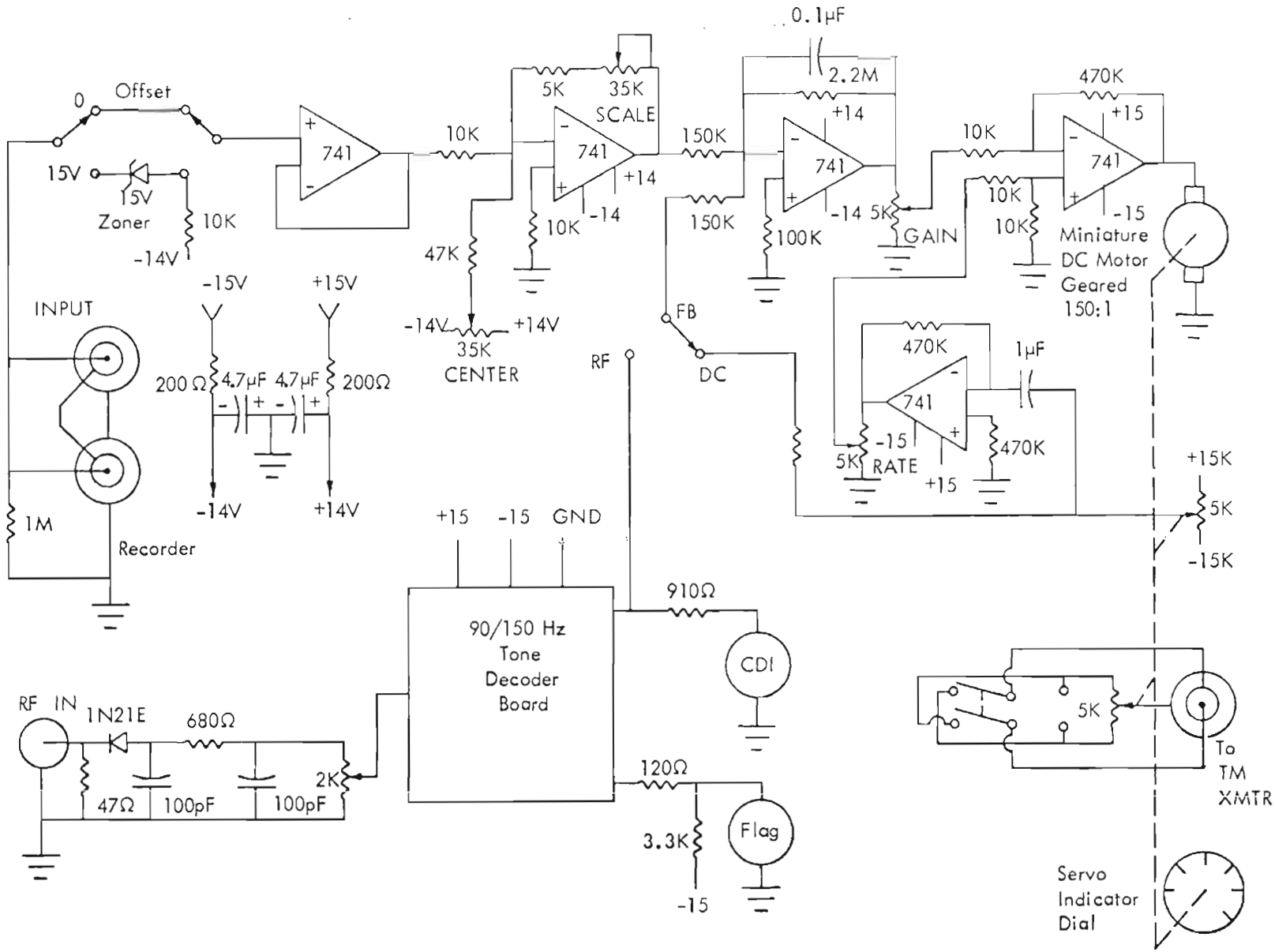

Figure 78. Complete Circuit Diagram of Converter/Display.

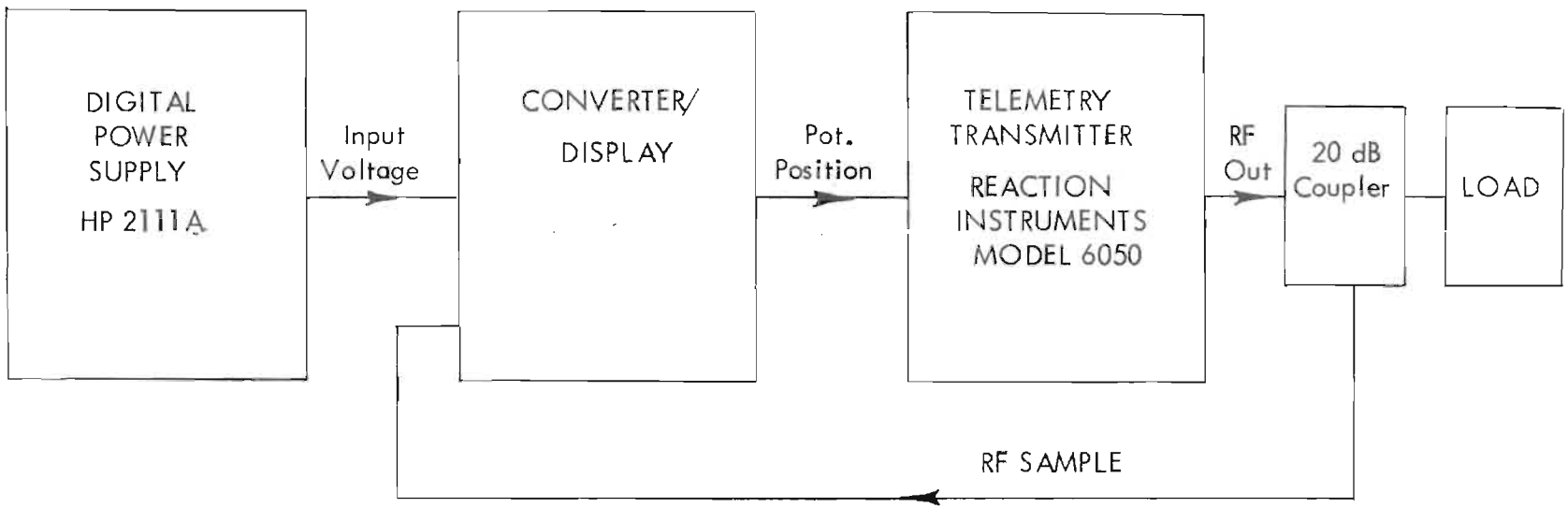

Figure 79. Test Setup for Converter/Display.

V_{in}	CDI Reading		TM Meter (DDM)
+5.000	150		0.180
+4.000	122		0.145
+3.000	92	90Hz	0.110
+2.000	61		0.072
+1.000	30		0.035
0.000	0		0
-1.000	30		0.035
-2.000	60	150Hz	0.070
-3.000	91		0.110
-4.000	122		0.148
-5.000	154		0.183

Table 4. Laboratory Test Data on Converter/Display Unit.

A second data set was taken, utilizing feedback available from the receiver's CDI circuit. This data appears in Table 5.

V_{in}	CDI Reading	TM Meter (DDM)
2.500	148	0.178
1.500	88	0.109
0.500	31	0.035
0.000	0	0
-0.500	29	0.033
-1.500	89	0.105
-2.500	145	0.175

Table 5. Laboratory Test Data on Converter/Display Unit (RF Feedback).

This data reveals a slightly higher error, averaging about 2 1/2 percent over the range. This increased error is attributed to non-linearities of the DDM modulator circuits in the telemetry transmitter. Figure 81 is a plot of this data.

Figure 82 presents a strip chart recording of the response of the converter/display unit to a stepped input. In this case, the potentiometer output was used as a voltage divider to provide the input voltage to the recorder. Excellent linearity is shown on the record.

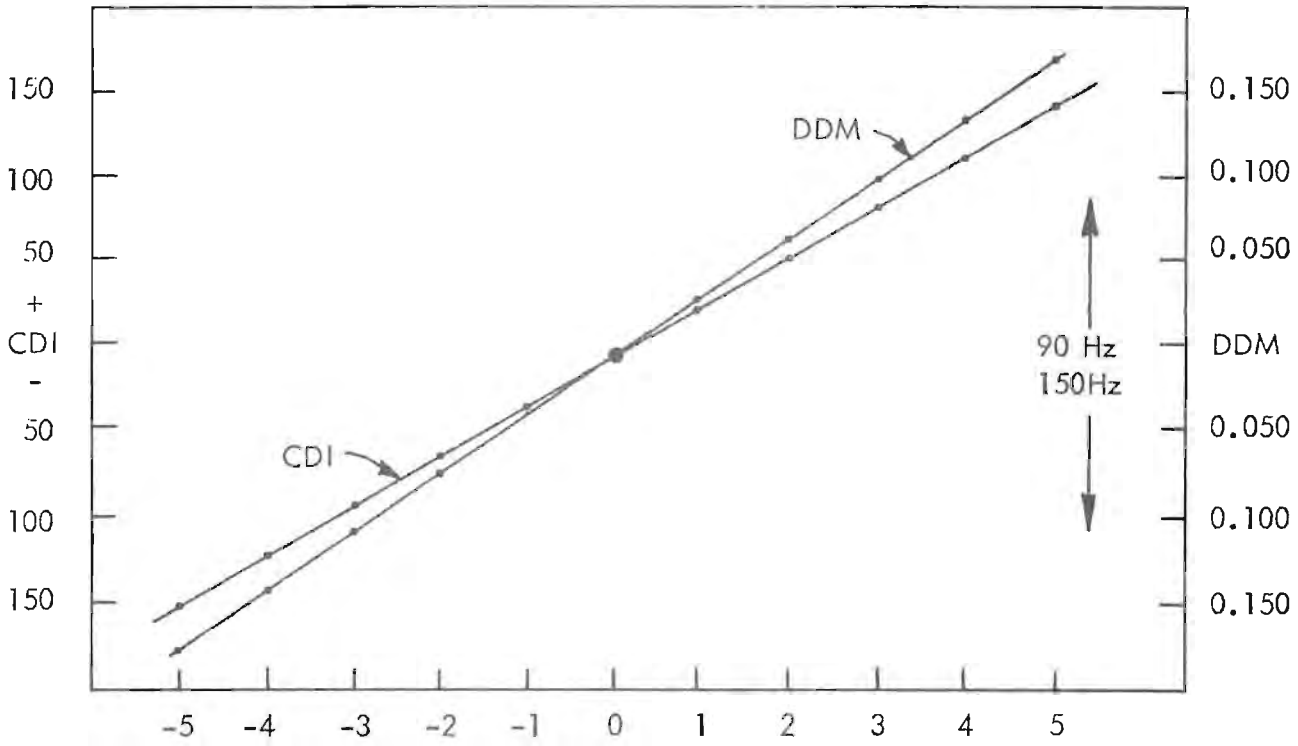

Figure 80. Calibration of Converter/Receiver Using DC Feedback.

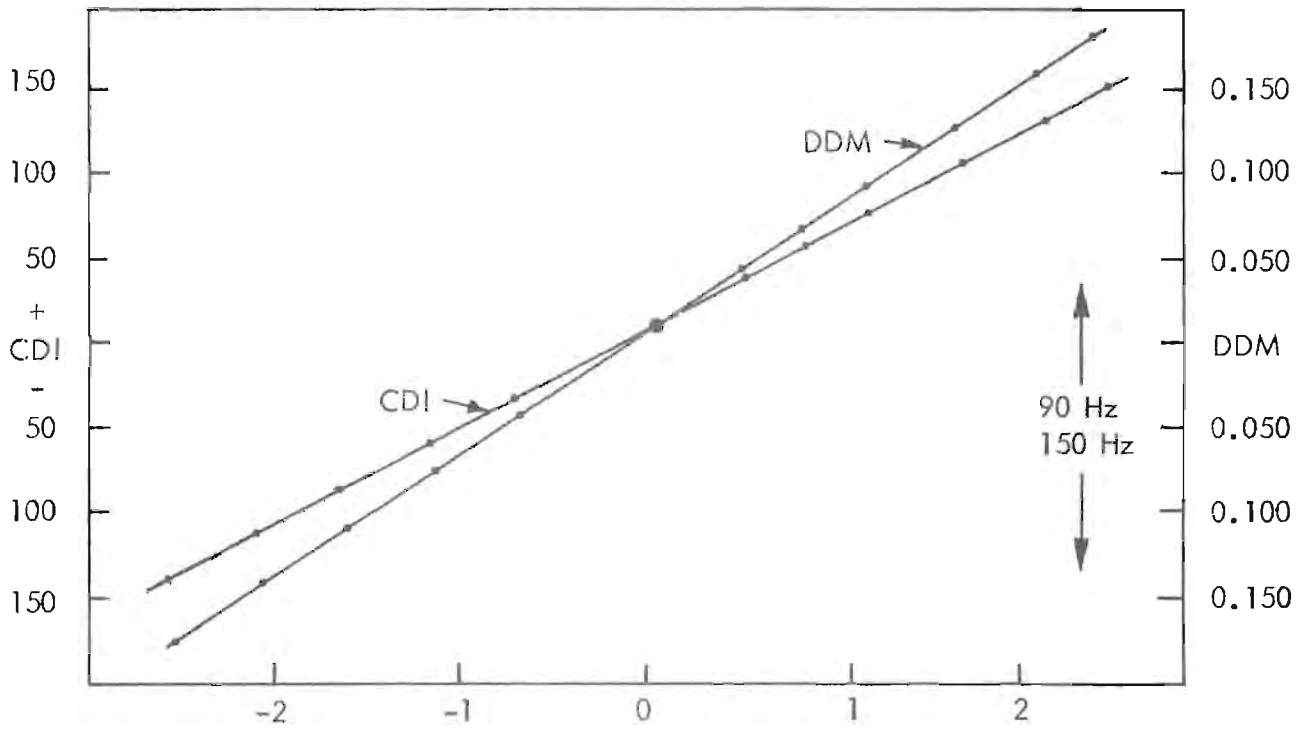

Figure 81. Calibration of Converter/Receiver Using RF Feedback.

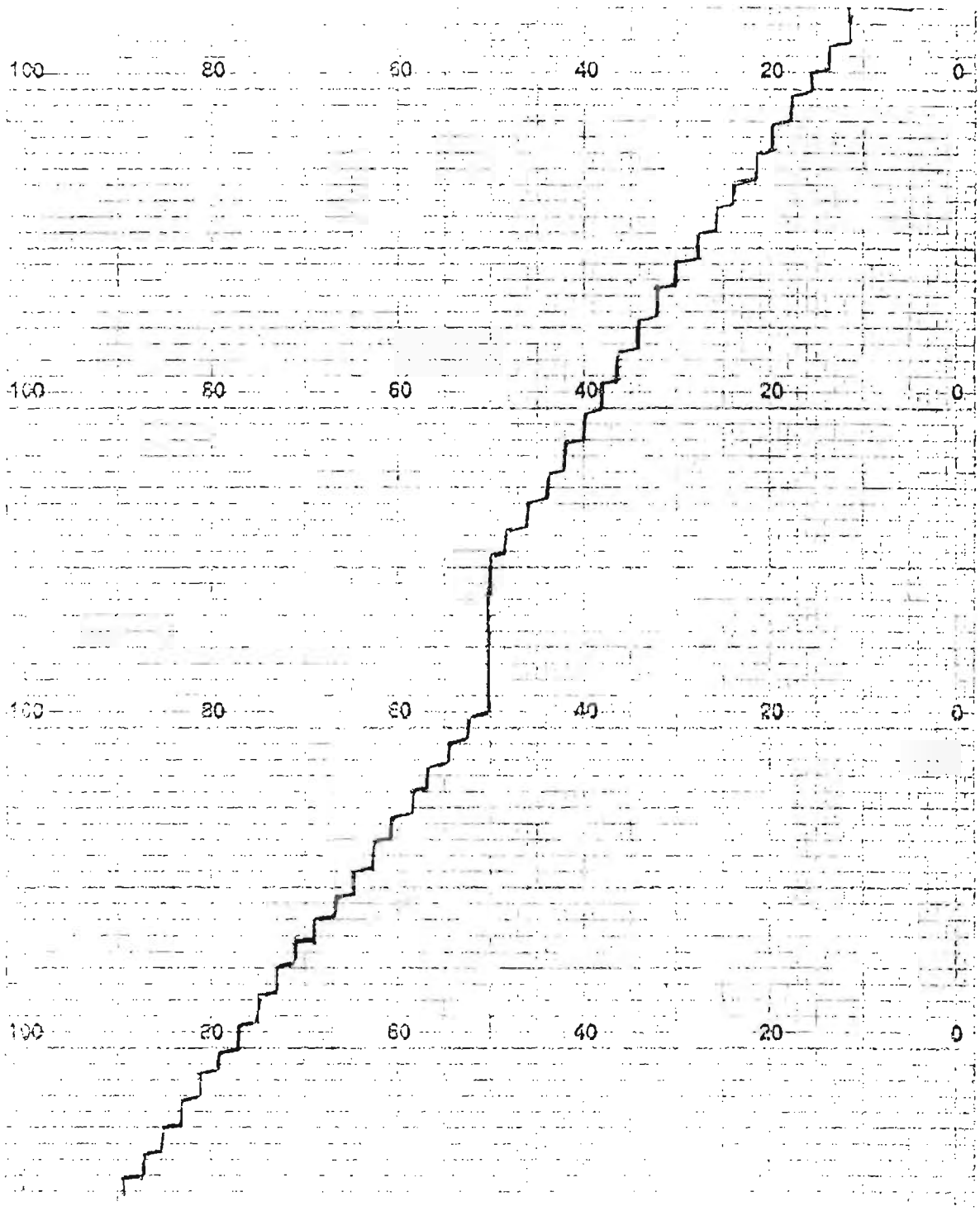

Figure 82. Stepped Response of Converter/Display Unit.

Finally, the dynamic response of the converter/display unit was taken to verify its ability to provide adequate "following" of the input signals. The record of this test is shown in Figure 83. It is seen that the response has its -3 dB point about 0.35 Hz, a frequency considered very adequate for the dynamics of the tracking problem.

4. Field Tests. The converter/display unit has been used in conjunction with the static ARTT tracker (See RD 74-214) on several occasions, including a demonstration for FAA officials and other interested persons at Oklahoma City on July 9, 1974. The interface unit has also been used satisfactorily with the video ARTT system during on-site flight checks.

D. Conclusions Concerning the Recently Fabricated ARTT Devices. The following conclusions are provided as a result of the tests and experiences obtained working with two versions of automatic tracking radio telemetering theodolites.

1. All models of automatic tracking theodolites investigated, in particular the two fabricated as a part of this program, involve at this time noticeable engineering tradeoffs. In simplest terms, the tradeoff is range versus operational capability for all light conditions. The video tracker optimizes with respect to range whereas the LED dynamic tracker optimizes with respect to operation during a variety of light and background conditions.

2. The video tracker has range capability greater than 5 miles with a 250-watt landing light source. With this and any other incandescent light source, control of the lens aperture must be affected to prevent excess light from degrading tracking accuracy when close-in.

3. Tracking accuracies obtained during initial tests with the video tracker show accuracies and repeatabilities comparable with an average manual track. Improvements are conceived that will permit the autotracker to exceed the manual capability.

4. Present video tracker operation is limited to nighttime; however, with special techniques such as reverse imaging and source modulation, opportunities exist for extending the period to include daytime.

5. Present packaging has not provided for operation in all environmental conditions, especially temperatures below 0°C, and high humidity.

6. A solid state detector, Model SC-10, with a dynamic tracker ARTT has been demonstrated under laboratory conditions to have a range of 1.5 miles during daytime, with a system noise equivalent to 0.02 degree. At a range of .7 mile the available look angle at the source was found to be a total of 8 degrees in both axes.

7. Theoretical calculations indicate that the LD-235 light emitting diode with its inherent 15-degree conical radiation pattern will provide a maximum range of 2 miles with the SC-10 photocell behind a 5-inch light gathering aperture.

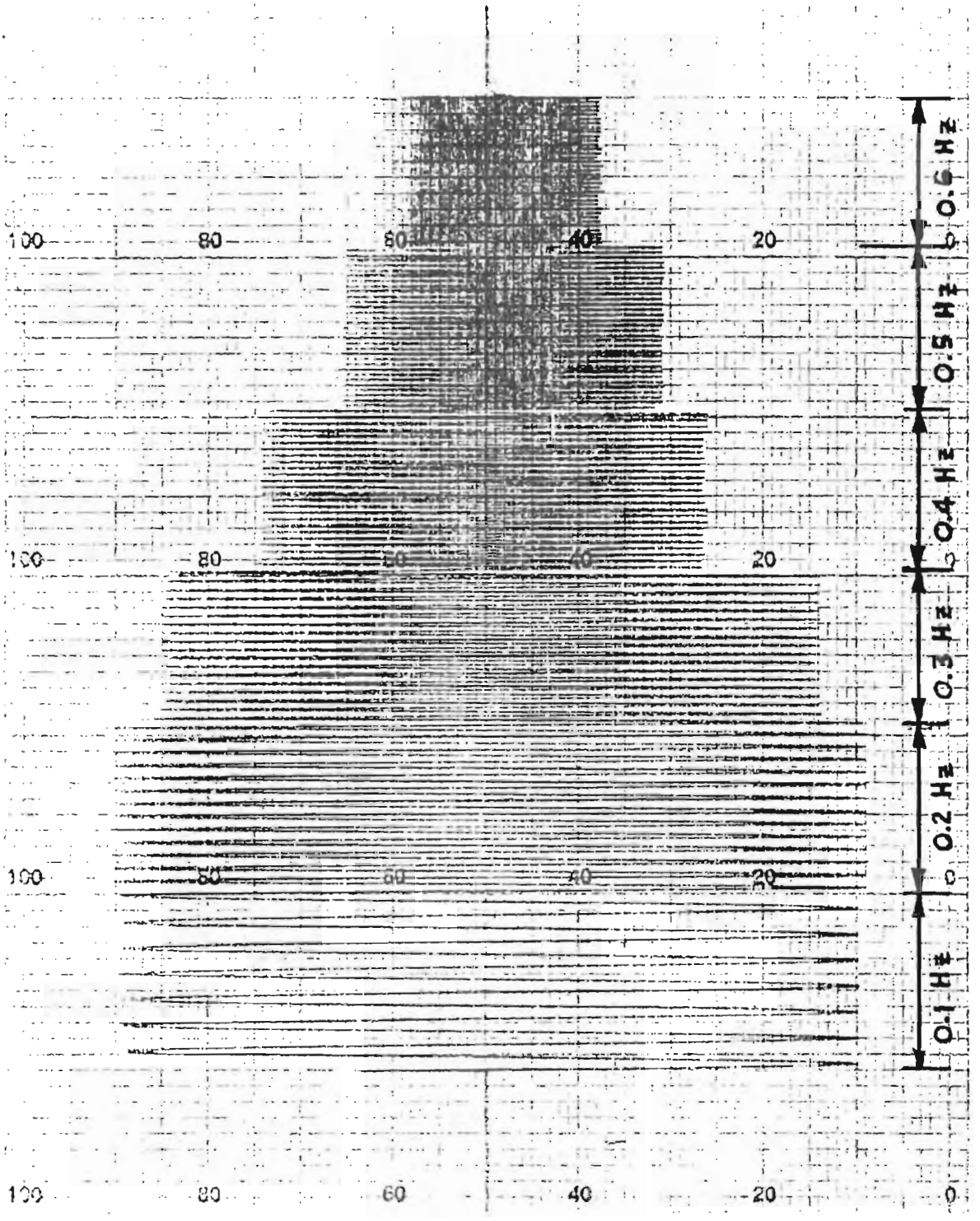

Figure 83. Dynamic Response of Converter/Display Unit.

VI INVESTIGATORS

Mr. Paul Blasche was the project engineer during final phases of the ARTT work program and coordinated the preparation of this report. He was assisted by Mr. David Herold and Mr. Larry Mitchell in circuit design on the dynamic tracker operating with the light emitting diode source.

Dr. James C. Gilfert was responsible for the design implementation and testing of the video tracker. Mr. Robert Rondini and Professor G. E. Smith consulted in this ARTT work.

Dr. Richard McFarland served as project director, performed flight measurements with the help of Aaron Swearingen and aided in production of this final report, particularly with respect to presentation of conclusions.

VII REFERENCES

[1] "Instrument Landing System Improvement Program, Fourth Interim Report," SRDS Report Number RD-73-137, Report EER 5-15, Avionics Engineering Center, Department of Electrical Engineering, Ohio University, Athens, Ohio, May, 1973.

[2] "United States Standard for Terminal Instrument Procedures (TERPS)," Second Edition, Department of Transportation, Federal Aviation Administration, February, 1970.

[3] United States Standard Flight Inspection Manual, Third Edition, OA P 8200.1, Departments of the Army, the Navy, and the Air Force, the United States Coast Guard, and the Federal Aviation Agency, May, 1963.

[4] Kennedy, William E. and Richard H. McFarland, "Instrument Landing System Improvement Program, Environmental Study of the 200 Foot Aperture Slotted Cable Localizer Antenna Array," FAA Report Number RD-74-94, Report EER 5-19, Avionics Engineering Center, Department of Electrical Engineering, Ohio University, Athens, Ohio, April, 1974.

[5] "Instrument Landing System Improvement Program, Final Report," SRDS Report Number RD-74-214, Report EER 5-20, Avionics Engineering Center, Department of Electrical Engineering, Ohio University, Athens, Ohio, December, 1974.

VIII APPENDICES

APPENDIX A. FIELD STRENGTH CONSIDERATIONS

I INTRODUCTION

The level of signal strength provided by an Instrument Landing System (ILS) is specified in the U. S. Flight Inspection Manual OA P 8200.1. Recent work with the Watts slotted-cable end-fire array has identified a problem of inadequate signal strength especially when low-power solid state transmitters are used in the system. Further adding to the problem of ascertaining adequacy of signal has been the apparent discrepancy between the readings taken by the FAA and Ohio University, especially when usable distance values were determined. This paper presents a discussion and documentation concerning field strength readings obtained in general with aircraft and with the Watts glide-slope system in particular. The past use of relatively high-powered vacuum tube transmitters for the ILS has provided an abundance of radio frequency energy in space for the operating aircraft, thus giving comfortable margins over specified minima*. The change to solid state equipment emphasizes the need for precise quantitative field strength measurements so that proper evaluations can be made and standards met. The elimination of excess energy in space is appropriate and consistent with energy and spectrum conservation and is obviously to be encouraged, further emphasizing the need for accurate signal strength determination.

Measurements of ILS field strength are accomplished principally to determine that an aircraft receiver will operate satisfactorily at a minimum altitude and maximum distance from the transmitter. There is usually no need to determine the electric field intensity in volts per meter at any given point in space. Therefore, a convenient measurement technique has been to establish an analog of the AGC voltage in the ILS receiver with a terminal voltage appearing at the receiver from a standardized signal generator. Using reasonable care with tube type receivers, the measurements were straightforward. However, solid state receivers required considerably greater attention to stability since the control circuits parameters are much more dependent on ambient temperature than are those of the tube receivers.

Aside from the receiver problems, the determination of absolute signal strength values for observation points in space has always been extremely tedious and difficult. To obtain an absolute value, the receiving antenna pattern must be known accurately; the transmission losses from the antenna to the receiver also must be determined. When the antenna is mounted on an aircraft, an irregular ground plane is present for the receiving antenna thus significantly affecting its receiving pattern, impedance, and transfer characteristics. To complicate matters, these usually vary with look angle, making the measurement a function of the orientation of the longitudinal axis of the aircraft. Calibration of an airborne system cannot simply be accomplished on the ramp. The presence of the earth close to the aircraft and sensitivity to the angle of reception of the signal makes the accuracy of any such calibration highly suspect.

---

*The U. S. Flight Inspection Manual specifies a minimum of 15 μv of signal for the glide slope and a minimum of 5 μv for the localizer[1]. ICAO Annex 10 specifies 400 μv/m for the glide slope and 40 μv/m for the localizer[2].

If one can become free of the requirement to obtain absolute values and settle for relative values, the problems of measurement are considerably diminished. Certainly because of this, nearly all measurements reported today are in terms of relative values most simply expressed in microvolts of signal at the receiver terminals. Some flaws which exist in this procedure have plagued the operation to obtain accurate determination of signal strength values for the Watts glide-slope system.

II UNITS FOR CALIBRATION

A confusion factor also exists when speaking of values of receiver terminal voltage. Some laboratory workers including those of the FAA introduce a 6 dB pad between their standard generator and the receiver to provide a more nearly constant impedance system. The result is to read voltage values on the signal generator for given responses of the receiver which are double those appearing at the receiver. Such calibrated voltage values are given the name of "hard" microvolts. This is in contrast to the "soft" microvolt value appearing at the terminals.

The standards expressed in the U. S. Flight Inspection Manual are assumed to be consistent and constant in the expression of "hard" microvolts. This means that when the manual specifies, for example, a 15 microvolts of signal strength requirement on the glide slope, it is requiring only 7.5 microvolts be present across the receiver terminals.

Clarification of units should also be accomplished at this point. From a purely technical standpoint, signal strength is not expressed in units of potential, rather in units of electric field intensity. These units in the MKSC system are given in volts per meter. Following is a short derivation of the relation between receiver terminal voltage (microvolts) and the electric field strength. For convenience, a one-half wavelength dipole is assumed to be the receiving antenna. The effective length for this antenna is given by Jordan[3] to be 0.3 wavelength or .273 meter at the glide-slope frequency of 330 MHz.

In Figure 1 v_o is shown to be the equivalent voltage generator for the Thevenin source which represents the receiving antenna. This value is given classically as

$$v_o = \int E \cdot dl$$

where E is the electric field strength in volts per meter and l is the length in meters over which the integration takes place. Using the effective length in effect accomplishes the integration to give

$$v_o = 0.273 \text{ E volts.}$$

Considering v_r at the receiver,

$$v_o = 2 v_r$$

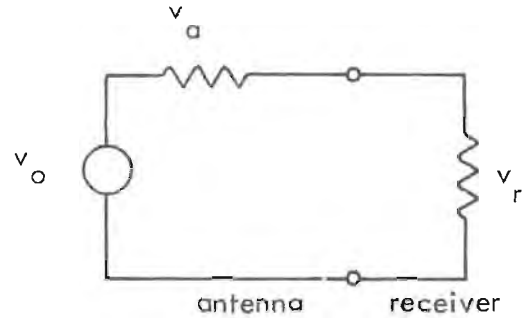

Figure A-1. Equivalent Circuit.

because of the matched condition which is assumed to exist. Therefore,

$$E = \frac{2}{.273} v_r = 7.33 v_r \text{ volts per meter.}$$

Considering the Flight Inspection Manual requirements, this would mean that a field strength of 7.33 times 7.5 or 54.97 microvolts per meter should exist based on the equivalent of a one-half wavelength dipole receiving antenna and lossless transmission lines. Experience has shown that this lossless condition is far from being met in many installations, thus indicating as much as double signal strength must exist to satisfy flight check requirements.

III EXTRAPOLATIONS FOR USABLE RANGE

It is useful at times to be able to determine the power increase needed to provide adequate usable distance given a receiver voltage reading at the minimum altitude, but at a distance other than the maximum. For example, if 10 microvolts is observed at 6 miles at the minimum intercept altitude with 4 watts at the antennas, what must be the power to provide minimum usable distance requirements?

To derive this relation, reference is made to the Flight Inspection Manual requirement of a minimum of 15 hard microvolts at 10 miles. Also, one may recall that signal strength changes inversely with distance, provided line of sight is maintained. Actually in the glide-slope problem the elevation angle is decreasing, thus moving the point of observation lower on the vertical lobe structure of the array pattern. In order to accommodate this factor realistically an exponential factor was derived from the empirical data. With the Watts array at Staunton, for example, 7.05 (2.5 x 2.82) hard microvolts was observed at 14.6 miles and 25.38 microvolts at 6 miles. This decrease was similar to 28.2 microvolts observed at 10 miles and 98.14 microvolts at 4.2 miles with the sideband reference system. The exponential factor is approximately 1.44 for both cases and seems to be quite representative for the Staunton site. However, data from the near-perfect Tamiami site indicates the exponential factor is 1.77 for the Watts end-fire system and 2.1 for the sideband reference system. To express this in mathematical terms let

R = Range ratio of d_2, the far distance of interest, usually the usable distance for the facility to d_1, the near distance of signal observation,

V_o = The receiver voltage observed at d_1 the near range,

V_1 = The receiver voltage observed at d_2 the far range, and

F = The exponential factor.

With this notation

$$R^F = \frac{V_o}{V_1} \tag{A-1}$$

or

$$F = \frac{\ln(V_o/V_1)}{\ln R} \quad . \tag{A-2}$$

If the factor F is considered as known, then

$$V_1 = \frac{V_o}{R^F} \quad . \tag{A-3}$$

Should the problem be one of finding usable distance given an observation of signal level V_o at a distance of d_1, then based on U. S. Flight Inspection Manual requirements, the usable distance d_2 is given by

$$\left(\frac{d_2}{d_1}\right)^F = \frac{V_o}{V_1} \tag{A-4}$$

or

$$d_2 = d_1 \; e^{(1/F)\ln(V_o/V_1)} \text{ miles usable distance.}$$

For example, if 30 microvolts is observed at the outermarker 5 miles from the runway, and a pessimistic factor of 2 is assumed for the Watts system, the usable distance would calculate to be 7.1 miles. Should a factor K of signal level increase need be determined in order that the Flight Inspection Manual requirements be met, the following equation comes directly from equation (A-1)

$$K = \frac{15}{V_o} \left(\frac{10}{d_1}\right)^F$$

If in the above example the increase in signal level to meet flight inspection requirements is desired, the following calculation can be made.

$$K = \frac{15}{30} \left(\frac{10}{5}\right)^2 = 2 \text{ or } 6 \text{ dB.}$$

For the Tamiami case where 2.31 microvolts was observed by Ohio University at 10 miles

$$K = \frac{15}{2.31 \times 2.82} \left(\frac{10}{10}\right)^2 = 2.30 \text{ or } 7.24 \text{ dB.}$$

To interpret this in terms of power required, one must add the requirement to boost the edge of the path at 8 degrees azimuth by 2.85 dB because of the azimuth pattern taper reported by the Watts Prototype Company for their new model slotted-cable antenna. The former antenna had approximately 8 dB of taper. An additional 3 dB of signal must be provided to permit operation down to the radio frequency alarm point. This means that a total increase of 13.09 dB must be provided for the new Watts array to meet operational requirements at Tamiami.

This amount of power can reasonably be expected to be obtained. First, a 12.6 dB increase can be obtained by relocating the transmitter hut closer to the center of the array and eliminating the feeder cable with a measured 12.6 dB of loss. Second, a corner reflector added to the slotted cables is calculated and measured by the Watts Prototype Company to produce a 4.9 dB increase in signal. Third and finally, replacement of 350 feet of one-half inch Spiroline Cable with 260 feet of seven-eighths inch Spiroline Cable will provide an increase of 3 dB. These three provide a total of 20.5 dB which gives a calculated margin of 7.41 dB.

IV COMPARISON OF WATTS ARRAY SIGNAL LEVELS WITH SIDEBAND REFERENCE

It is noted that the sideband reference system has been found in practice to provide adequate signals to meet FAA standards with solid state transmitters and directional antennas. Accordingly, it is reasonable to assume that if the Watts system can provide signal levels equal to or greater than those produced with the sideband reference system, then the Watts signal levels should be acceptable. Motivated by this logic, a set of airborne readings was made at Tamiami with the Watts array and with a new collinear dipole array in a corner reflector currently being manufactured for use with image glide-slope systems. This antenna was mounted on the image glide-slope tower at the height for sideband reference operation (SBR). The typical 3 dB power split loss for the SBR was provided for these measurements.

Airborne measurements showed the Watts system to be 18.8 dB below the SBR at 10 miles and 20.7 dB lower at 5 miles. As calculated in the preceding section, an additional 20.5 dB is expected from Watts system modification so that signal levels comparable with

the SBR can be expected. Azimuth tapers for both the SBR directional antennas and the new model Watts antenna are nearly the same and alarm limits for the RF power will be identical for the two systems, hence these are not factors of concern in this calculation.

V COMPARISON OF CALIBRATION SYSTEMS

FAA Calibration and Aircraft Setup

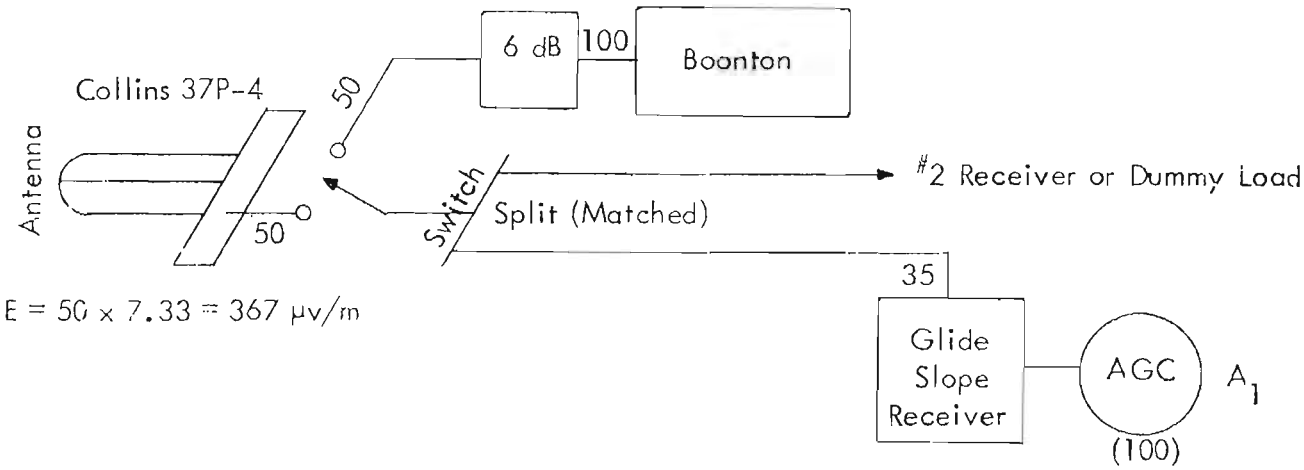

E = 50 x 7.33 = 367 μv/m

100 μv-Boonton gives 50 μv at splitter (assumes matched). This produces 35 μv at each receiver for AGC value A_1. This requires 367 μv/m field strength, assuming lossless cable and equivalance to dipole.

Ohio University Calibration and Aircraft Setup

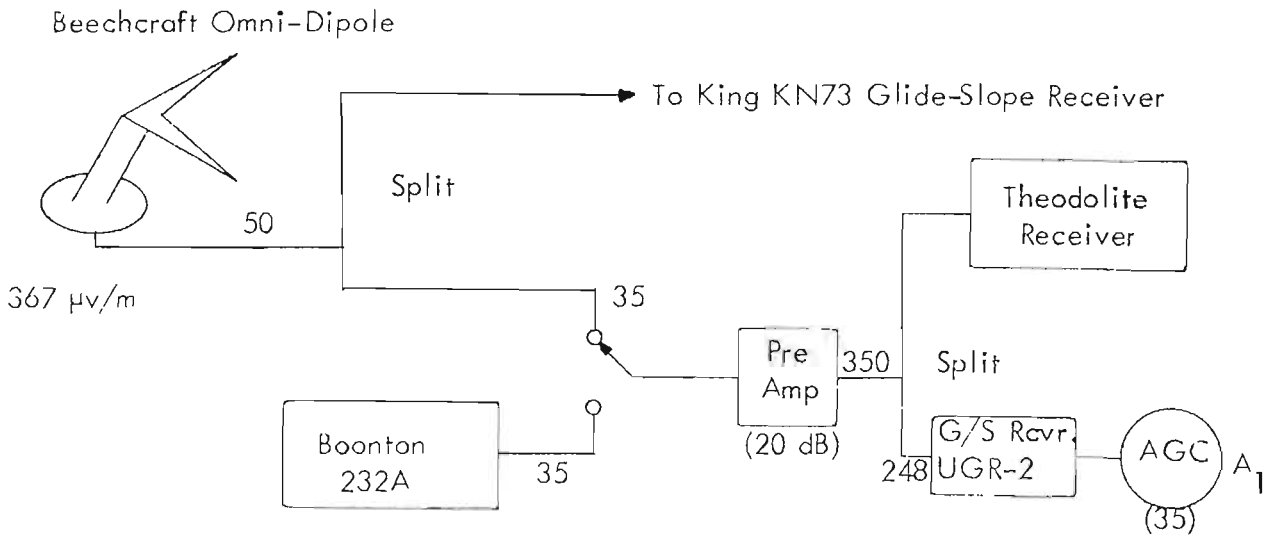

367 μv/m field strength gives 35 μv to preamp and an AGC value A_1. Boonton reading will be 35 μv.

The conversion between Ohio and FAA readings is 2.82 x Ohio = FAA.

VI REFERENCES TO APPENDIX A

[1] United States Standard Flight Inspection Manual, Third Edition, Departments of the Army, the Navy, and the Air Force, the United States Coast Guard, and the Federal Aviation Agency, May, 1963, pp. 14 and 15.

[2] International Standards and Recommended Practices, Aeronautical Telecommunications, Annex 10 to the Convention of International Civil Aviation, Third Edition of Volume I, International Civil Aviation Organization, July, 1972, pp. 217-24 and 217-27.

[3] Jordan, E. C., Electromagnetic Fields and Radiating Systems, New York: Prentice-Hall, Inc., 1950, p. 336.

APPENDIX B. CIRCUIT DIAGRAMS FOR VIDEO ARTT PROCESSOR

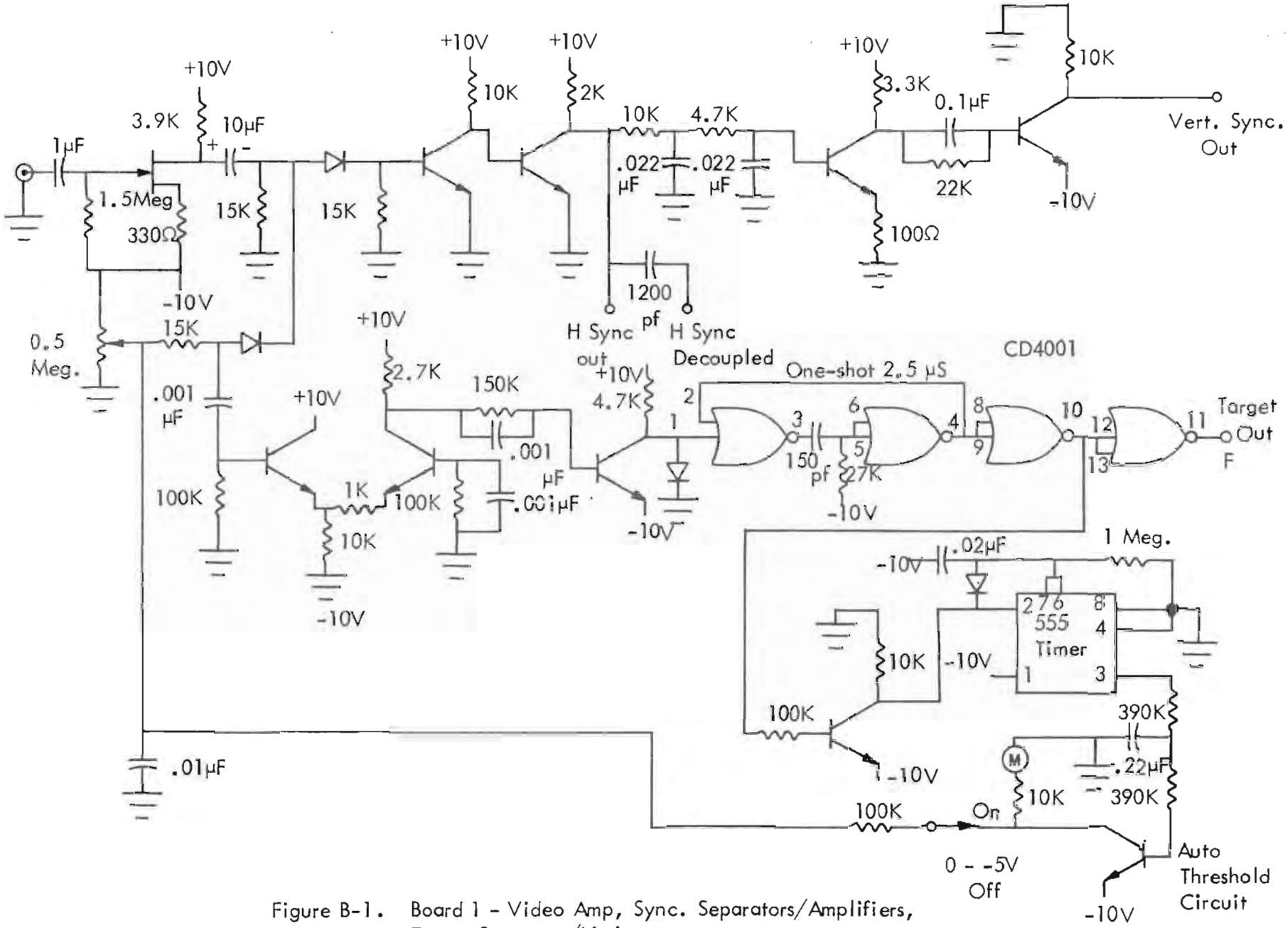

Figure B-1. Board 1 - Video Amp, Sync. Separators/Amplifiers, Target Separator/Limiter.

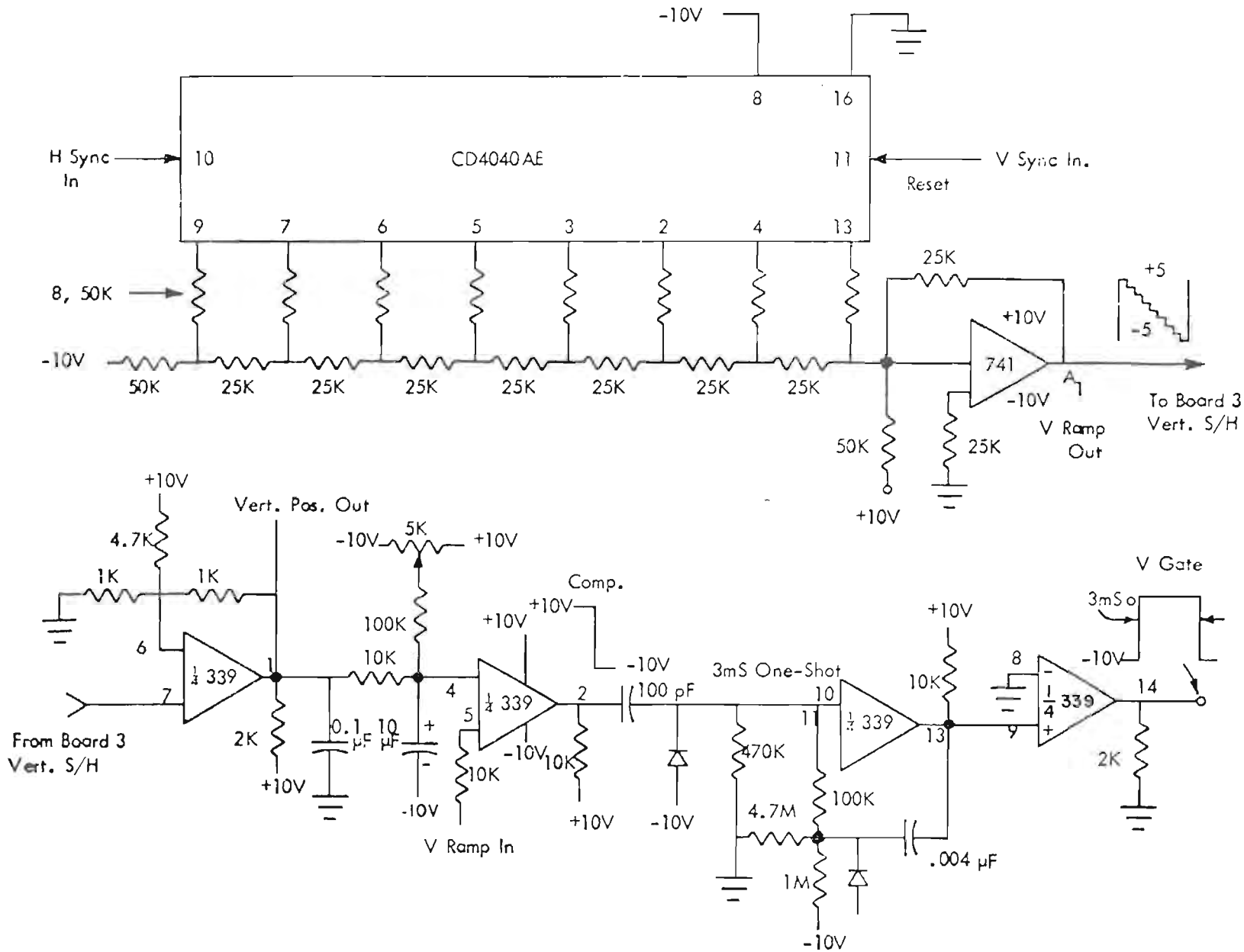

Figure B-2. Board 2 - Vertical Ramp Generator and Gate Generator.

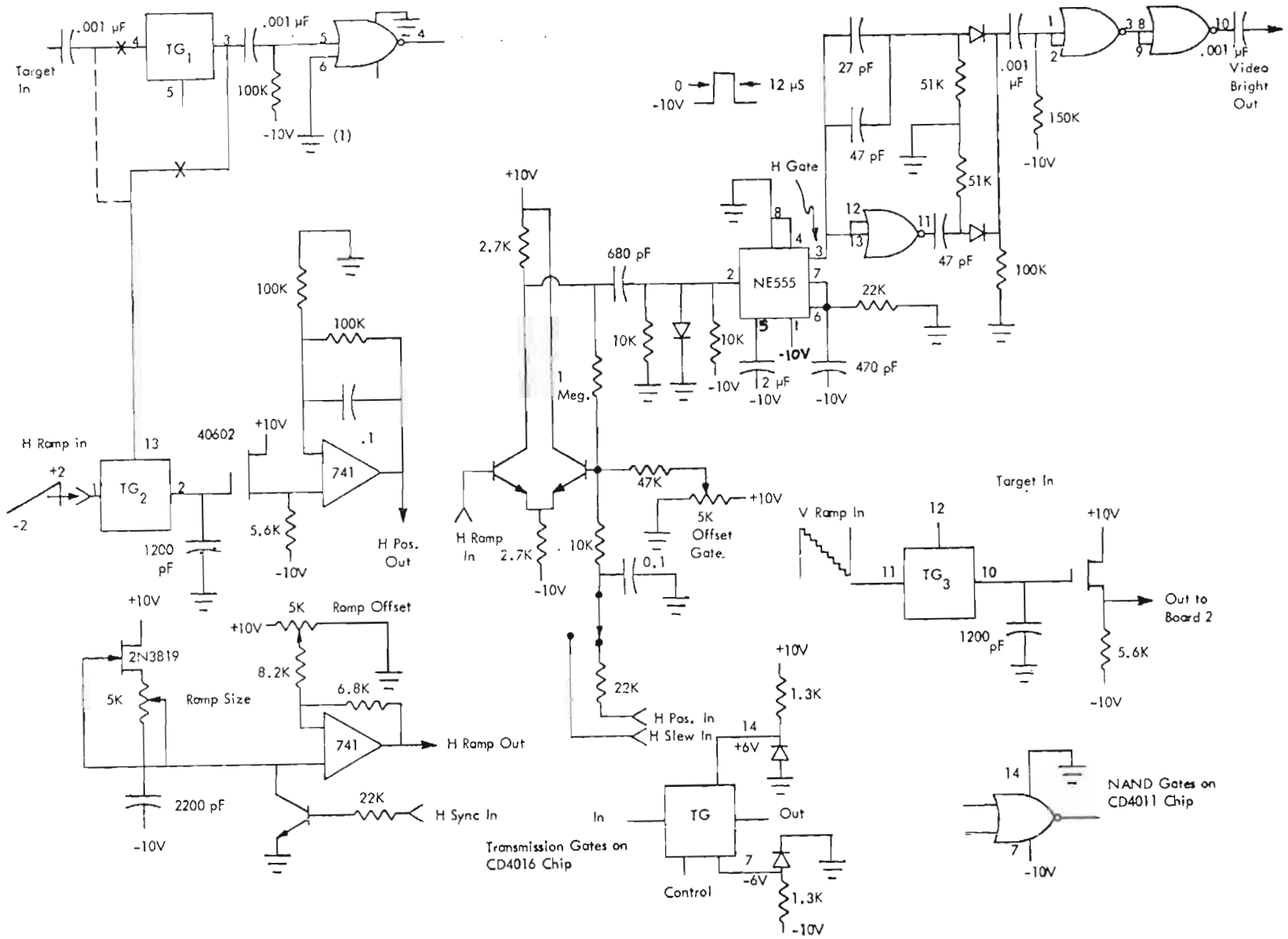

Figure B-3. Board 3 - Horizontal and Vertical Sample/Holds, Ramp Generators, Location Detectors, Gate Generators, and Bright-Line Generators.

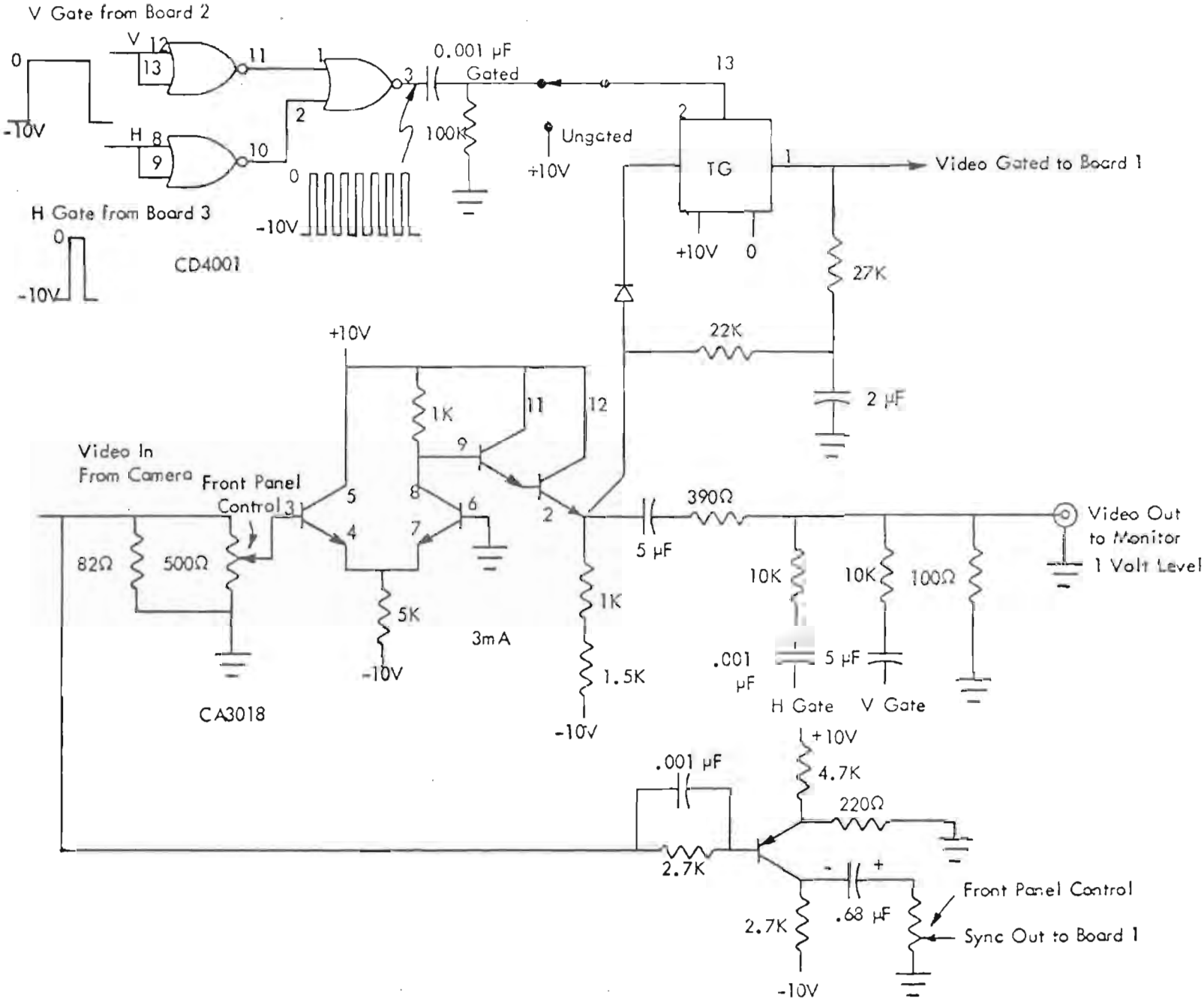

Figure B-4. Board 4 - Video Booster/Isolator, Video Gating, Cursor Adder.

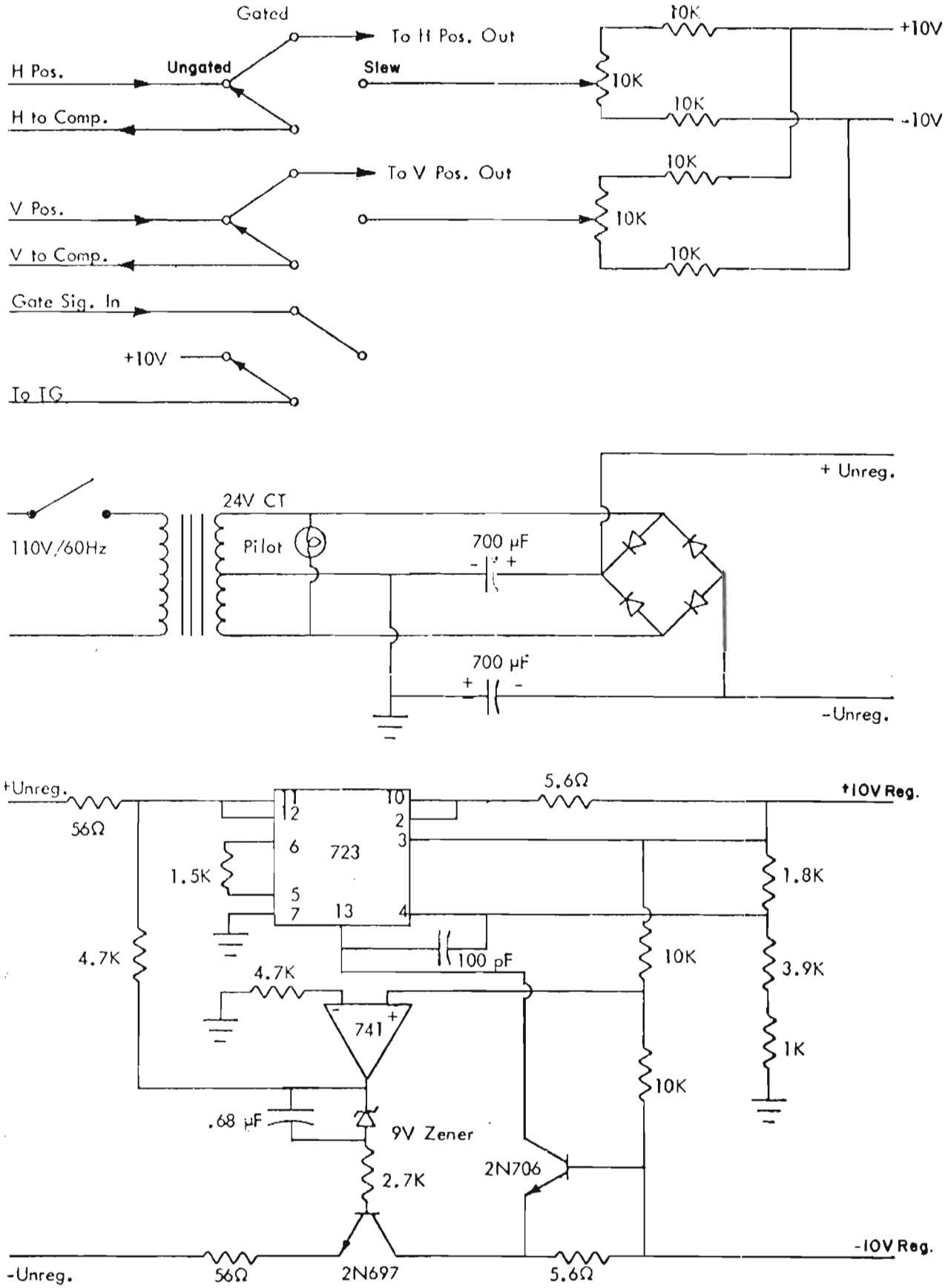

Figure B-5. Cabinet-Mounted Functions - Mode Switch and Power Supply and Tracking Regulator.

ELECTRICAL CHARACTERISTICS

	SC/10	UNITS
Position Sensitivity		
At spectral peak	1.6	μa/mw/.001"
White light 2850 °K	.8	μa/mw/.001"
Position Linearity		
0.05" from center	1	Percent
75% of distance from center to edge	6	Percent
Intensity Sensitivity (responsitivity)		
At spectral peak	.25	μa/μw
White light 2850 °K	3600	μa/lumen
R_s (equivalent series resistance -see equivalent circuit)	20	K ohms
Capacity (typ.)		
10 volts	450	pf
50 volts	200	pf

EQUIVALENT CIRCUIT

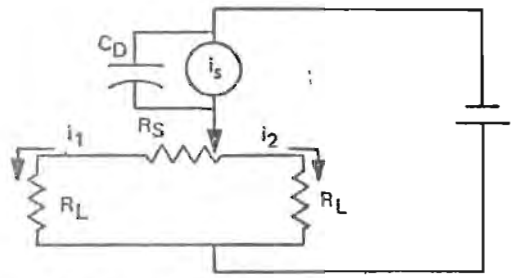

R_S = Sheet resistance—see electrical characteristics

R_L = Load resistance

i_s = Signal current

C_D = Detector capacitance

NOTE: $i_1 = i_2$ at null

$i_1 + i_2 = i_s$

MECHANICAL DETAILS

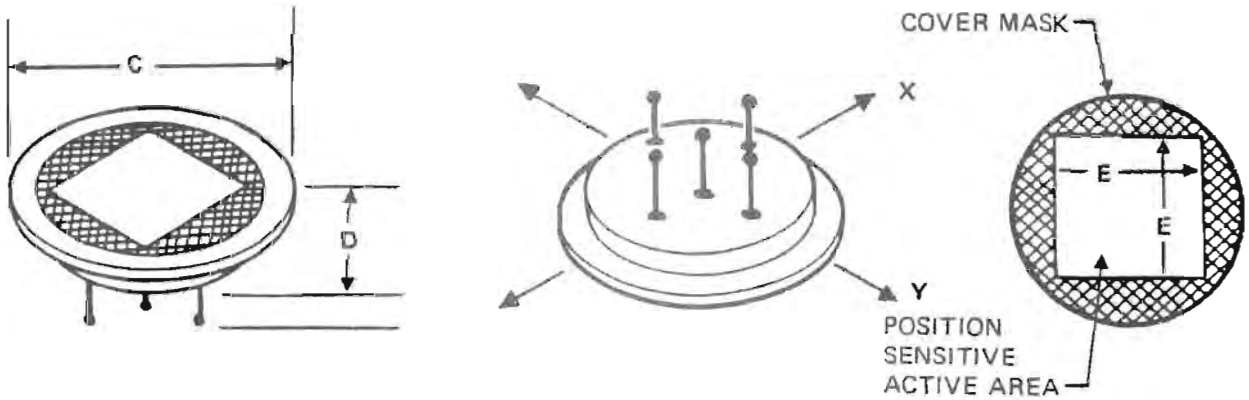

SC/10 AND SC/25